



Texas Tech University – Space Raiders
Preliminary Design Review 2017 – 2018

Davis Hall

I) Contents	
II) Summary	2
III) Changes to Proposal	3
IV) Vehicle Criteria	4
1. Selection, Design, and Rationale	4
2. Launch Vehicle	5
3. Recovery Subsystem	26
4. Mission Performance Prediction.....	48
V) Dynamic Apogee Control System	57
1. Designs.....	57
2. Parts Selection.....	58
3. Logic	61
4. Testing	63
VI) Payload Criteria	66
1. Payload Summary.....	66
2. Changes Since Proposal.....	66
3. Payload Experiment Goals	67
4. System Level Design.....	68
5. Leading Payload Design	82
6. Verification Plan	93
7. Recovery Subsystem	93
8. Recovery Subsystem	94
9. Line Item Budget.....	94
10. Payload Team Gantt Chart	95
VII) Project Planning	96
1. Vehicle Requirement	96
2. Pre-Launch Checklist	99
3. Budgeting	100
4. Timeline	106
VIII) Safety	107
1. Safety Procedures	107
2. Safety Budget	112
XI) Bibliography	113

II) Summary of PDR

a. Team Summary

b. Launch Vehicle Summary

The launch vehicle will provide a means of transportation of a scientific payload up to exactly one-mile AGL. The Vehicle will be re-usable and meet all requirements specified by the student handbook, as well team sanctioned requirements.

c. Payload Summary

III) Changes Made Since Proposal

I) Integrating DACS

- a. The idea to incorporate a dynamic apogee control system was proposed shortly after submission of the proposal. This system (DACs) for short will be classified as a second payload due to the complexity of the system. DACs is on board to correct the actual altitude of the launch vehicle to a set target, assuming it will overshoot the target height. More information over DACs can be found in section V

II) Considering Transition body

- a. A transition body, going from large front to skinny rear would reduce the drag of the airframe and therefore be a more efficient design. Research into this topic went on and complications arose, therefore making this option only a strong consideration and not necessarily our final choice. More information over this can be found in section IV.

III) Refined Motor selection

- a. The Motor selection went from a broad range during the proposal to a set of 4 options that we can choose from when narrowing down final weight. A thrust plate is also proposed as the motor retention system. Details of this research can be found in section IV.

IV) Long Elliptical Nosecone

- a. From research the team has brought up the idea of 3D printing a long elliptical shape nosecone. This differs from the originally proposed parabolic fiberglass nosecone in multiple ways. Details over nosecone research can be found in section IV.

V) Rail Buttons

- a. Originally proposed rail buttons were set to be 3D printed from ABS plastic, however due to the sheer size and mass of the launch vehicle, the ABS plastic could potentially fail under a moment force thus causing the rocket to go ballistic at the time of launch. This problem can be avoided by using commercially available Delrin 1515 rail buttons. More information over rail buttons can be found in section IV

VI) Parachute Size Change

- a. The original design in the proposal called for a 14 foot diameter parachute but this was a rough estimate based off the original estimations for the mass of different components throughout the rocket. After going through and revamping the distribution of mass, and then limiting the amount of kinetic energy upon impact we have reached the conclusion that we will need a 16 foot diameter main chute. Along with the main parachute size changing we recalculated the size of the drogue parachute and came to the conclusion that we must increase the diameter from the originally proposed 4 foot diameter to one with a 2 foot diameter.

VII) Shock cord size and Material

- a. The shock cords we originally proposed were three quarter inch tubular elastic but with some further research we were unable to find any supplier where we could buy tubular elastic with that specific dimension. Instead we looked at different options mostly Nylon or Kevlar alternatives.

VIII) Recovery system Redundancy

- a. In the proposal we never specified or looked into the redundancy of the overall system and decided to add another altimeter and additional separation charges in order to insure a safe decent of the rocket and successful delivery of our payload.

IV) Vehicle Criteria**4.1 Selection, Design, and Rationale****4.1.1 Mission Statement**

Space Raiders has a mission to design, build, test and launch a high-powered rocket that carries and deploys a payload of a rover containing folding solar panels. In order to achieve the desired altitude of 5280 ft, we will implement the Dynamic Apogee Control System (DACs). As a team, we pride ourselves on our ingenuity and teamwork as well as the interest in aerospace and STEM that we bring to the community.

4.1.2 Mission Success Criteria

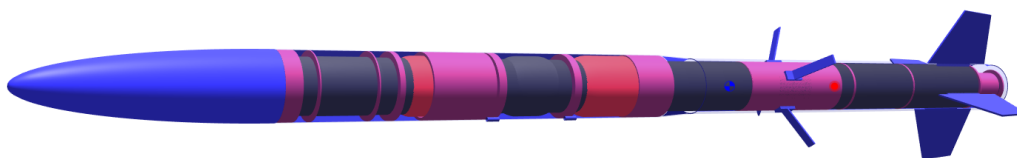
- Build and Design a rocket-powered launch vehicle within a budget of \$2000
- Achieve a target altitude of 5280 ft
- Provide a secure platform for the mounting of the payload bay
- Implement the Dynamic Apogee Control System (DACs) to control vehicle velocity after burnout
- Achieve a velocity at the exit of the take-off ramp of 52 ft/s
- Implement safe fabrication as well as testing practices
- Launch vehicle must be completely reusable after launch, landing, and payload deployment
- Safely deploy stages and separations using black powder charges and altimeters
- Have successful drogue parachute deployment at apogee
- Have successful main parachute deployment at 750 ft
- Safely land vehicle and payload at a velocity of 14.753 ft/s
- Safely land vehicle and payload at a kinetic energy of 70.993 ft-lb

4.2 Launch Vehicle

The Launch vehicle must be designed and built following a strict set of requirements in order to ensure a successful mission. The work for this section has been divided amongst vehicle team members to ensure every subsystem was researched thoroughly and to create areas topics of expertise within each member. Each subsystem was addressed with, material selection, price, complexity, and then weighed with pros and cons using decision matrices to determine an ideal model to use for simulations. A GANTT chart was used to reach our goals and work on the PDR. This was a very effective tool in assigning roles, setting deadlines and overall organization. (see chart below)



(GANTT Chart: Vehicle Team PDR)



(Conceptual rendering)

4.2.2 Motor selection

Motor choice could be considered one of the most pivotal aspects of a successful launch. Due to the importance of selecting the correct engine option, a considerable amount of thought and discussion has gone into the calculations, simulations and research on this topic. Incorporating ideas of tail cones, thrust plates, and casing securing methods to increase the desired performance have also been considered in the overall selection. Factoring in the many changing parameters that will occur during the finalization of the different team's designs, our team has

done an analysis of multiple scenarios in which different systems are simulated to confirm mission goals are still met. An excel spreadsheet was created in order to help simplify and condense the possible engine candidates. After reviewing the data received from our simulations and the excel file, the team decided on four ideal engine possibilities which will fit the criteria needed for a successful launch. Since the weight of the rocket was variable throughout the design process, we classified the different engines by the final weight suited for the engine type. Allowing a flexibility and adaptability to changes made as the designs continued to progress forward. This selection criteria was also useful in establishing a clear path forward.

*Motor chart containing all reviewed motors is included in the appendix

4.2.2.1 *Cesaroni L1395 – BS*

The Cesaroni blue streak L1395 is one of the first engines we moved to into the ideal engine selection stage. The motor showed a specific impulse capable of delivering a sustained thrust suited for a rocket of medium to heavyweight. The simulations showed this engine would place us around the desired apogee and would also meet the required rail exit velocity with the weight class selected.

Engine Specifications

4 Grain, 75mm (2.953")

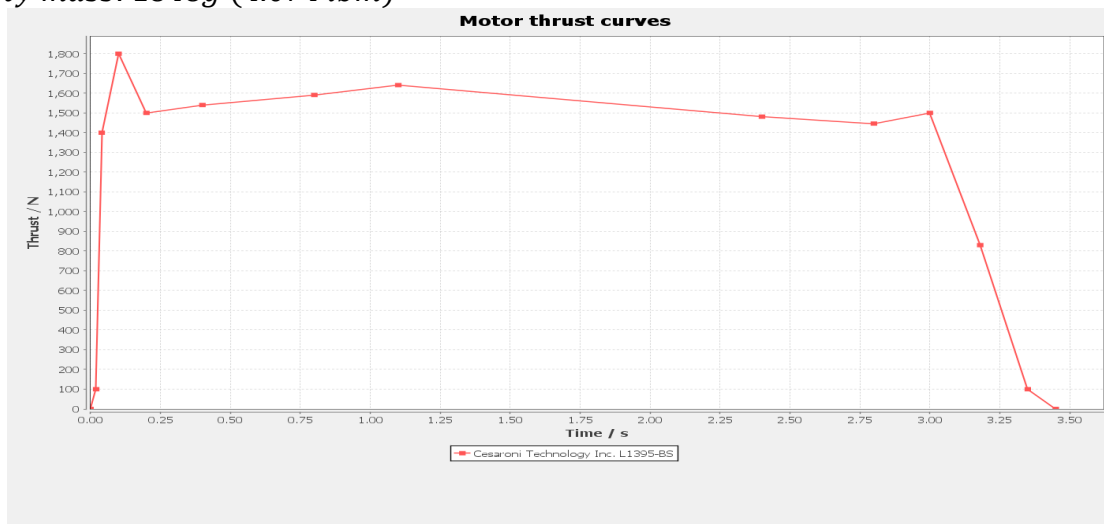
Total Impulse: 4895N · s (1100.439 lbf · s)

Average Thrust: 1463N (328.895 lbf)

Max Thrust: 1800N (404.656 lbf)

Launch Mass: 4323g (9.531 lbm)

Empty mass: 1848g (4.074 lbm)



4.2.2.2 *Cesaroni L1410 – SK*

The Cesaroni L1410-SK turned out to be the best candidate for ideal engine selection. The current estimated weight shows that selecting this motor would couple perfectly with the medium weight class our rocket falls into. One trait of this motor that should be mentioned is that the fuel grain it consumes does produce smoke during the burn. The Cesaroni L1410-SK will be the engine selected if the estimated weight of the rockets stays relatively constant throughout the design process.

Engine Specifications

5 Grains, 75mm (2.953")

Total Impulse: 4828N · s (1085.378 lbf · s)

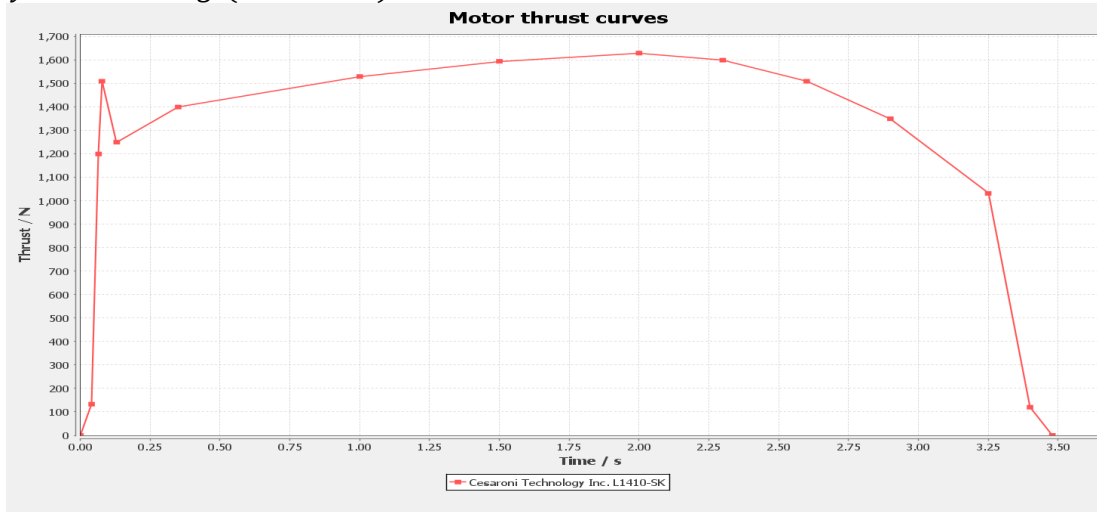
Average Thrust: 1419N (319.003 lbf)

Max Thrust: 1630N (366.439)

Burn Time: 3.4s

Launch Mass: 5115g (11.277 lbm)

Empty Mass: 2240g (4.938 lbm)



4.2.2.3 Aerotech L2200G

The Aerotech L2200G was selected as an ideal engine choice for a scenario in which the weight greatly exceeds the original estimation. The motor is the most powerful engine that our team could find available for purchase online. In the case where our weight does fall over the estimation, this engine will have the thrust to reach desired apogee, but a concern would be that the total impulse falls only 16 N · s (3.597 lbf · s) under the limit of 5104 N · s (1147.425 lbf · s).

Engine Specifications

4 Grain, 75mm (2.953")

Total Impulse: 5104N · s (1147.425 lbf · s)

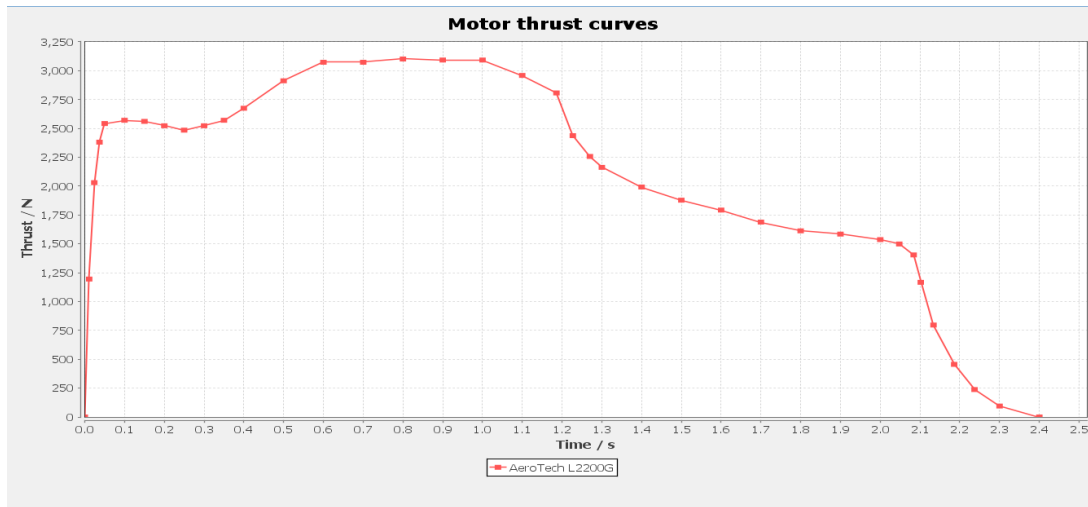
Average Thrust: 2243N (504.246 lbf)

Max Thrust: 3102N (697.357 lbf)

Burn Time: 2.27s

Launch Mass: 4751g (10.474 lbm)

Empty Mass: 2235g (4.927 lbm)



4.2.2.4 Aerotech L1420R

The Aerotech L1420R made it into the ideal engine selection as an optimal candidate for a scenario in which the total weight of the rocket comes out to be less than our estimated value. This engine accomplishes this by burning at a slower rate than the other engines considered to be ideal. This quality is displayed in the red flame produced as a byproduct. A downside of this engine is the difficulty encountered during the ignition process.

Engine Specifications

4 Grain, 75mm (2.953")

Total Impulse: 4603N · s (1034.795 lbf · s)

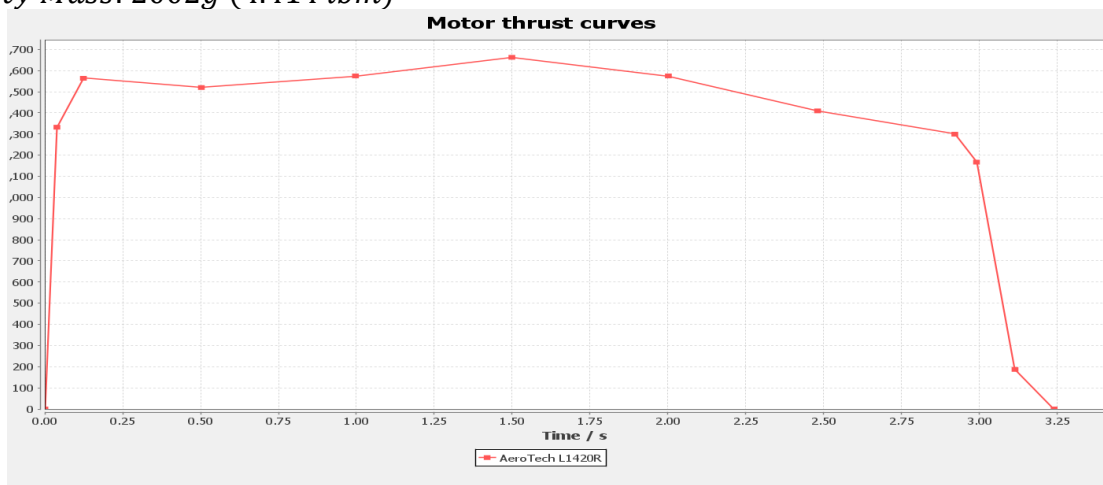
Average Thrust: 1420 N (319.228 lbf)

Max Thrust: 1814 N (407.803 lbf)

Burn Time: 3.2s

Launch Mass: 4562g (10.057 lbm)

Empty Mass: 2002g (4.414 lbm)

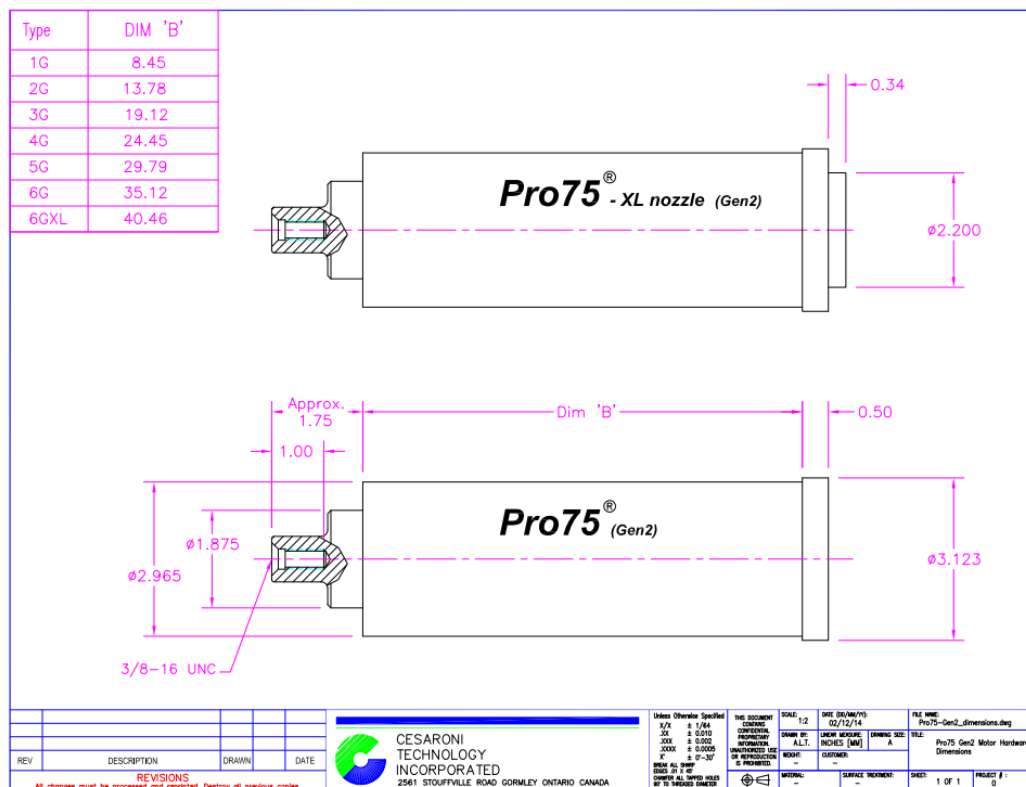


4.2.3 Hardware

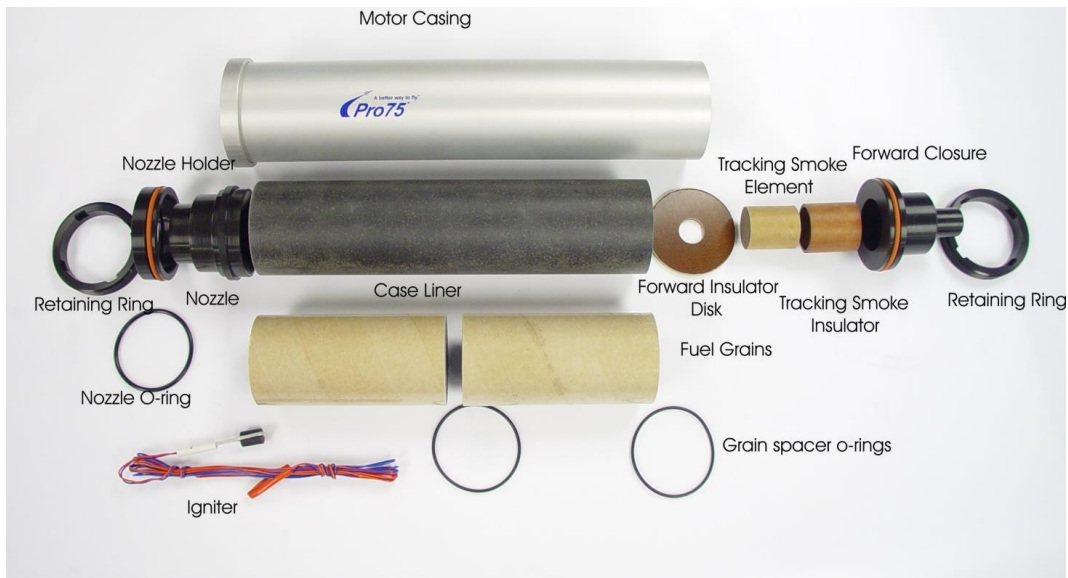
Each of the motor selection options has a compatible casing that is manufactured by the same company to allow for easy reloading and increased longevity. Below are the two options of our motor selection.

4.2.3.1 Cesaroni Casing

The casing and hardware that is used for Cesaroni motors is manufactured by the same company and is directly compatible with their motors. The motor casing will come with forward and rear closures, threaded retaining rings, as well as the nozzle holder. It is CNC machined out of 6061-T6 aluminum and anodized for corrosion resistance. This casing has a cost of this hardware set is \$309.95.



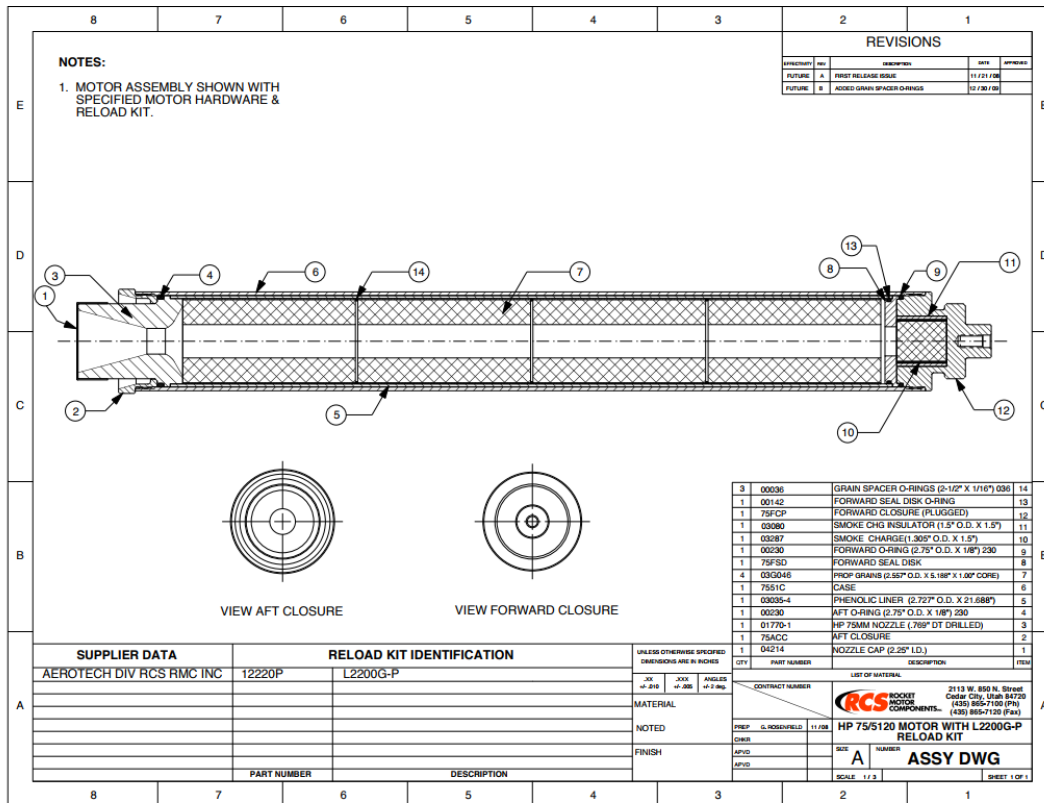
Cesaroni Casing detailed drawing



Cesaroni Hardware Set

4.2.3.2 Aerotech Casing

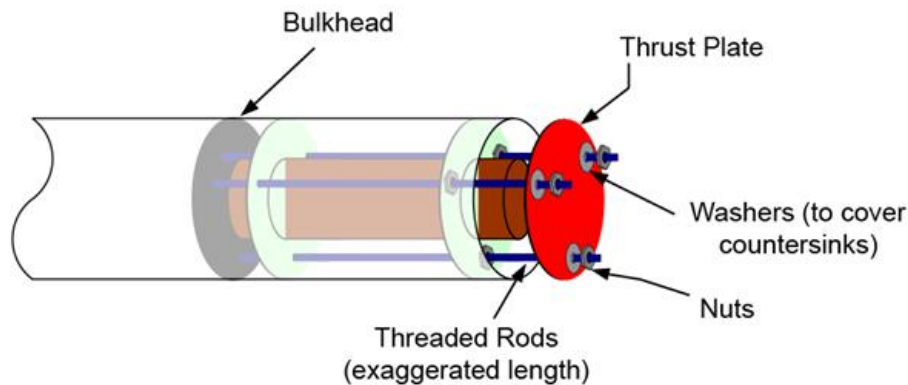
The compatible motor casing for the L2200G and the L1420-R is specially designed for use with Aerotech 75mm (2.953”) motors reaching a total max total impulse of $5120 N \cdot s$ ($1151.021 lbf \cdot s$). It is manufactured by the same company and is sold as a set that contains all essential hardware for assembly similar to the Cesaroni casing seen above. The cost of this hardware set is \$550.



Aerotech Casing detailed drawing

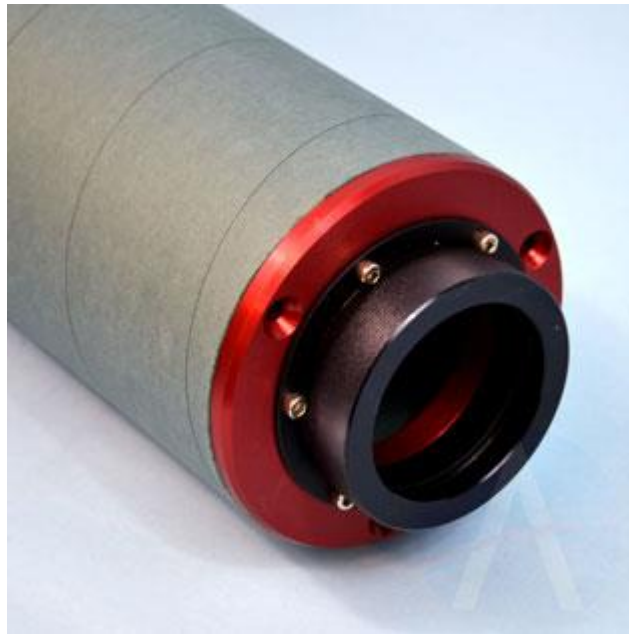
4.2.3.3 Retaining rings

The 3 retaining rings will serve the purpose of holding the motor casing/hardware assembly in position inside of the launch vehicle's airframe. They will be made out of 0.635cm (1/4") thick plywood which has a density of $0.9 \frac{g}{cm^3}$ ($0.0325 \frac{lbm}{in^3}$). The outside diameter will be the same as the inside diameter of the 13.97cm (5.5") blue tube which is 13.6144cm (5.36") and have an inner diameter of 7.8994cm (3.11"). They will be secured with high strength epoxy resin and have either holes for threaded rods or use screws to fasten a thrust plate if it is decided to use one.



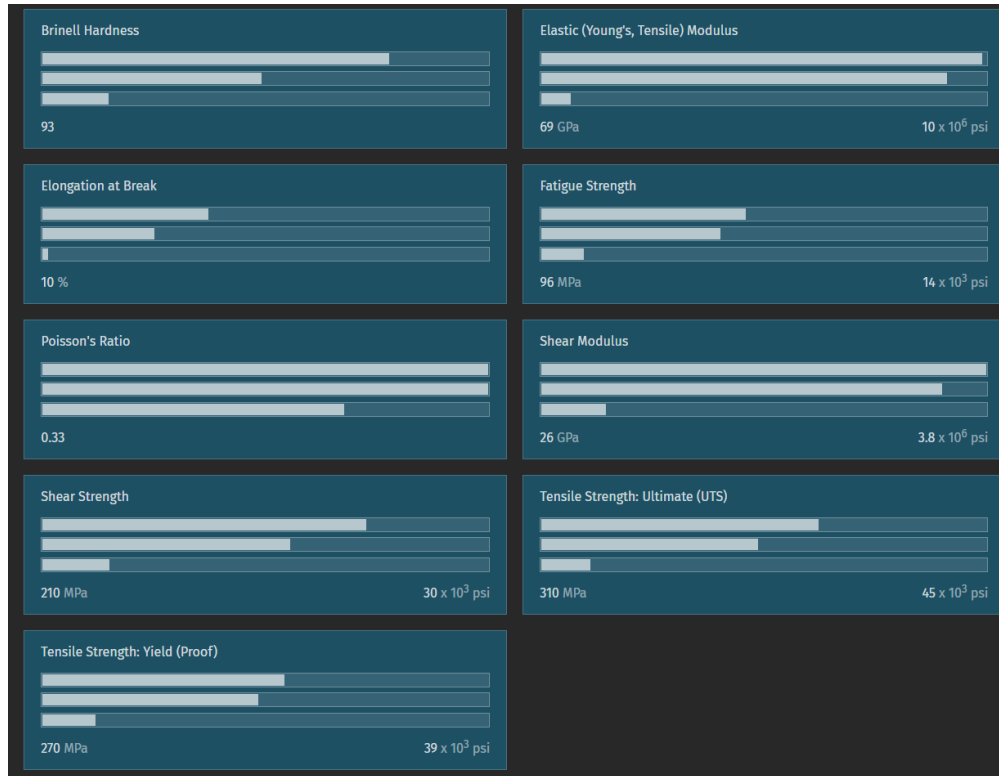
4.2.3.3 Thrust Plate

A thrust plate is being considered as an addition to the motor assembly as it can be utilized to disperse the force of the motor throughout the airframe instead of concentrating on the centering rings. This will reduce the stress created on the epoxy fillets and ensure the longevity and re-usability of the launch vehicle. The Thrust plate would be secured using threaded rods as fasteners that run parallel to the motor casing as seen in the figure above. This component is sold commercially for the exact application that we are using it for and therefore has been proven to be a reliable component.

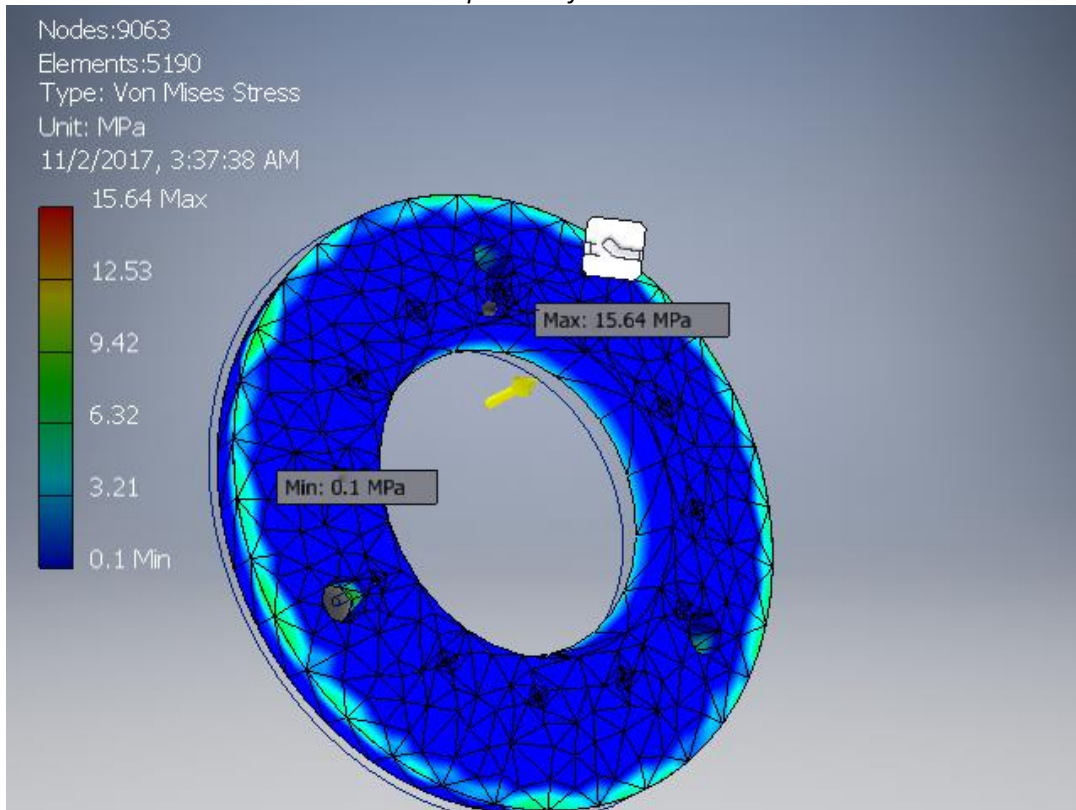


4.2.3.3.1 Stress Analysis

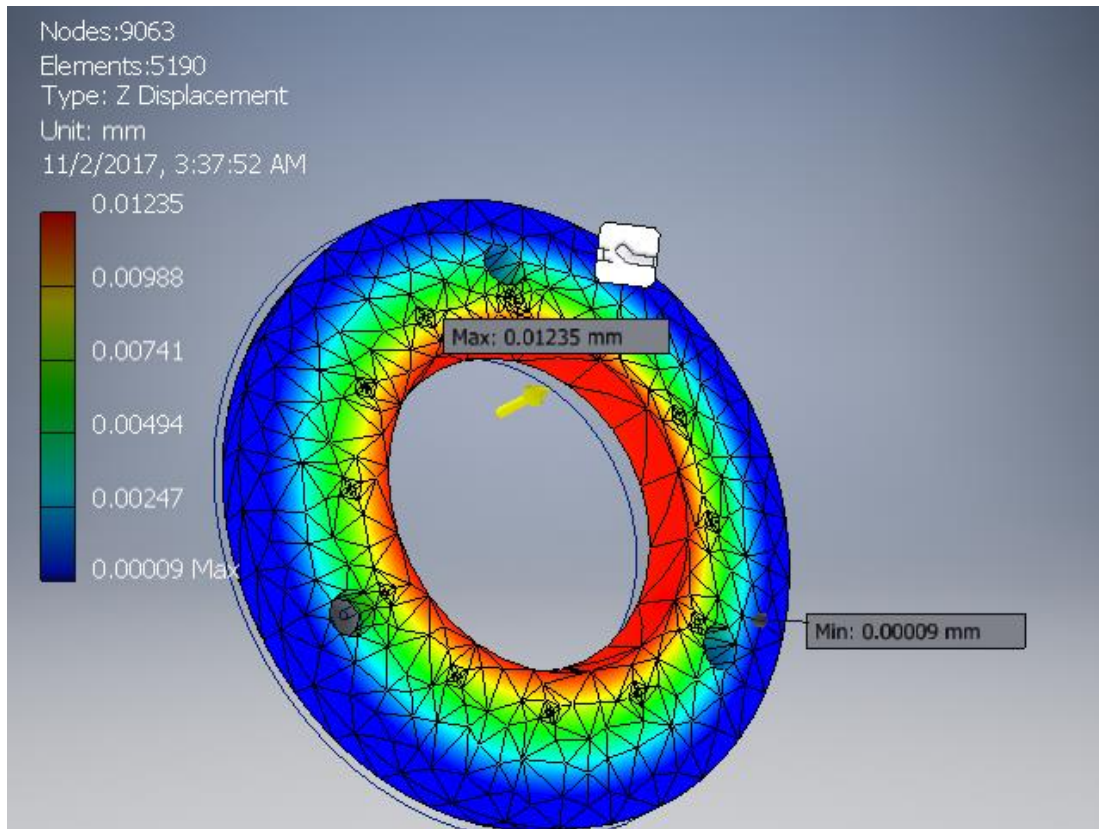
The thrust plate was modeled in Autodesk inventor for the same size as the one predicted with a 13.97cm (5.5'') aft diameter. It is made out of 6061 Aluminum and had a force of 1800N (404.656 lbf) applied directly to the face that simulates the max thrust of the motor. This simulation is intended to verify the robustness of the motor retention system. Maximum Von Mises stress was found to be 15.64MPa (2.268ksi) and the tensile strength (yield) is 270MPa (39.160ksi). The total displacement in the z direction (along the rocket body) is $.01235\text{mm}$ (0.000486''), which is not large enough to worry about component failure. After stress analysis we can deduce that the thrust plate will not be at risk to fail.



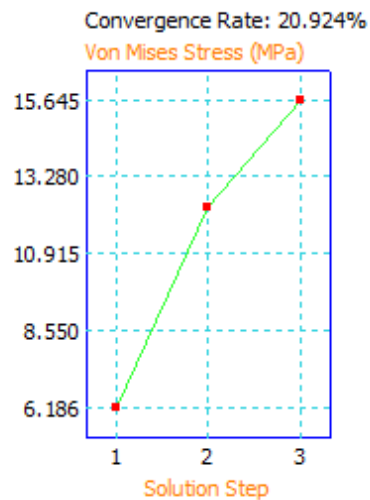
Material Properties of 6061 Aluminum



Max stress is 15.64MPa (2.268")



Displacement in the z direction is .01235mm (0.000486")



Plot shows convergence

4.2.3.4 Bulkheads

The bulkheads will be made out of 0.635cm (1/4") thick plywood that will be cut into concentric circles and laminated together with crosshatched grains. The bulkheads that will be connected to the shock chords will have to be very robust and therefore we will use three circles to reach

1.905cm($\frac{3}{4}$ "). The material selection for the bulkheads is focused towards saving money and achieving maximum rigidity. G10 is an option for bulkheads, however they are more expensive and provide less surface area for mounting to the airframe. A CNC router will be used to cut the bulkheads to a perfect fit inside of the airframe.

4.2.4 Airframe

4.2.4.1 Material Considerations:

We considered a few options that are used regularly in model rocketry. Of these options are, carbon fiber, Blue Tube 2.0, and phenolic tubing.

- **Carbon Fiber:**

Carbon fiber is defined as “a strong, stiff, thin fiber of nearly pure carbon, made by subjecting various organic raw materials to high temperature, combined with synthetic resins to produce a strong, lightweight material used in construction of aircraft and spacecraft” (dictionary.com). It is a very lightweight material and it ends up being a very strong material relative to its weight. Out of our options this is the strongest and lightest material.

Safety concern and consideration:

Carbon fiber if handled with the improper equipment can be extremely dangerous. Carbon fiber inhalation should be taken seriously and anyone handling carbon fiber should reference the MSDS over carbon fiber before use.

- **Blue Tube 2.0**

Blue Tube 2.0 is vulcanized cellulose fiber. It is tolerant to high temperatures, and not prone to shattering or cracking when encountered with high forces at impact. Below is data from testing done on Blue Tube. The density of the Blue Tube 2.0 is $1.502 \frac{g}{cm^3}$. The density was taken from the given weights and measurements of the Blue Tube 2.0.

3/12/2009

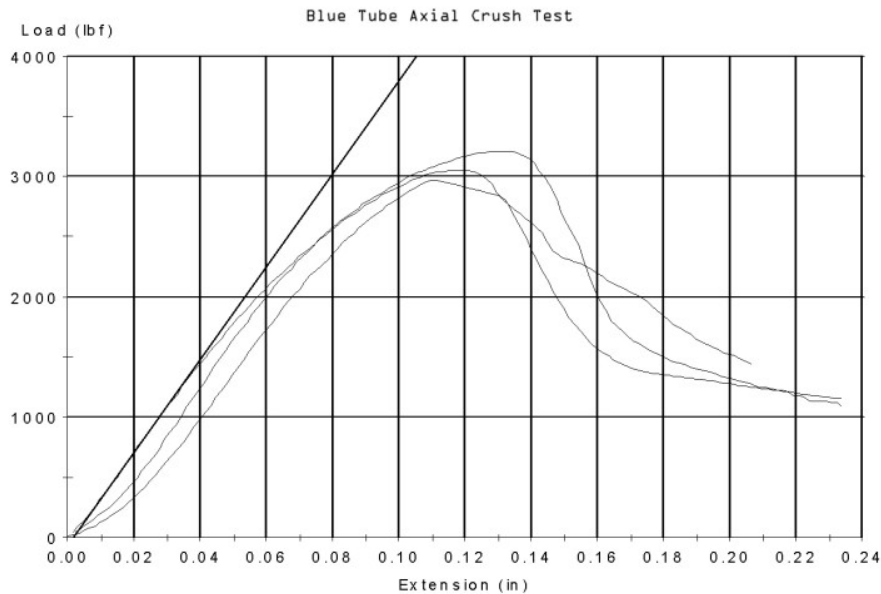
Sample ID: BlueTube.mss
 Method: Tube Compression (Simple Servo).msm

Test Date: 3/11/2009
 Operator: MTS

Sample Results:**Specimen Results:**

Specimen #	Specimen Comment	Inner Diameter in	Outer Diameter in	Platen Separation in	Area in ²	Modulus ksi	Load At Yield lbf
1		3.002	3.128	9.00000	0.60662	559.60219	2974.13082
2		3.002	3.128	9.00000	0.60662	607.10291	3211.11207
3		3.002	3.128	9.00000	0.60662	574.09091	3052.63859
Mean		3.002	3.128	9.00000	0.60662	580.26534	3079.29383
Std. Dev.		0.000	0.000	0.00000	0.00000	24.34486	120.71828

Specimen #	Stress At Yield MPa	Peak Load lbf	Peak Stress psi	Energy To Peak ft*lbf	Break Load lbf	Elongation at Peak in
1	33.80322	2974.13082	4902.72798	14.11096	1504.89966	0.11156
2	36.49669	3211.11207	5293.38147	20.93077	1607.34466	0.13095
3	34.69552	3052.63859	5032.14469	18.27847	1534.46427	0.11815
Mean	34.99848	3079.29383	5076.08472	17.77340	1548.90286	0.12022
Std. Dev.	1.37205	120.71828	198.99895	3.43785	52.72665	0.00986



- **Phenolic tubing**

This is a type of tubing that is used in model rocketry. People experienced with using phenolic material will generally coat the tubes with a layer of fiberglass to try to prevent cracking or shattering and to strengthen the tube.

Our material decision and reasoning:

We are favoring Blue Tube 2.0. Some people inside of our team have experience with Blue Tube 2.0 and know its versatility of strength, price, and ease of use. We came to the decision as a team that we were not going to pursue the carbon fiber tubing route due to its price if it comes pre-made. We agreed that we do not have enough time in the middle of a project to perfect the

process of making precise and accurate carbon fiber tubing. We agreed that because of the complexity of the production process of carbon fiber and the strict schedule we have to adhere to, we marked it as a not viable option for this project. In regards to phenolic tubing, phenolic tubing is less shatter proof and more prone to cracking than our choice of Blue Tube 2.0. Even though it is lighter than Blue Tube 2.0, the strength and flexibility of Blue Tube 2.0 is a good trade for the weight difference than what would be offered with phenolic. The members in our project who have worked with Blue Tube 2.0 before have no doubts about its ability to be able to complete the objective.

4.2.4.2 Things to keep in mind:

During the construction process of the airframe there are known risks when altering the airframes. Most of the risks stem from the use of power tools. All necessary safety precautions listed in section IV that are relevant to the situation should be followed and kept in mind when operating equipment to alter the airframe. Necessary precautions should be taken before attempting to alter the airframe to make accurate measurements and changes. If there is a change that needs to be made to the length of the body tube, the measurements should be made, marked onto the tube, the measurements should be remade to check to make sure the original measurement was correct.

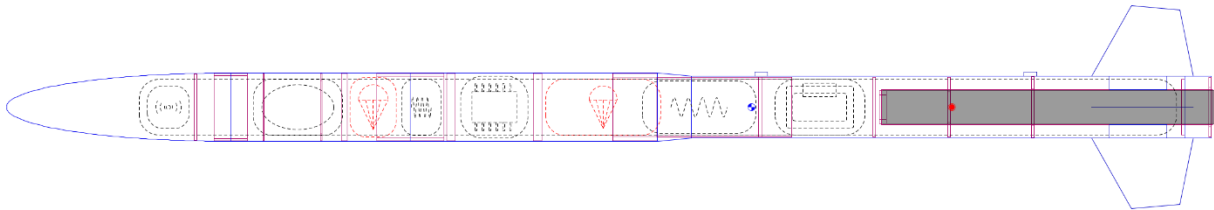
4.2.4.3 The design and shape of the rocket:

For the design of the rocket, we majorly considered two options, the DETS design and an updated version of our proposal design named the "Straight 6" due to its six inch diameter and its straight profile relative to the DETS design. To help with our decision-making process, we used decision matrices where each cell contained a number one through five. In our decision matrix, the number, one, will be what we consider the worst for that process and the number, five, will be what we consider the best for the specific process. The total numbers for each design are then added together and the sum is something we took into account for our design favorability as well as material favorability. The decision matrix is a method of how we weighed the pros and cons of each design.

4.2.4.4 The DETS Design:

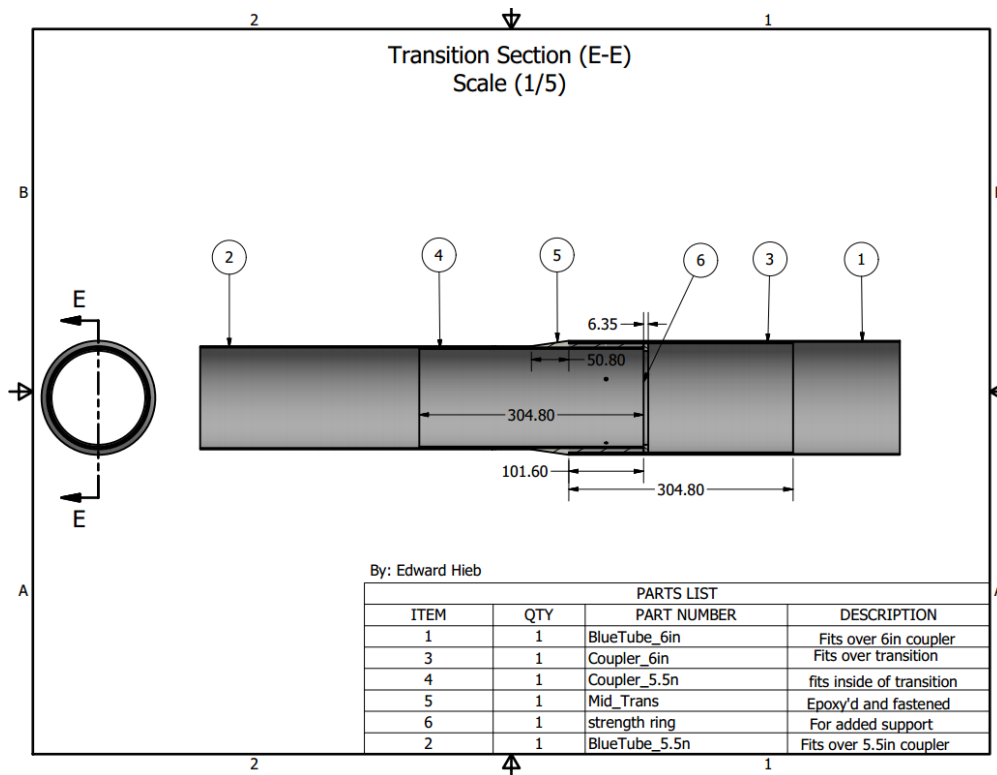
DETS is an acronym for "Drag Elimination by Teardrop Shape". The DETS design is a design being considered that would have an overall lower drag coefficient than the design in our proposal. Our goal with this design was to eliminate unnecessary drag that would take us further from our goal and be able to optimize our altitude and bring the rocket as close to a mile as possible. The vehicle team drew inspiration for this design from the fact that in subsonic speeds a teardrop shape has a very low drag coefficient. We attempted to model this tear drop shape by having a transition piece that connects the front section 15.4 cm (6" Blue Tube 2.0), to the rear section of the rocket 14.02 cm (5.5" Blue Tube 2.0). Our plan for this design was to maximize our accuracy to a mile with the theoretical low drag approach and also by implementing a system that will increase in surface area when it predicts that the rocket will be going over the one-mile mark. This system responsible for this increase in drag is the DACS. The intricacies of this system are referenced in this section . The DETS body The shape is shown below. The

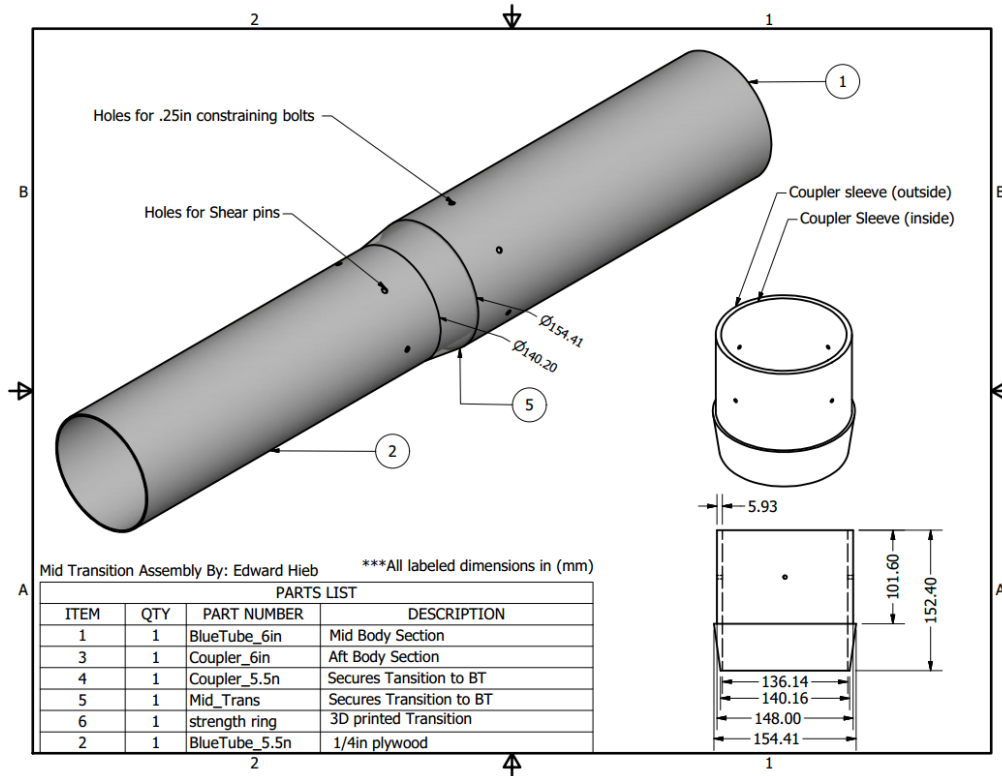
theoretical pros of this design is its lower drag coefficient and higher stability. The cons of this design is the complexity of the building process.



4.2.4.5 In-depth DETS transition piece design:

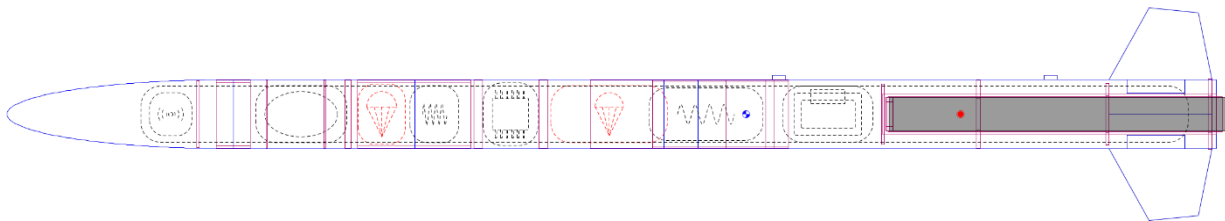
This transition piece would have precisely dimensioned diameters that allow for perfect fitting to concentric couplers. The couplers are necessary to attach the body sections as opposed to using flanges that protrude 5.08cm (2") from the 3D printed transition piece alone. Mounting hardware such as nuts, and bolts will be necessary along with epoxy to attach the components in a way that ensures no accidental separation occurs. This assembly would also use a 6.35mm ($\frac{1}{4}$ ") thick plywood strengthening ring attached to inside of the 15.24cm (6") coupler and against the transition piece.





4.2.4.6 Straight 6”:

The Straight 6” is the design that we used in our proposal with updated Blue Tube 2.0 dimensions accurate to what is available for Blue Tube 2.0. This design has accurate weights and like in the DETS design, it has the DACS system implemented as well. This design consists of a 15.4 cm outer diameter body tube (Blue Tube 2.0) that stretches the length of the rocket instead of having a transition and a section of the rocket that has a smaller diameter body tube like in our DETS design. The internal weights of the Straight 6” design is modeled. The Straight 6” body shape is shown below. The pros of this design is the simplicity of the building process. The cons of this design is its drag coefficient.



4.2.4.7 Our decision and reasoning:

We as a team favor the Straight 6” because the drag coefficients between the DETS design and the Straight 6” are not significant enough to account for the more complex DETS rocket build (see drag coefficient tables below). The DETS design has a drag coefficient of 0.44 and the Straight 6” has a drag coefficient of 0.47. The drag difference between the two designs is almost negligible (0.03 drag coefficient difference). The DETS design will not have enough of a noticeable impact on our drag to account for the more complex building process which could statistically leave more room for error in the building process. In conclusion, because of the higher complexity of the build of the DETS and the negligible difference in drag coefficients between both designs (listed below is the decision matrix for the design), we are going to be favoring the Straight 6”. Our decision matrix is below. For information on how we structured our decision matrices, please reference the “Introduction” of this design of the airframe section.

Decision Matrix for Body Shape

	Drag(x2)	Complexity	Price	Rail Button Location	Total
DETS Design	3	4	2	3	15
Straight 6”	3	2	3	1	12

Drag Coefficient of DETS Design

Stability	Drag characteristics	Roll dynamics			
Component	Pressure C _D	Base C _D	Friction C _D	Total C _D	
Nose cone	0.02 (5%)	0.00 (0%)	0.04 (9%)	0.06 (14%)	
Body tube	0.00 (0%)	0.00 (0%)	0.04 (9%)	0.04 (9%)	
Body tube	0.00 (0%)	0.00 (0%)	0.05 (12%)	0.05 (12%)	
Transition	0.00 (0%)	0.00 (0%)	0.01 (2%)	0.01 (2%)	
Body tube	0.00 (0%)	0.00 (0%)	0.10 (22%)	0.10 (22%)	
Freeform fin set	0.02 (4%)	0.00 (0%)	0.04 (10%)	0.06 (14%)	
Launch lug	0.00 (1%)	0.00 (0%)	0.00 (0%)	0.00 (1%)	
Launch lug	0.00 (1%)	0.00 (0%)	0.00 (0%)	0.00 (1%)	
Tail Cone	0.00 (0%)	0.11 (24%)	0.01 (1%)	0.11 (26%)	
Total	0.05 (10%)	0.11 (24%)	0.29 (65%)	0.44 (100%)	

Drag Coefficients of Straight 6”

Component	Pressure C _D	Base C _D	Friction C _D	Total C _D	
Nose cone	0.02 (4%)	0.00 (0%)	0.04 (8%)	0.06 (13%)	
Body tube	0.00 (0%)	0.00 (0%)	0.04 (8%)	0.04 (8%)	
Body tube	0.00 (0%)	0.00 (0%)	0.05 (11%)	0.05 (11%)	
Transition	0.00 (0%)	0.00 (0%)	0.01 (2%)	0.01 (2%)	
Body tube	0.00 (0%)	0.13 (28%)	0.11 (24%)	0.24 (51%)	
Freeform fin set	0.02 (4%)	0.00 (0%)	0.04 (9%)	0.06 (13%)	
Launch lug	0.00 (1%)	0.00 (0%)	0.00 (0%)	0.00 (1%)	
Launch lug	0.00 (1%)	0.00 (0%)	0.00 (0%)	0.00 (1%)	
Total	0.05 (10%)	0.13 (28%)	0.30 (63%)	0.47 (100%)	

(Data collected from open rocket component analysis)

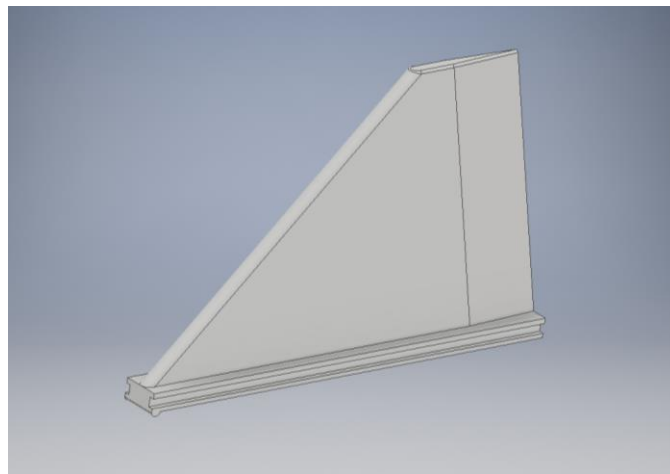
4.2.5 Fins:

We considered several different materials for the fins. Among the materials considered we are considering G10 fiberglass, plywood and a range of 3D printable filament. Each material has a different set of pros and cons and selection and is analyzed in the section below.

4.2.5.1 3D printed fin can:

During the brainstorming process, we came up with a 3D printed modular fin can concept. This is our most innovative option due to the flexibility of design and application of new 3D printing technology. The fin can would be seated directly on the external face of the airframe and have 4 receiver grooves that allow for individual fin integration. Epoxy and possibly hardware would be used to attach this system to the airframe. The fin can will also create a factor of customizability that will not limit fin design to the first launch when traditional fins are permanently mounted. Having disposable fins solves the problem of fin breakage upon landing and will be extremely beneficial during test flights while having a lower projected weight than the G10 alternative. The ideal fin shape is an airfoil design and that would be easily achievable due to our limitations being endless in 3D CAD design. Assuming ABS plastic is used and fins are designed to be disposable, the concept would work if it does not violate the “reusability” factor that is a requirement of the launch vehicle. The cost of producing these fins out of common filament is staggering low at \$0 due to access to the TTU Mechanical Engineering machine shop. The shop has a selection of filament that can be chosen to match desired material properties. In the event that any breakage and disposable fin is not allowed, research has gone into continuous filament printing which would allow for printing in composites such as fiberglass and carbon fiber and thus create a high strength fin that could withstand high impact forces that are applied at landing. We plan on reaching out to companies that specialize in advanced continuous filament printing to request samples that would be tested as fins. Ideally the company would be extremely interested and provide a sponsorship by supplying high strength 3D printed fins for research purposes.

(See appendix for ABS and Composite filament data)



4.2.5.2 G10

G10 fiberglass is a type of fiberglass that is extremely heat resistant and has a very tensile strength. Matweb.com describes it as a “glass-epoxy specified for its extremely high strength and high dimensional stability over temperature” (matweb.com) The pros for G10 fiberglass is its strength, flexibility and its heat resistance. The cons for G10 is that has a relatively high density of $1.85 \frac{g}{cm^3}$ and it is more expensive than the other considerations.

Mechanical Properties	Metric	English
Hardness, Rockwell M	110	110
Tensile Strength at Break	262 MPa	38000 psi
	310 MPa	45000 psi
Flexural Strength	448 MPa	65000 psi
	517 MPa	75000 psi
Flexural Modulus	16.5 GPa	2400 ksi
	18.6 GPa	2700 ksi
Compressive Strength	448 MPa	65000 psi
Izod Impact, Notched	6.41 J/cm	12.0 ft-lb/in
	7.47 J/cm	14.0 ft-lb/in

[This information from matweb.com shows the tensile strength and flexural strength of G10 fiberglass.](#)

Safety concern with G10: Fiberglass inhalation is a very serious concern and should not be taken lightly. Long term exposure can lead to lung disease and short-term exposure can lead to irritation of the throat, nose, eyes, and lungs. Reference the material safety data sheet over G10 for more information

4.2.5.3 Plywood:

Plywood is defined as “a structural material consisting of sheets of wood glued or cemented together with the grains of adjacent layers arranged at right angles” (merriam-webster.com). The utilization of alternating the wood grains will work to strengthen the material. The mechanical properties for plywood are shown in the image below from matweb.com. Pros for plywood is that it is lightweight and is relatively strong for its weight. The con is that it is not as strong as G10 fiberglass.

Mechanical Properties	Metric	English
Tensile Strength	27.6 - 34.5 MPa	4000 - 5000 psi
Modulus of Rupture	0.0483 - 0.0689 GPa	7.00 - 10.0 ksi
Flexural Modulus	8.20 - 10.3 GPa	1190 - 1490 ksi
Compressive Strength	31.0 - 41.4 MPa	4500 - 6000 psi
Shear Modulus	0.138 - 0.207 GPa	20.0 - 30.0 ksi
	0.586 - 0.758 GPa	85.0 - 110 ksi
Shear Strength	1.72 - 2.07 MPa	250 - 300 psi
	5.52 - 6.89 MPa	800 - 1000 psi

4.2.5.4 Our decision:

We as a team came to the conclusion that G10 fiberglass would be what we are going to be favoring. Some people in the team have experience handling and are familiar with G10 fiberglass. The reason for this decision is its extremely high tensile strength and the knowledge that it is more than capable of doing what it needs to do. We can order the G10 fiberglass in a 0.635 cm (1/4 inch) wide sheet and sand down the width until we reach our desired width while following required safety guidelines.

4.2.5.5 Things to consider:

During the construction process of the fins there are known risks when altering the fin design. Most of the risks stem from the use of power tools and materials used. All necessary safety precautions listed in section IV that are relevant to the situation should be followed and kept in mind when operating equipment to manufacture the fins. Necessary precautions should be taken before manufacturing the fins. Measurements should be made multiple times before any changes are made to manufacture the fins.

4.2.6 Nose Cone

The shape of the nose cone is one of the many determining factors for calculating the drag of the rocket. Because of this, choosing a nose cone shape with the least amount of drag is crucial for designing the rocket. According to Figure One, a round shaped nose is the best option. When looking at the graph in Figure Two which compared drift to mach, a parabolic shape is best choice for sub-mach conditions while ogive ranked 4 overall. An experiment published on Apogee Rockets compared the drag of different shapes of nose cones and found that long elliptical shaped nose cone has the least amount of drag with parabolic being ranked second (Milligan). From these experiments and graphs from our research, we have determined that long elliptical shape is the ideal shape for the nose cone.

The shape of the nose cone is quite limited when it comes to purchasing a premade one due to having a 15.240cm (6") diameter body. There are three options we have found which include a 3D printed nose cone. A 15.240cm (6") diameter fiberglass ogive from Apogee Rockets, and a 15.240cm (6") diameter fiberglass Ogive from Public Missiles. With 3D printing a nose cone, our team has the benefit of freedom of design. With this, the nose cone will be a long elliptical shape which is the best aerodynamic compared to other nose cone shapes. The material would be ABS plastic with a 50.8cm (20") exposed length with a shoulder length of 13.97cm (5.5"). The second option is a nose cone from Apogee Rockets. This nose cone has an exposed length of 76.2cm (30") with 13.97cm (5.5") shoulder length. With this option the benefit is the strength of fiberglass. The third option of the nose cone from Public Missiles is a nosecone identical to the nose cone from Apogee Rockets with exception of the exposed length of 60.960cm (24"). The negative side to both the nose cone from Apogee Rockets and Public Missiles are that the cost is about one hundred and five dollars and the shape being ogive which has a higher drag coefficient based off the research. Although there were other nose cone options with fiberglass material and different shape, the price was higher and little to no information about dimensions was provided which made us steer away from those

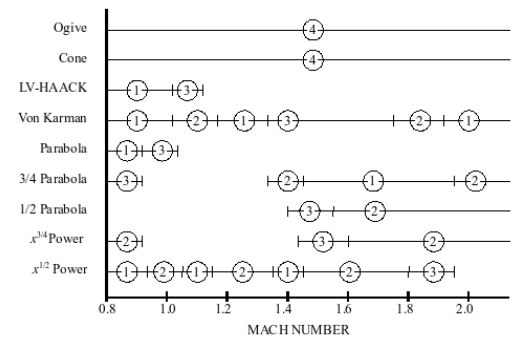
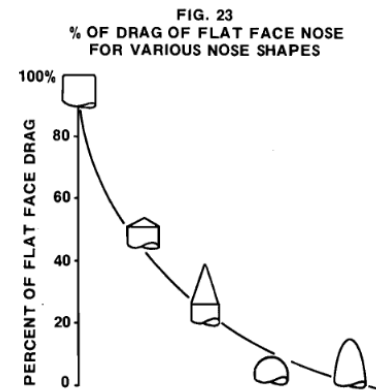


Figure Two: Rating of Nose Cone Shapes in Different Mach Numbers (1 = superior, 2 = good, 3 = fair, 4 = inferior) (Nose Cone Design)

options. From these three options, we decided 3D printing the nose cone is the best option because of cost, shape, and ease of access. With the cost being free and having the printers available to us, this helps with budget and ease of access. Another advantage for the nose cone being 3D printed is that it allows us to make changes to the design before printing in case we need to change length. The downside to 3D printing a large nose cone is we have to design it in sections which makes the design have some complexity. Overall by being able to choose the long elliptical shape, we will have a lower drag coefficient compared to ogive shape.

The equation for making a long elliptical nose cone is

$$V = \frac{\pi d^2 h}{6}$$

and

$$y = R \sqrt{1 - \frac{x^2}{L^2}}$$

where r equals the radius, x is, and L is the exposed length of the nose cone with exception of shoulder.

4.2.7 Bulkheads

The bulkheads will be made out of 0.635cm ($\frac{1}{4}$ ") thick plywood that will be cut into concentric circles and laminated together with crosshatched grains. The bulkheads that will be connected to the shock chords will have to be very robust and therefore we will use three circles to reach 1.905cm ($\frac{3}{4}$ "). The material selection for the bulkheads is focused towards saving money and achieving maximum rigidity. G10 is an option for bulkheads, however they are more expensive and provide less surface area for mounting to the airframe. A CNC router will be used to cut the bulkheads to a perfect fit inside of the airframe.

4.2.8 Rail Buttons

Rail buttons will be changed from the original design if using a transition body piece on the airframe. This is because the staggering of the body from 15.24cm (6") to 13.97cm (5.5") makes a 0.635cm ($\frac{1}{4}$ ") standoff from the section of the aft section of the body where the rail buttons are located, and thus the rail buttons must be offset to correct the difference of diameter.



(Rail buttons)

4.2.9 Scale Model Overview

In the handbook one of the requirements is that we build and launch a small-scale rocket with accurately scaled weights and measurements. This is to attempt to simulate how the full-scale launch will react when launched.

4.2.9.1 Method

We plan on scaling down the measurements by a third and have exact geometric similarity to our full-scale design. For example, if we used a six-inch diameter blue tube then go to a 2-inch diameter blue tube. We would scale the weights in their appropriate section to end up with the same stability as the full-scale rocket. We will select a motor based on the thrust to weight ratio of the scaled rocket to achieve as close to the simulated full-scale results. For more information on the motor selection **REFER TO ENGINE SELECTION AREA**

Due to the planned complexity of implementing the DACS in a two-inch diameter tube, we will not be implementing the DACS in our sub-scale launch. Although we are not implementing the DACS in the sub-scale launch, we plan to be wind tunnel testing the full-scale DACS during the time we are building the sub-scale design. The members who plan on wind tunnel testing the DACS are required to undergo safety training before using the wind tunnel.

Vehicle Parts List DETS

Vehicle Parts						
Part Name	Amount	Cost (ind.)	Weight Total (g)	Material	Part Total	
Nose Cone	1	0	1443	ABS Plastic	0	
					0	
Airframe					0	
Coupler (6in)	1	20	334.98	Blue tube	20	
Coupler (5.5in)	1	20	301	Blue tube	20	
6in Frame	1	67	806	Blue tube	67	
Bulkhead (3/4in)	1	10	840	Plywood	10	
Bulkhead (1/4in)	1	5	70	Plywood	5	
5.5in Frame	1	56	1164	Blue tube	56	
Fins	2	54	1146	G10	108	
Transition	1	0	50	ABS Plastic		
RocketPoxy (2 quarts)	1	60	453	Epoxy	20	
					0	
Motor Assembly					0	
Thrust Plate	1	60	254	Aluminum	60	
Hardware set	1	310	2268	Aluminum	310	
Centering Rings	1	10	128	Plywood (1/4in)	10	
Fuel Grain	2	600	5115	Amonium Perchloarate	1200	
					1886	

4.3 Recovery Subsystem

4.3.1 Electronics Bay

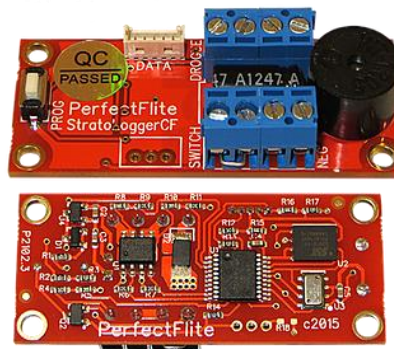
Altimeters: Altimeter choices were based on price, dual deployment, and size. The three choices we decided on are the FeatherWeight Raven3, Missile Works RRC3 Xtreme, and the PerfectFlite StratologgerCF. All require a 9v battery and a USB to retrieve data. The main altimeter and backup we will be using is the StratologgerCF, the backup will also be the one used for NASA.

FeatherWeight Raven3: This altimeter is a dual deployment altimeter that measures altitude, velocity, and acceleration. Also tests all sensors and outputs to verify that all wiring is working. It has a $\pm 0.3\%$ accuracy. The flight data that is stored can be accessed on a computer through a USB-mini cable. A reason for not choosing this altimeter is that it was too expensive and the accuracy wasn't as good as the StratologgerCF

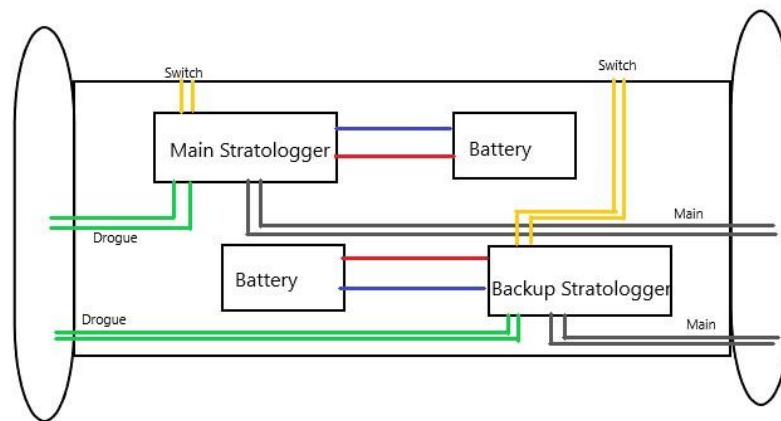
Missile Works RRC3 Xtreme: A dual deployment altimeter that measures altitude, velocity, and other events. It is programmable, meaning you can change the default settings. The flight data recorded can be obtained by a USB-IO. We did not choose this altimeter because it was the largest out of all three and we wanted a small one due to weight and compatibility in the avionics bay.

PerfectFlite StratologgerCF: The StratologgerCF is a dual deployment altimeter that records altitude, velocity and other events. On startup the StratologgerCF will test if all wiring is connected. It has a calibration accuracy of $\pm 0.05\%$ and a measurement precision of $\pm 0.1\%$ + 30.48cm (1ft). The reason we chose the StratologgerCF is that it is the cheapest option but also will get the job done. A con of getting it is that we have to purchase a USB kit in order to get the data.

Proposed Items List					
Distributor	Model	Unit Dimensions	Unit Cost	Qty.	Total Cost
FeatherWeight	Raven3	1.75" (44.45mm)L x 0.80" (20.32mm)W x 0.23oz (6.6g)	\$155.00	2	\$310.00
Missile Works	RRC3 Xtreme	3.92" (99.5mm)L x 0.925" (23.5mm)W x 0.60oz (17g)	\$79.95	2	\$159.90
PerfectFlite	StratologgerCF	2.0" (0.05m)L x 0.84" (0.02m)W x 0.38oz (10.77g)	\$54.95	2	\$109.90



Both altimeters will be mounted on 6.35mm ($\frac{1}{4}\text{in}$) plywood between two bulkheads. Another option for the sled was 3D printing it. If we 3D printed it, it would be lighter and cheaper but, we chose plywood since it is sturdier and can be easily drilled into. Also since we will be using plywood for other parts of the rocket, it is simpler to take from that. There will be two 9v Duracell batteries on the sled with the altimeters. Both altimeters will be programmed to deploy the drogue and main parachute, the second StratologgerCF is a backup of the first. The sled will be glued to the drogue bulkhead with two threaded rods holding it in place. We also considered having one threaded rod but chose two because it had more stability than one.



Predictions: We believe that all wiring will be connected correctly and both batteries will not fail. Also the main altimeter will collect data properly without being disturbed and will deploy the drogue parachute at apogee and the main parachute at 750ft. If this does not happen then, the backup altimeter will work properly and do what the main should have. Ejections will occur on time and correctly.

Risks: Wiring could fail either with the batteries or altimeters. If the wiring to the ejection charges fails this could cause a premature explosion or no explosion at all causing the rocket to become projectile. If wiring failed with batteries they could catch on fire. Also if the altimeters detect a false apogee this would cause the drogue to deploy earlier than programmed. Another risk would be when arming the altimeters, the ejection charges could go off once arming it.

Precautions: Make sure all wiring is connected properly before arming altimeters to ejection charges. Test to make sure switches work correctly. Be careful when arming altimeters when they are attached to ejection charges.

4.3.2 Parachute Selection

Parachutes can either be made or bought. Buying materials to hand-make a parachute is a much less expensive option. Though it is cheaper, making the parachute requires a lot of time and tedious work to complete with a higher potential for error outside of size calculations. A commercially bought parachute best fits our need for the recovery system. Buying a parachute presents several options in terms of the shapes and designs available. Two design options are chosen to focus on spill-hole and standard elliptical parachutes. Spill-hole parachutes, although more expensive, provide an advantage in reducing drift and rocking upon the vehicle descending. Standard elliptical parachutes provide the basic principles of reducing the rate of descent upon decent but increase the drift significantly after deployment of the main parachute. The cost-to-benefit comparison of both options determines the standard elliptical parachute to be the leading option in our recovery system. Parachute options with their respective vendors are listed below.

Main Parachute Options and Vendors		
Distributor	Model (Diameter)	Price
Rocketman Enterprises	Standard Low-Porosity Ripstop 1.1 (16')	\$ 170.00
Rocketman Enterprises	Low-Porosity Ripstop 1.9 (16')	\$ 225.00

Drogue Parachute Options and Vendors		
Distributor	Model	Price
Rocketman Enterprises	Standard Low-Porosity Ripstop (2')	\$ 25.00
Topflight	PAR-24 TFR Standard Type (24")	\$ 10.95
Apogee Rockets	Nylon Parachute (24")	\$ 9.79

We are leaning towards the cheaper of the two options for the main parachute due to the decrease in cost overall and the reduction in weight in comparison to the 1.9 Ripstop option. For the drogue shoot we are leaning towards the Rocketman parachute mostly due to the high reliability of their chutes while the increase in cost is a burden we will have to bear for an added factor of safety.

4.3.2.1 Parachute Sizing Calculations

Assuming the total weight of the vehicle at landing to be 47.1 pounds, calculations will be made to determine descent velocity required for the vehicle to land with a kinetic energy of less than 75-foot pound force. The following calculations assume constant velocity and strict motion occurring vertically downward. The rate of descent is determined as follows:

$$\begin{aligned}
 v &= \text{descent rate} \\
 \text{Total Weight} &= 47.1 \text{ lbs} \\
 g &= 32.2 \text{ ft/s}^2 \\
 KE &= \frac{1}{2}mv^2 < 75 \text{ ft} \cdot \text{lb}f
 \end{aligned}$$

Solving for v provides the following relation:

$$v < \sqrt{\frac{2 * g * KE}{W}}$$

Then solving for descent rate gives:

$$v < \sqrt{\frac{2 * 32.2 \text{ ft/s}^2 * 75 \text{ ft} \cdot \text{ lbf}}{47.1 \text{ lbs}}} < 10.127 \text{ ft/s}$$

Given the calculations above, the landing descent rate must be lower than 10.127 feet per second to land with a kinetic energy of less than 75-foot pound force as specified by guidelines.

Understanding the required descent rate allows for a minimum parachute diameter to be solved for. Using 10.127 feet per second as the descent rate, calculations are as follows:

$$\begin{aligned} \sum \text{Forces}_y &= D - W = ma = 0 \\ \rho &= \text{density of air} = 0.075 \text{ lb/ft}^3 \\ S &= \text{surface area of the main parachute} \\ C_d &= \text{coefficient of drag} = 2 \\ W = D &= \frac{1}{2} \rho v^2 S C_d \end{aligned}$$

Solving for surface area provides the following relation:

$$S = \frac{2W}{\rho v^2 C_d} = \frac{2 * 47.1 \text{ lbs}}{0.075 \frac{\text{lb}}{\text{ft}^3} * \left(10.127 \frac{\text{ft}}{\text{s}}\right)^2 * 2} * \frac{32.2 \text{ lb}}{1 \frac{\text{lbf s}^2}{\text{ft}}} = 190.460 \text{ ft}^2$$

Based on the above surface area, you can determine the minimum diameter of the main parachute by the area of a circle.

$$\begin{aligned} d &= \text{minimum diameter of the main parachute} \\ A &= \text{area of circle} = \frac{\pi}{4} d^2 \\ d &= \sqrt{\frac{4 * S}{\pi}} = \sqrt{\frac{4 * 183.979 \text{ ft}^2}{\pi}} = 15.572 \text{ ft} \end{aligned}$$

Given the above results, the minimum diameter required for the main parachute to land with a kinetic energy of less than 75-foot pound force is rounded up to a 16-foot diameter. The diameter is rounded up to account for the commercial availability of parachute sizes. Now the exact

descent rate at landing can be solved for accounting for a parachute diameter of 16 feet. The calculations for the total surface area are as follows:

$$A = S = \frac{\pi}{4} d^2 = \frac{\pi}{4} * (16ft)^2 = 201.062 ft^2$$

Now, using prior equations, the new descent rate at landing is solved for using the below relation:

$$v = \sqrt{\frac{2W}{\rho C_d S}} = \sqrt{\frac{2 * 47.1 lbs * 32.2 ft/s^2}{0.075 \frac{lb}{ft^3} * 2 * 201.062 ft^2}} = 10.029 ft/s$$

Therefore, the maximum descent rate at landing is now 10.029 feet per second given a 16-foot main parachute diameter. This descent rate takes into account the maximum kinetic energy allowed at landing. With the method outlined above, we are assuming a worst case scenario where the total weight of the rocket is used to calculate the minimum descent rate based on kinetic energy.

Predictions: The chosen parachute will deploy and open at the correct time. Also, the descent rate will be lower than 10.127 feet per second which will allow for a kinetic energy less than 75 foot-pounds.

Risks: The descent rate could change based on unplanned conditions which could cause a higher kinetic energy upon landing. If the parachute were to not open properly this would also cause the decent rate to be more thus causing a higher kinetic energy at landing.

Precautions: We will make sure to have all calculations correct in order to have the descent rate and kinetic energy be in a safe range. We will also fold and pack the parachute in a way that it can open correctly.

4.3.2.2 Kinetic Energy

The heaviest section of the rocket will be maxed out at 27.13 lbs which will reduce the total kinetic energy at impact. With this being said our simulations predict that our final descent will be faster than the values calculated above. The main reason for the calculation above was to predict the size of our parachute in order to comply with the kinetic energy limitation set by NASA. The following table outlines the kinetic energy of each independent section:

Kinetic Energy			
Drogue Deployment	Section 1	Section 2	
Mass (g)	5153.000	13151.000	
Mass (lbs)	11.360	28.993	
Velocity (m/s)	37.785	37.785	
Velocity (ft/s)	123.967	123.967	
Kinetic Energy (J)	3678.485	9387.882	
Kinetic Energy (ft * lbs)	2713.111	6924.145	
Main Deployment	Section 1	Section 2	Section 3
Mass (g)	5081.200	2122.000	9752.000
Mass (lbs)	11.202	4.678	21.499
Velocity (m/s)	4.443	4.443	4.443
Velocity (ft/s)	14.577	14.577	14.577
Kinetic Energy (J)	50.152	20.944	96.253
Kinetic Energy (ft * lbs)	36.990	15.448	70.993

To elaborate on the breakdown of the table above after drogue deployment we will have two sections connected by a shock cord. Section one will be made up of the payload bay, nosecone, transmitter/receiver, and rover ejection charges. Section two will consist of the motor casing, electronics bay, main parachute, D.A.C.S, and ejection charges.

After deployment of the main parachute our rocket will be split into three sections all connected by a single shock cord. Section one will not be changed and remain the same as stated previously. Section two will be between the payload section and the section containing the motor housing; this section will contain the electronics bay. Section three will be the same as stated above minus the main parachute and electronics bay.

4.3.2.3 Parachute Protection

Two options are present for parachute protection: deployment bags or fireproof cloth. Deployment bags provide an easy storage inside the vehicle that is made of 2,000-degree flameproof NOMEX fabric provided the bag is bought from Rocketman Enterprises. Other options include fireproof cloth sheets that would be hand-packed into the airframe to serve as an insulated barrier between the parachute and any charges. Although the option is less expensive, slip may occur exposing parts of the parachute if not packed correctly. Parachute deployment bags are to be used to avoid any safety hazards that may occur mid-flight or at deployment.

Parachute Protection Options (Main Parachute)		
Distributor	Model	Price
Rocketman Enterprises	16ft. Deployment Bag	\$ 65.00
Apogee Rockets	Sunward 18in Nomex Protector	\$ 10.49
Top Flight Recovery	Chute Protector FCP-18x18"	\$ 10.95

Parachute Protection Options (Drogue Parachute)		
Distributor	Model	Price
Rocketman Enterprises	2ft. Deployment Bag	\$ 25.00
Apogee Rockets	Sunward 18in Nomex Protector	\$ 10.49
Top Flight Recovery	Chute Protector FCP-18x18"	\$ 10.95

The main and drogue parachutes are made of rip-stop nylon sewn together at contact points with shroud lines. Each parachute will have four shroud lines to reduce the probability of entanglement at any stage in the flight or deployment. Shroud lines will be held together by 660 pound tested quick links which are connected to swivels. Torsion will be heavily experienced while the vehicle descends, so 1000 pound tested swivels will be utilized to reduce this effect torsion may have on the airframe. Swivels will be connected between the quick links attached to the shroud lines and shock cord for both the main and drogue parachute.

Swivel and Quick Links		
Distributor	Model (Diameter)	Price
Topflight Recovery	SW- 1000 Swivel	\$ 6.00
Topflight Recovery	QL- 3/16" Quick Link	\$ 1.35
Apogee Rockets	1/4" Quick Link	\$ 3.94
Commonwealth Rocketry	SWLR8 900 lb Swivel	\$ 1.99
Commonwealth Rocketry	1/4" Stainless Steel Quick Link	\$ 2.90

Predictions: Parachute protection will fully protect both parachutes. Swivels and quick links will effectively hold together and not tangle the shroud lines.

Risks: The parachute could not open correctly if the parachute bag gets caught on it or if the shroud lines get tangled. The parachutes could disconnect if the swivels or quick links are not tied on properly.

Precautions: To avoid these risks we will attach the swivels and quick links correctly and test them in order to ensure they do not come apart. We will also pack the parachutes in such a way that they can fully open.

4.3.3 Drift

Now that the maximum descent rate is understood, the amount of drift that will be experienced will be determined. The following calculation takes into account the maximum descent rate and a horizontal wind velocity of 20 miles per hour, or 29.3333 feet per second.

$h = \text{change in altitude after deployment}$
 $v = \text{descent rate}$
 $W = \text{wind velocity acting horizontally}$

$$Drift = \frac{h}{v}(W)$$

$$Drift = \frac{500 \text{ ft}}{10.029 \frac{\text{ft}}{\text{s}}} * \left(29.333 \frac{\text{ft}}{\text{s}}\right) = 1462.409 \text{ ft}$$

The drift experienced between the main parachute, deployment, and landing is 1463 feet. This estimation allows for the drift experienced between apogee and the main parachute deployment to be 1037 feet in order to follow within the 2500-foot radius from the launch pad. From the drift calculations above, the descent rate from apogee to the main parachute deployment can be calculated. The following calculations solve for the descent rate from apogee to the main parachute deployment:

$$Drift = \frac{h}{v}(W)$$

Solving for the descent rate gives:

$$v = \frac{h * W}{Drift} = \frac{(5280 - 500) \text{ ft} * 29.333 \frac{\text{ft}}{\text{s}}}{1037 \text{ ft}} = 135.209 \frac{\text{ft}}{\text{s}}$$

The estimated descent rate shown above can now be utilized to determine a drogue parachute size that is appropriate to allow a 138.471 foot per second descent rate from apogee to the main parachute deployment. Taking into consideration the surface area relationships previously used, the minimum diameter of the drogue parachute is calculated as follows:

$$S = \frac{2W}{\rho v^2 C_d} = \frac{2 * 47.1 \text{ lbs} * 32.2 \frac{\text{ft}}{\text{s}^2}}{0.075 \frac{\text{lb}}{\text{ft}^3} * \left(138.471 \frac{\text{ft}}{\text{s}}\right)^2 * 2} = 1.055 \text{ ft}^2$$

$$A = S = \frac{\pi}{4} d^2$$

Solving for diameter gives:

$$d = \sqrt{\frac{4A}{\pi}} = \sqrt{\frac{4 * 1.055 \text{ ft}^2}{\pi}} = 1.159 \text{ ft}$$

From the above calculation, the minimum diameter for the drogue parachute given the previous calculations is 1.159 feet. A two-foot diameter parachute is selected to ultimately account for the kinetic energy at landing and the estimation of drift in order to land within the 2500-foot radius from the launch pad. The current frontrunners for the main and drogue parachutes are listed below:

Main Parachute Options and Vendors		
Distributor	Model (Diameter)	Price
Rocketman Enterprises	Standard Low-Porosity Ripstop (16')	\$170
Rocketman Enterprises	Standard Low-Porosity Ripstop (2')	\$25

All of the calculations were based off worst-case situations that are nearly impossible to encounter in the real world. The section on drift calculations more clearly outlines the impractical aspects of the calculations above.

4.3.3.1 Drift Calculations

With the equations outlined in the above section combined with the proposed parachute dimensions, we are able to calculate the drift of the rocket upon its descent. From this, we took into account the worst possible situations in terms of drift when looking to comply with the requirements listed by NASA. Our previous calculations were based on the terminal velocity of the rocket as it descends under the maximum listed wind speed. The table below works on refining our calculation by using the average velocity after deployment of the drogue parachute then deployment of the main parachute. With our parachute size calculations being so close to one foot in diameter we also ran drift simulations on a one-foot drogue to see how it affected the total drift of our rocket.

1 Foot Drogue Drift					
Drift Calculations, Minimum Decent Velocity					
Wind Speed (mph)	0.000	5.000	10.000	15.000	20.000
Wind Speed (ft/s)	0.000	7.333	14.667	22.000	29.333
Wind Speed (m/s)	0.000	1.524	3.048	4.572	6.096
Drift - Main (ft)	0.000	366.259	732.569	1098.828	1465.087
Drift - Drogue (ft)	0.000	139.193	278.404	417.597	556.789
Drift - Main (m)	0.000	111.636	223.287	334.923	446.559
Drift - Drogue (m)	0.000	42.426	84.858	127.283	169.709
Total Drift (ft)	0.000	505.452	1010.973	1516.425	2021.876
Total Drift (m)	0.000	154.062	308.144	462.206	616.268
Drift Calculations, Average Decent Velocity					
Wind Speed (mph)	0.000	5.000	10.000	15.000	20.000
Wind Speed (ft/s)	0.000	7.333	14.667	22.000	29.333
Wind Speed (m/s)	0.000	1.524	3.048	4.572	6.096
Drift - Main (ft)	0.000	66.096	132.200	198.296	264.391
Drift - Drogue (ft)	0.000	224.362	448.755	673.118	897.480
Drift - Main (m)	0.000	20.146	40.295	60.441	80.587
Drift - Drogue (m)	0.000	68.386	136.781	205.166	273.552
Total Drift (ft)	0.000	290.458	580.956	871.414	1161.871
Total Drift (m)	0.000	88.532	177.075	265.607	354.138

Velocities used for drift Calculations:

1ft Drogue Velocity	(ft/s)	(m/s)
Velocity after Drogue 1ft	239.705	73.062
Velocity Average	148.711	45.327
Velocity after Main	15.016	4.577
Velocity Average	83.209	25.362

2 Foot Drogue Drift					
Drift Calculations, Minimum Decent Velocity					
Wind Speed (mph)	0.000	5.000	10.000	15.000	20.000
Wind Speed (ft/s)	0.000	7.333	14.667	22.000	29.333
Wind Speed (m/s)	0.000	1.524	3.048	4.572	6.096
Drift - Main (ft)	0.000	362.302	724.654	1086.957	1449.259
Drift - Drogue (ft)	0.000	269.145	538.328	807.473	1076.618
Drift - Main (m)	0.000	110.430	220.875	331.304	441.734
Drift - Drogue (m)	0.000	82.036	164.082	246.118	328.153
Total Drift (ft)	0.000	631.448	1262.982	1894.429	2525.877
Total Drift (m)	0.000	192.465	384.957	577.422	769.887
Drift Calculations, Average Decent Velocity					
Wind Speed (mph)	0.000	5.000	10.000	15.000	20.000
Wind Speed (ft/s)	0.000	7.333	14.667	22.000	29.333
Wind Speed (m/s)	0.000	1.524	3.048	4.572	6.096
Drift - Main (ft)	0.000	155.071	310.163	465.234	620.305
Drift - Drogue (ft)	0.000	330.787	661.619	992.406	1323.193
Drift - Main (m)	0.000	47.266	94.538	141.803	189.069
Drift - Drogue (m)	0.000	100.824	201.661	302.485	403.309
Total Drift (ft)	0.000	485.858	971.782	1457.640	1943.498
Total Drift (m)	0.000	148.089	296.199	444.289	592.378

Velocities used for drift Calculations:

2ft Drogue Velocity	(ft/s)	(m/s)
Velocity after Drogue 2ft	123.967	37.785
Velocity Average	100.866	30.744
Velocity after Main	14.573	4.442
Velocity Average	35.466	10.810

All of the above calculations were based off an apogee of 5300ft, drogue chute deployment within one second of reaching apogee, and then a min chute deployment of 750ft. This altitude for deployment of the main parachute was strongly based on our mentors' recommendations and then backed up by simulations. Looking at the drift under 20mph winds with a two-foot drogue we see that our drift exceeds the limitation. This simulation is based on the worst case and seemingly impossible situations. When simulating the drift in this section we were using the terminal velocity of the rocket with the parachute fully deployed. With terminal velocity under the main chute deployment being the slowest the rocket is traveling on its decent it would bring amount the greatest amount of drift. This assumption stems from the thought that once the main

chute is deployed the rocket immediately decelerates to $14.573 \frac{ft}{s}$ and keeps that velocity for the remainder of its decent. In order to overcome this error in our simulations, we took the average decent velocity between each stage. The logic behind making this assumption was based on the linear aspect of the deceleration data. To compute this average we simulated the launch and recover of the rocket in Open Rocket.

4.3.4 Shock Cords

With shock cords, we have a verity of options which range in size and material. After a little research and narrowing down the vast pool of option on the market we have come up with five leading option that consists of mainly Nylon or Elastic. The five different options for shock cords are listed below:

Swivel and Quick Links		
Distributor	Model (Diameter)	Price
RocketMan	Kevlar Covered Tubing with Nylon Webbing - 1" x 30'	\$ 55.00
RocketMan	Tubular Nylon Webbing - 1" x 30'	\$ 40.00
RocketTarium	Red Elastic - 5/8" x 30'	\$ 12.50
RocketTarium	Neon Orange Tubular Nylon - 5/8" x 30'	\$ 20.90
RocketTarium	Neon Orange Tubular Nylon - 1" x 30'	\$ 24.90

The current sizes are all based on or above our mentors' advice when he was given a rough estimate of the mass of our rocket. The two sizes for shock cord, one inch or five eights of an inch, are selected from the commercially available options that are still within reasonable cost estimates.

Kevlar Covered Tubing with Nylon Webbing: Of the option above it is the most costly but it is also the strongest in terms of tensile strength with a test strength of 4200 lbs. Along with the high tensile strength, it comes with pre-sewn loops and Quick Links at each end. These Quick Links have a yield strength greater than that of the Nylon/Kevlar shock cord so the possibility of failure at the Quick Links is minimal. This biggest con of this option would be the cost and weight seeing how it is one of the larger options we are looking at a total increase in mass from what we originally estimated.

Tubular Nylon Webbing: One of the more expensive options, it still offers supreme strength with a test strength of 4200 lbs. With this being another component from RocketMan it comes with Quick Links on both ends attached to pre-sewn loops, yet again it is one of the heavier options on our list. In comparison to some of the other options, Red Elastic mostly, this component would not do as well with absorbing as much energy upon deployment of the main chute due to the increased rigidity of Nylon in comparison to elastic.

Red Elastic: The only option on our list that does not have a Nylon base and from this has the added benefit of being able to absorb much more energy than any other option we have listed. This ability to absorb energy is due to the increased elasticity of the material but this comes with a con of being more prone to failure due to large impulse forces. Another downside

to this option is that we would have to source our own Quick Links and secure our own loops to the end of the shock cords which greatly increases the possibility of failure due to fabrication error. Furthermore, this is the largest option we could find for elastic shock cord and is still very close to the recommendation from our mentor and has a relatively small factor of safety in comparison to all the other options.

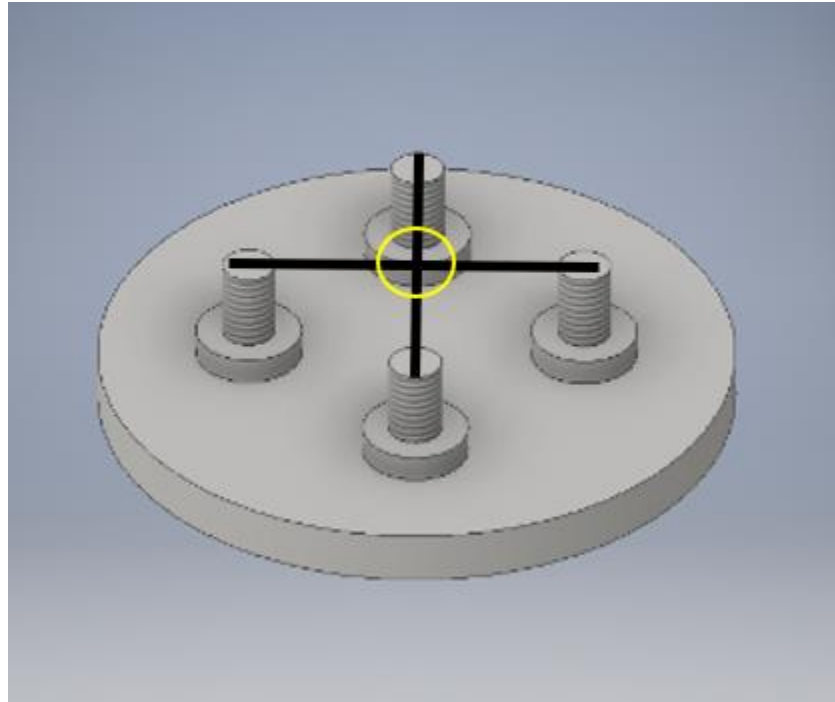
Neon Orange Tubular Nylon (5/8"): This option is one of the thinner materials that we are looking at and in turn is one of the weaker options. Another con about this product is that no hard data could be recovered on the actual yield strength of this component. This option does not come with its own Quick Links so we would have to source our own links as well as devise some way to secure the shock cord to the body of the airframe which, again, increases. The biggest advantage with using five eighths tubular Nylon is the fact that it is the lightest option we are looking at. With this option being the second cheapest it is an ideal candidate for securing the nosecone to the airframe when that section is ejected to deploy the rover. This option will be the ease to work with and doesn't need the extreme strength that the main and drogue shock cords require in order not to fail. Further details of the separation process will be outlined in the charge and size calculations for nosecone ejection.

Neon Orange Tubular Nylon (1"): This option, is again, one of the thicker options and from this, it is one of the stronger options we have outlined. For this size of shock cord, it is by far the cheapest option yet no hard data on the yield strength of the cord is given. For this option, the biggest con we have is that it does not have any Quick Links or loops built into the cord and would have to devise some way of attaching them to the airframe. From the options provided above the most viable option appears to be the Tubular Nylon Webbing is not only the most cost-effective option but it is also the strongest option in terms of yield strength. Because of its strength, this option would provide the most redundancy within the shock cords and does the most to eliminate the possibility of failure within this part of the recovery system. One of the biggest risks that we have with this option for shock cords is the stress concentrations build up in knots within in the shock cord which is impossible to get around seeing how we are attaching the parachutes directly to the shock cords. The system of attaching the shroud lines from the parachute to the shock cord will utilize a bowline knot and is outlined in the

4.3.4.1 Shock Cord Connecting to the Bulkhead:

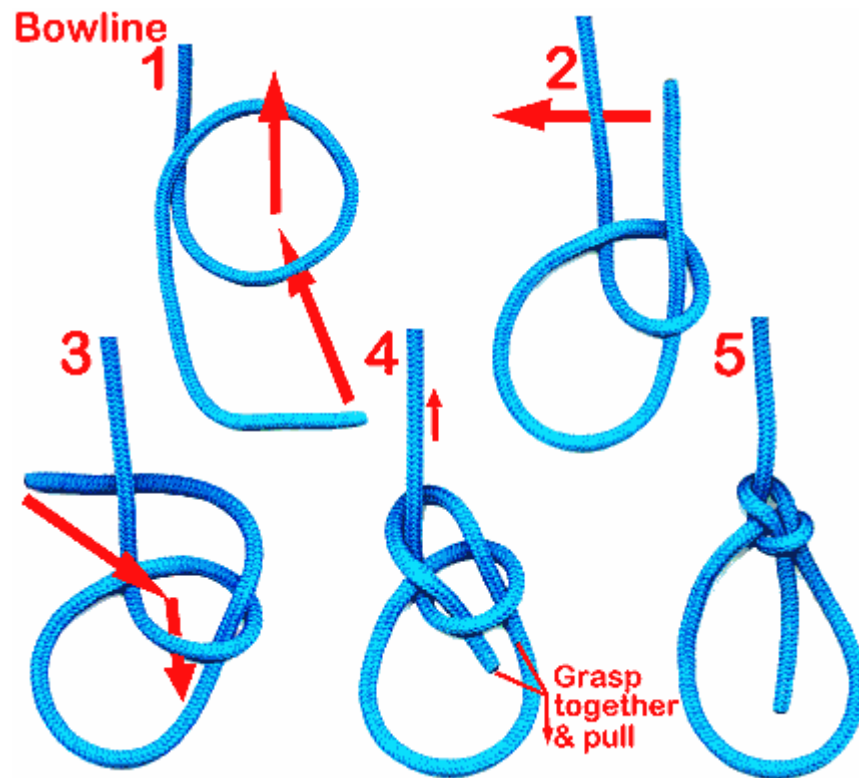
In regards to how the shock cord is going to be connected, there will be four eye bolts that will be threaded through a base plate. There will be a harness that will be created by having a line going from the eye bolts threaded across from each other creating an "x" that will create one connection point for the shock cord to connect to. This connection point and how the eye bolts will be connected is visualized in the figure down below. The line that we will be using to create this harness that will serve as the connection point for the shock cord to the bulkhead is solid braid KnotRite nylon rope 1/4-inch size which has a weight capacity of 1100lbs which is strong enough to serve as a harness for the connection point. The eye bolts that we will be using will have a shank diameter of 3/8 giving the bolt a weight capacity of 1550lbs to reduce the possibility of a failure from the forces acting on the system. The connection point between the line and the shock cord is identified in the figure below by the yellow circle. To connect the

shock cord and the harness we will be using a Topflight recovery quick link 3/16-inch. By using the harness set up and the four connection points we will be able to better spread out the forces that will be acting on the system. The possible risks are that the nylon harness could shred due to the large amount of force that the system will sustain so in order to minimize it we are going to weave the nylon through the bolts three times to increase the strength and the capacity of the harness.



4.3.4.2 Parachute Connections to Shock Cord

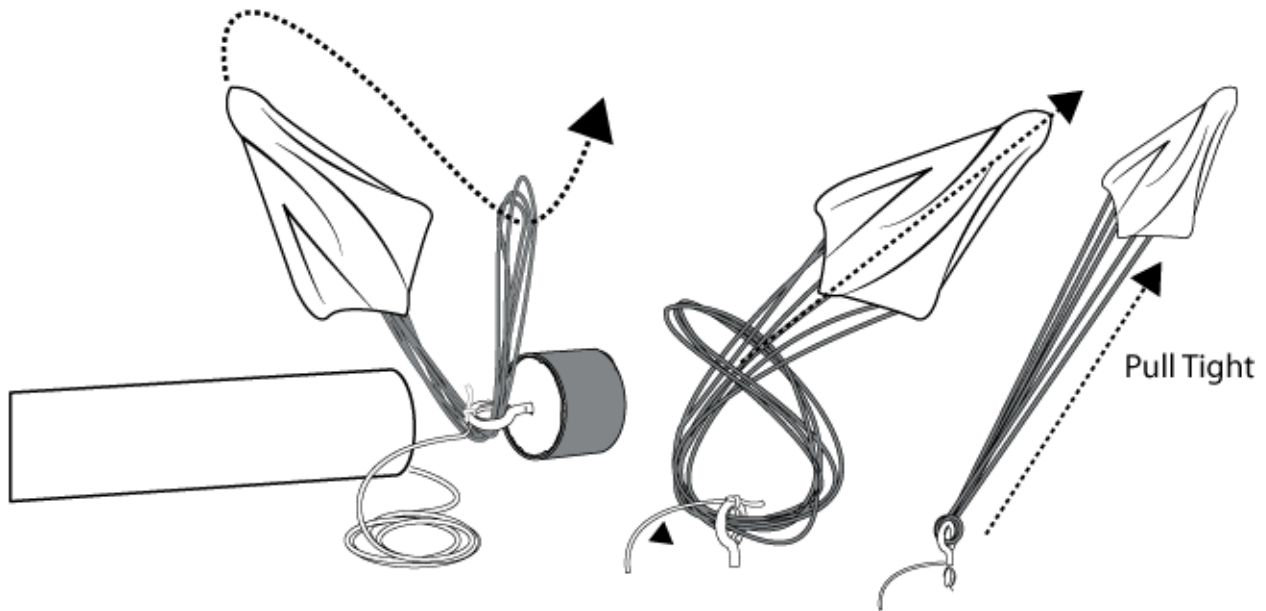
Looking at different ways to attach the parachutes to the rocket the two leading designs were to attach the parachute directly to the airframe or to attach the parachute to the shock cord which runs between the different sections of the rocket. When connecting the parachute directly to the bulkheads we run into problems of the initial shock of the main parachute, when it fully deploys, ripping the bulkheads out of the airframe due to the extreme stress caused by the negative acceleration of such a large rocket. The main advantage of this system of attachment is the simplicity of the build yet this does not overcome the massive downside of the extreme stress the airframe is put under upon deployment of the main parachutes. The second option, where we attach the parachutes to the shock cord and then attach the shock cord to the bulkhead with four points of contact. The main advantage of this system is the reduced stress on the airframe seeing how the shock cord takes a majority of the initial load and helps dissipate the stress to the airframe. The largest downside to this design is the fact that we have to tie a knot in the shock cords which can lead to an increase in stress within the shock cord and ultimately cause a failure within the shock cord itself and ultimately failure of the recovery system as a whole. In order to reduce the risk of failure in the shock cord because of the loop tied in the shock cord, we will tie a bowline knot which is most commonly used in sailing on lines under extreme tension. Instructions on how to tie a bowline knot are below:



<http://www.boatsafe.com/nauticalknowhow/bowline.gif>

With that being said we are looking at the later design, attaching the parachute directly to the shock cords, because of the reduced stress to the bulkheads and connection of the electronics bay to one of the bulkheads shared with the main parachute. Because the electronics bay will be connected to the bulkhead it is empirical that all measures are taken to reduce the risk of failure within the bulkhead.

In order to overcome any torsion that may build up in the shroud lines and shock cord, we will be using swivels rated up to 1000lbs to reduce any and all torsion in the different parts of the parachute. The swivel will then be connected to the shock cord with a quick link. In order to connect the parachute to the swivel, we will use the method outlined below:



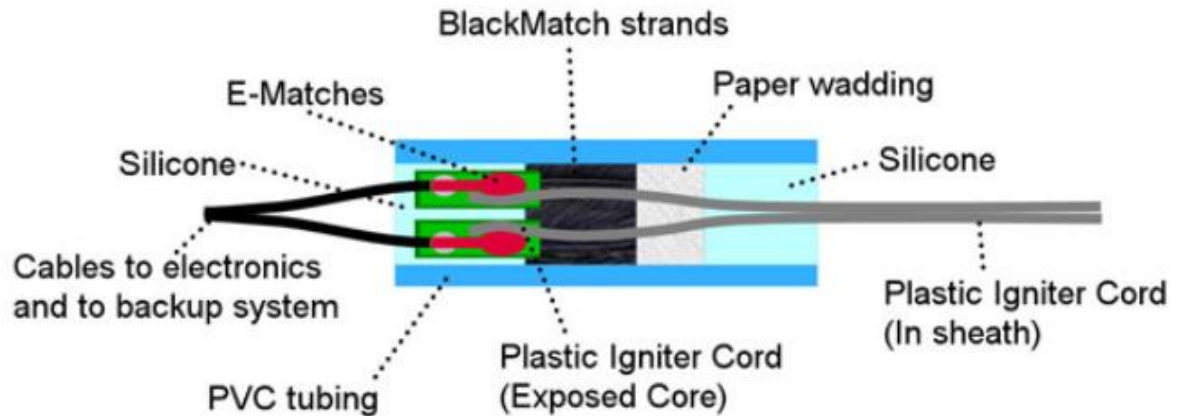
4.3.5 Ejection Canisters Design and Selection

To set off the black powder separation charges we have decided to go with the XL variable-capacity Ejection Canister from Apogee Rockets. This was the only viable option we could find when we looked for different ejection charge canisters as it was the only one large enough to house our required amount of black powder.

Predictions: The ejection canister is a filament-based ignition system that will ignite the black powder separation charges. The canisters will be going off once at apogee to deploy the drogue chute and again at 750 feet to deploy the main chute. The ignition is accomplished through the heating element inside of the canister and is a safe ignition system. The maximum amount of gunpowder per canister is 6.8 grams.

Risks: Possible issues that could arise from the ignition system is a failure to properly heat the black powder to initiate the separation sequence. Another possible problem that could occur is a premature detonation due to a malfunction with the wiring and could be a serious safety concern for the team members.

Precautions: The Company from whom we are purchasing tests their canisters to make sure they are working properly before being shipped off. If there is a failure that occurs for one of the canisters there will be other canisters tied into the system to ensure that the separation sequence is able to be initiated. We will also be following all of our safety procedures when handling the canisters and not wiring them completely until just before launch to ensure there is no premature detonation of the black powder.



4.3.6 Black Powder Selection

In regards to what kind of black powder we will be using we considered two options which were 3F black powder and 4F black powder. With the 3F black powder it is a smaller explosive charge making it a safer option to use in terms of handling however it may not have the force necessary to separate the two sections effectively. The other option we have considered is the 4F black powder which is a more powerful explosive that has the necessary force required to initiate the separation sequence.

Risks: As discussed before the possible risk using the 3F powder is that it will not have the necessary force in order to properly separate the sections because it is not a powerful enough explosive. A general precaution with black powder is that it must be properly handled and stored as it must be kept away from heat, sparks, and flames and it must avoid impact, friction and static electricity. If the black powder is not handled properly or not properly loaded into the rocket a team member could get severely injured.

Precautions: To mitigate the risks that handling black powder poses we will be following all the safety procedures that are required by Texas Tech University to handle and store black powder. Team members that will be handling and loading the black powder and charges will have the necessary training and be made aware of the precautions of handling black powder. In regards to ensuring that the separation charges have enough force to properly carry out the sequence we have decided to use the 4F black powder since it has a larger explosive force between the two black powder options considered. For MSDS on black powder and for safe handling instructions please refer to the safety section in the document.

4.3.7 Nylon Pin Shear Strength

The force required to shear the pins was calculated using experimental data (rocketmaterials.org). It was found that #2 nylon screws withstood 24.64 lbf which was rounded to 25 lbf. The data also showed that #4 screws withstood 40.30 lbf, which was rounded to 40lbf. These numbers were the

most conservative of the dataset, in order to ensure that calculated charge sizes would be sufficient. The dataset used to derive these values is provided below:

#2 Nylon Screws			#4 Nylon Screws		
# of Pins	Peak Load (lbs)	Peak Load (Each Pin)	# of Pins	Peak Load (lbs)	Peak Load (Each Pin)
2	53.123	26.56	2	81.304	40.65
2	45.952	22.98	2	85.148	42.57
2	50.848	25.42	2	75.944	37.57
2	51.799	25.90	2	80.391	40.20
2	47.924	23.96	2	80.908	40.45
Avg	49.93	24.64		80.75	40.30
3	62.637	20.88	3	119.273	39.76
3	60.569	20.19	3	110.999	37.00
3	64.395	21.47	3	99.969	33.32
3	62.413	20.80	3	113.554	37.85
3	68.760	22.92	3	116.208	38.73
3	66.643	22.21	3	121.121	40.37
			3	123.689	41.23
Avg	64.24	21.41		114.97	38.32
4	86.699	21.67	4	143.405	35.85
4	86.855	21.71	4	152.368	38.09
4	78.771	19.69	4	142.026	35.51
4	84.269	21.07	4	160.489	40.12
4	85.617	21.40	4	153.302	38.33
4	90.402	22.60	4	154.766	38.69
			4	160.368	40.09
Avg	84.44	21.36		152.38	38.21

4.3.8 General Charge Size Equation

The general formula used to calculate black powder charge sizes, for 4F black powder, is given as:

$$mass_{BP}(grams) = \frac{P_{req} * V}{\left(266 \frac{in * lbf}{lbm}\right) * (3307 R)} * \left(454 \frac{g}{lbf}\right)$$

The volume of the compartment where the charge is placed is given by:

$$V = \frac{D^2}{4} \pi * L$$

The P_{req} is the pressure required, given as:

$$P_{req} = \frac{F_{req}}{A_{cross-sectional}}$$

4.3.8.1 Charge Size Calculation for Drogue Parachute Deployment

For the drogue parachute shear pins, #2 nylon screws are the leading design. The reasoning behind this option is that it is best to minimize the size of the black powder charges, where possible, in order to ensure safe deployment of the parachute. The #2 nylon screws, with a diameter of $3/32''$, will shear easier than the #4 nylon screws, thus requiring less force to shear the pins. The leading design calls for 8 of these #2 nylon screws.

The force required to separate the section, via shearing the screws, can be found via:

$$F_{req} = N_{screws} * F_{max} = 8 * 25 \text{ lbf} = 150 \text{ lbf}$$

Using the F_{req} found above, we can calculate the pressure required to be produced by the charge by taking the F_{req} and dividing by the cross-sectional area of the bulkhead. P_{req} is then scaled by a design factor of 1.25 in order to ensure that sufficient pressure is provided to ensure separation, is given by:

$$P_{req} = \frac{F_{req}}{\frac{D^2}{4} \pi} * 1.25 = \frac{150 \text{ lbf}}{\left(\frac{3}{32} \text{ in}\right)^2 \frac{\pi}{4}} * 1.25 = 6.63 \text{ psi}$$

The required pressure is then plugged into the charge size formula to obtain the charge size in grams. The length of the section is approximately 10 inches.

$$mass_{BP}(\text{grams}) = \frac{6.63 \text{ psi} * \frac{\left(\frac{3}{32} \text{ in}\right)^2}{4} \pi * 10 \text{ in}}{\left(266 \frac{\text{in} * \text{lbf}}{\text{lbm}}\right) * (3307 \text{ R})} * \left(454 \frac{\text{g}}{\text{lbf}}\right) \approx .97 \text{ g} \approx 0.034 \text{ oz}$$

The required charge is found to be .034 ounces of 4F black powder for our leading design.

4.3.8.2 Charge Size Calculation for Main Parachute Deployment

For the main parachute shear pins, #4 nylon screws are the leading design. The reasoning behind this option is that it minimizes the risk of the section being broken off at drogue deployment, as the force on the pins will have to sustain the change in acceleration and the weight of the lower sections. There are 2 options in terms of the number of pins we can use, the leading option being 8 pins with the alternative being 6.

The pros of using 8 pins is that the section will be more secure, with less risk of shearing prior to detonation of the charges. The cons of this design option are that the black powder charge will have to be larger, thus increasing risk of damage to the airframe. The major pro of a 6 pin design is the lower charge size, thus reducing risk to the airframe. A con is that the design does reduce the strength of the coupler.

The calculation for the F_{req} and the P_{req} for the 8 pin #4 nylon screw design yields:

$$F_{req} = N_{screws} * F_{max} = 8 * 40 \text{ lbf} = 320 \text{ lbf}$$

$$P_{req} = \frac{F_{req}}{\frac{D^2}{4} \pi} * 1.25 = \frac{320 \text{ lbf}}{\left(\frac{3}{32} \text{ in}\right)^2 \pi} * 1.25 = 14 \text{ psi}$$

The P_{req} , and the length of the section, $L = 20 \text{ in}$, is substituted into the charge size equation.

$$mass_{BP}(\text{grams}) = \frac{14 \text{ psi} * \frac{\left(\frac{3}{32} \text{ in}\right)^2}{4} \pi * 20 \text{ in}}{\left(266 \frac{\text{in} * \text{lbf}}{\text{lbm}}\right) * (3307 \text{ R})} * \left(454 \frac{\text{g}}{\text{lbf}}\right) \approx 4.09 \text{ g} \approx 0.144 \text{ oz}$$

The calculation for the F_{req} and the P_{req} for the 6 pin #4 nylon screw design yields:

$$F_{req} = N_{screws} * F_{max} = 6 * 40 \text{ lbf} = 240 \text{ lbf}$$

$$P_{req} = \frac{F_{req}}{\frac{D^2}{4} \pi} * 1.25 = \frac{240 \text{ lbf}}{\left(\frac{3}{32} \text{ in}\right)^2 \pi} * 1.25 = 10.61 \text{ psi}$$

This P_{req} is then substituted into the charge size equation:

$$mass_{BP}(\text{grams}) = \frac{10.61 \text{ psi} * \frac{\left(\frac{3}{32} \text{ in}\right)^2}{4} \pi * 20 \text{ in}}{\left(266 \frac{\text{in} * \text{lbf}}{\text{lbm}}\right) * (3307 \text{ R})} * \left(454 \frac{\text{g}}{\text{lbf}}\right) \approx 3.21 \text{ g} \approx 0.113 \text{ oz}$$

The required charge is found to be .144 ounces of 4F black powder for our leading design.

4.8.3.3 Charge Size Calculation for Nosecone Ejection

Our leading design for the deployment of the rover, involves the ejection of the nosecone from the payload section, such that the rover can be deployed from the area between its compartment and the nosecone. The nosecone charge will have to be detonated remotely via a longwave receiver in the nosecone, and attached to a bulkhead attached to the payload section via shock cord. The shock cord will be slightly smaller in diameter than the drogue and main parachute connections with the leading design being the five eighths inch thick tubular nylon seeing how this shock cord will only be used to keep the nosecone attached to main airframe. Please refer to the shock cord selection above for the logic behind this decision. The nose cone will be protected from the explosive detonation with a removable bulkhead that will be ejected with the ejection of the nosecone. Further testing will be required to determine the final material selection for this component.

When the charge is detonated, the payload will then be ejected from the airframe as the shock cord pulls taught with the nosecone. There are currently 2 pin layout we are considering, with an 8 pin #4 nylon screw design being the leading design, and a 6 pin #4 nylon screw layout being an alternative. The 8 pin design is currently being considered over the 6 pin design because of its security with regard to its coupled strength to the payload section. The 6 pin design is being considered because of the lower charge size, thus minimizing potential damage to the payload.

The calculation for the F_{req} and the P_{req} for the 8 pin #4 nylon screw design yields:

$$F_{req} = N_{screws} * F_{max} = 8 * 40 \text{ lbf} = 320 \text{ lbf}$$

$$P_{req} = \frac{F_{req}}{\frac{D^2}{4} \pi} * 1.25 = \frac{320 \text{ lbf}}{\left(\frac{3}{32} \text{ in}\right)^2 \pi} * 1.25 = 14 \text{ psi}$$

The P_{req} , and the length of the section, $L = 4.75 \text{ in}$, is substituted into the charge size equation.

$$mass_{BP}(\text{grams}) = \frac{14 \text{ psi} * \frac{\left(\frac{3}{32} \text{ in}\right)^2}{4} \pi * 4.75 \text{ in}}{\left(266 \frac{\text{in} * \text{lbf}}{\text{lbm}}\right) * (3307 \text{ R})} * \left(454 \frac{\text{g}}{\text{lbf}}\right) \approx 0.97 \text{ g} \approx 0.0341 \text{ oz}$$

The calculation for the F_{req} and the P_{req} for the 6 pin #4 nylon screw design yields:

$$F_{req} = N_{screws} * F_{max} = 6 * 40 \text{ lbf} = 240 \text{ lbf}$$

$$P_{req} = \frac{F_{req}}{\frac{D^2}{4} \pi} * 1.25 = \frac{240 \text{ lbf}}{\left(\frac{3}{32} \text{ in}\right)^2 \pi} * 1.25 = 10.61 \text{ psi}$$

This P_{req} is then substituted into the charge size equation:

$$mass_{BP}(\text{grams}) = \frac{10.61 \text{ psi} * \frac{\left(\frac{3}{32} \text{ in}\right)^2}{4} \pi * 4.75 \text{ in}}{\left(266 \frac{\text{in} * \text{lbf}}{\text{lbm}}\right) * (3307 \text{ R})} * \left(454 \frac{\text{g}}{\text{lbf}}\right) \approx .74 \text{ g} \approx 0.0261 \text{ oz}$$

The charge size for the leading design is .0261 ounces of 4F black powder.

4.3.9 Transmitter and Receiver Selection and Design for Nosecone Ejection

The transmitter and receiver for the detonation of the nosecone charge will be a standalone system on a standalone circuit located in the nosecone. The leading design's receiver is the Adafruit Feather 32u4 RFM96 LoRa Radio, a microcontroller with an onboard receiver that has a range of 1.2 miles, with wire quarter-wave antennas. This microcontroller will also be capable of relaying instructions to the rover, and will act as an intermediary between mission control and the landing site.

The microcontroller will be placed near a thinner edge of the nosecone, in order to negate any RF shielding effects from the ABS plastic cone. At \$34.95, the microcontroller is an affordable option, with utility aside from detonating the charge. This is currently a system still in the process of being fleshed out, and will be elaborated upon in detail in the CDR.

Leading Part Selection

Looking at the different possible options we could buy for this part of the rocket we had to consider the reliability of the different components along with the cost in order to present a final parts list. With cost being one of the main limiting factors for component selection we had to look at where we could make compromises without compromising the safety of the rocket and the recovery system as a whole. Listed below are the leading components for the recovery system as a whole:

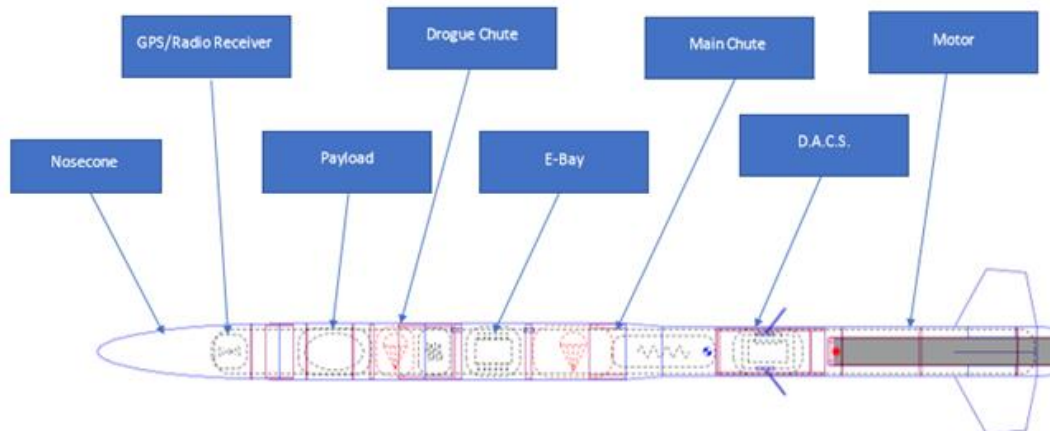
	Parts	Quantity	Unit Cost	Total Cost
Electronics Bay				
	Plywood	1	\$ -	\$ -
	1/2" carriage bolts Long	2	\$ 2.65	\$ 5.30
	1/2" Nuts	6	\$ 0.20	\$ 1.20
	Terminal block	2	\$ 3.41	\$ 6.82
	Perfect Flight StratologgerCF	2	\$ 60.00	\$ 120.00
	9v Battery	4	\$ 11.03	\$ 44.12
Chute				
	1000lbs Swivle	2	\$ 6.00	\$ 12.00
	Standard Low-Porsity Ripstop	1	\$ 170.00	\$ 170.00
	2' Drogue - Pro 1.9	1	\$ 25.00	\$ 25.00
	2ft Deployment Bag	1	\$ 17.00	\$ 17.00
	16ft Deployment Bag	1	\$ 15.00	\$ 15.00
	Tubular Nylon Webbing - 1" x 30'	2	\$ 40.00	\$ 80.00
Seperation				
	Apogee XL Ejection Charge Canister	4	\$ 2.75	\$ 11.00
	Black Powder 6.8g max	4	\$ -	\$ -
	1" 30ft Tubular Kevlar / Nylon	2	\$ 55.00	\$ 110.00
	1/4" 50ft solid braid KnotRite Nylon Rope	1	\$ 8.50	\$ 8.50

Nose Cone				
	Apogee XL Ejection Charge Canister	2	\$ 2.75	\$ 5.50
	Missile Works T3 GPS Tracking System	1	\$ 75.00	\$ 75.00
	9V Battery	2	\$ 11.03	\$ 22.06
	Terminal block	1	\$ 3.41	\$ 3.41
	Adafruit Feather 32u4 RFM96 LoRa Radio	1	\$ 34.95	\$ 34.95
			Total Cost:	\$ 766.86

4.4 Mission Performance Predictions

Open rocket is the primary tool that we used for running flight simulations, data collection, and design optimization. It is a very powerful open-source software package that is backed by the community and has complex built-in functions for finding CG, CP, calculating stability, calculating the coefficient of drag etc. Simulations have been ongoing and that are directly correlated to the research of parts and materials of the launch vehicle. As information from each team was presented, design variants were made and tested to determine the effects on flight characteristics. As the design process went on we narrowed motor options down to a list of four that are shown in simulation data below.

Two designs were simulated; the straight 6" body tube and the transition body. It was found that the difference that the transition piece makes is negligible, and the weight reduction of not including the transition piece balances out with the reduction of drag



(Internal component placement)

4.4.1 Vehicle Information:

Simulations for the DETS were run with an airframe that is made out of 15.24cm (6") and staggering to 13.97cm (5.5") Blue Tube, with an ABS transition piece, G10 fins, an ABS plastic long elliptical shaped nosecone simulated weight for the DACS, as well as the payload bay, E-bay and an included 907.185 g (2lbm) that accounts for epoxy, wires, and hardware. The DACS was not deployed on any of the simulations and therefore we are looking for an apogee that is above 1.609km (1 mile). The total mass of the launch vehicle is 21.364kg (47.1lbm) and length is 273.05cm (107.5"). Simulations for the straight 6" were run with a 6" airframe running the whole length of the rocket. The straight 6" uses the same nosecone, fin design, and same masses of internal components.

4.4.2 Simulations:

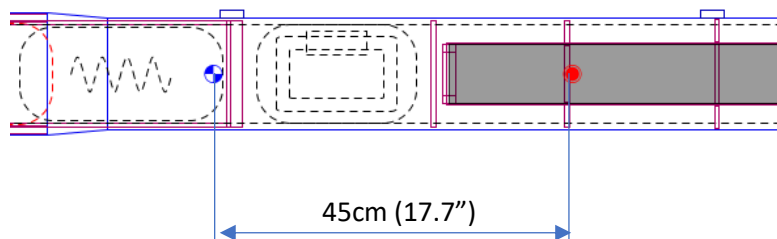
Simulations were made with weather conditions mirroring the average climate data of Huntsville Alabama in the month of April obtained from the weatherspark.com. We used motor data from the 4 motor options and compared the flight characteristics between both the straight 6" design and the DETS design.

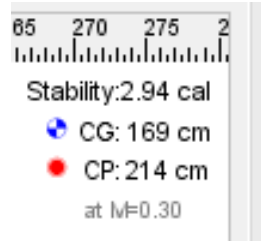
Temperature: High (deg F)	74
Temperature: Low (deg F)	50
Humidity	<30%
Wind Speed (mph)	6.5
Latitude	34.73deg
Longitude	-86.586deg
Elevation(ft)	669

4.4.2.1 Vehicle Stability:

The Vehicle stability was calculated by hand as well as pulled from OpenRocket. The hand calculations verified the accuracy of the software. The calculations were made with the rocket at the bottom of the launch rail and at the top of the launch rod which came out to be: 2.94 and 2.97 respectfully.

$$\frac{(CP - CG)}{d} = \text{Stability Factor}$$





4.4.2.2 Thrust to weight ratio:

The thrust to weight ratio is a critical factor with regards to safety, as this also contributes to the stability of the rocket. A higher thrust to weight ratio will create a more stable rocket with a rule of thumb to always remain above 5.

$$\frac{\text{Thrust}}{\text{Weight}} = \text{Thrust to weight ratio}$$

Calculated thrust to weight ratio is: 6.87 on the pad.

Cesaroni L1395-BS

Straight 6" body

Apogee: 1775m (5826ft)

Rail Exit Velocity: $19.3 \frac{m}{s}$ (63.32fps)

Max Velocity: $210 \frac{m}{s}$ (688.98fps)

Max Acceleration: $79.5 \frac{m}{s^2}$ ($260.83 \frac{ft}{s^2}$)

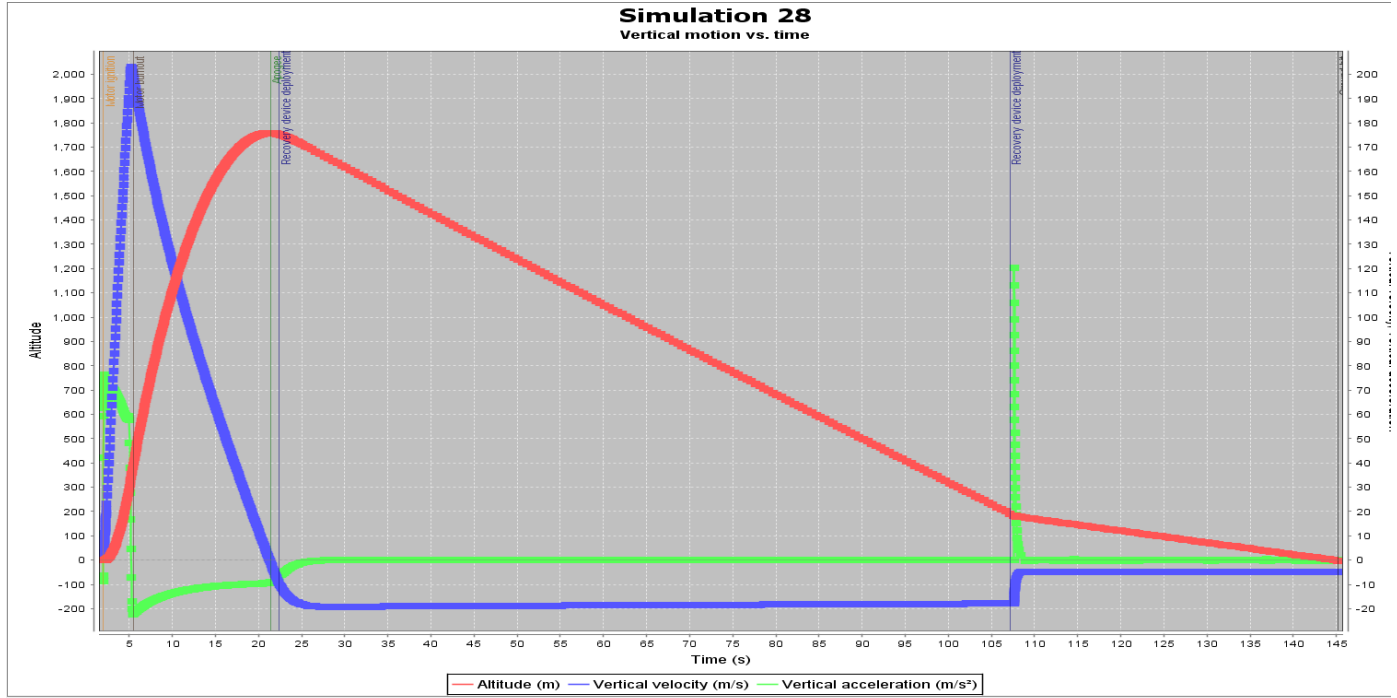
DETS Body

Apogee: 1750m (5741ft)

Rail Exit Velocity: $19.1 \frac{m}{s}$ (62.7fps)

Max Velocity: $202 \frac{m}{s}$ (662.7fps)

Max Acceleration: $76.1 \frac{m}{s^2}$ ($249.7 \frac{ft}{s^2}$)



4.4.4 Aerotech L2200G

Straight 6" Body

Apogee: 1856m (6089.24ft)

Rail Exit Velocity: $24.6 \frac{m}{s}$ (80.7fps)

Max Velocity: $226 \frac{m}{s}$ (741.5fps)

Max Acceleration: $147 \frac{m}{s^2}$ ($482.2 \frac{ft}{s^2}$)

DETS Body

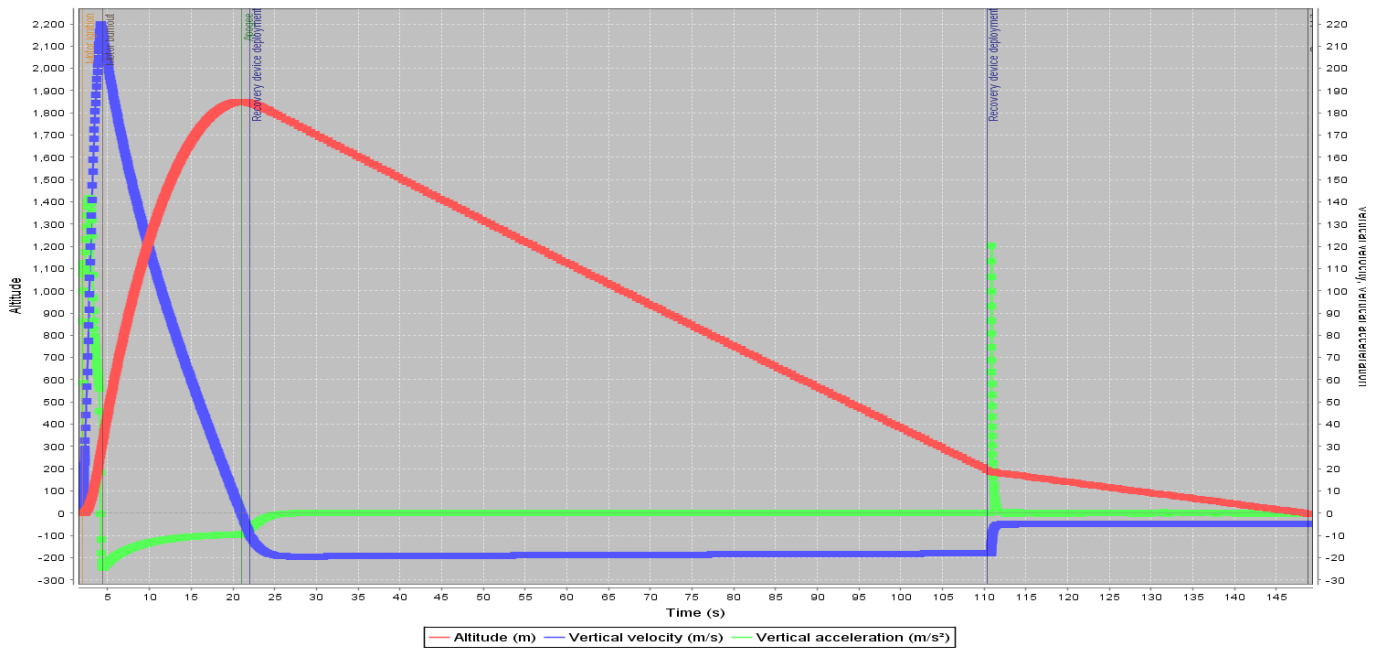
Apogee: 1843m (6046.5ft)

Rail Exit Velocity: $24.7 \frac{m}{s}$ (81.0fps)

Max Velocity: $219 \frac{m}{s}$ (718.5fps)

Max Acceleration: $141 \frac{m}{s^2}$ ($462.6 \frac{ft}{s^2}$)

Simulation 30
Vertical motion vs. time



4.2.5 Aerotech L1420R-P

Straight 6" Body

Apogee: 1629m (5344.5ft)

Rail Exit Velocity: $19.4 \frac{m}{s}$ (63.6fps)

Max Velocity: $198 \frac{m}{s}$ (649.6fps)

Max Acceleration: $74.5 \frac{m}{s^2}$ (244.4 $\frac{ft}{s^2}$)

DETS Body

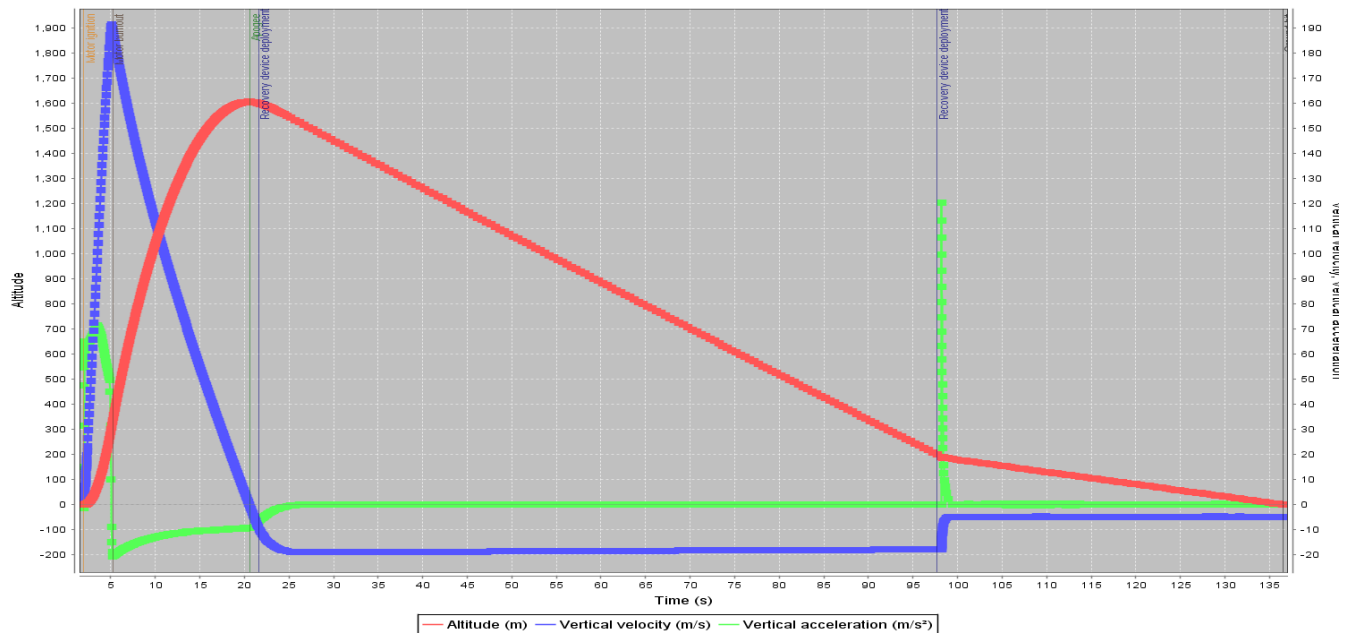
Apogee: 1595m (5232.9ft)

Rail Exit Velocity: $18.5 \frac{m}{s}$ (60.7fps)

Max Velocity: $191 \frac{m}{s}$ (626.6fps)

Max Acceleration: $71.1 \frac{m}{s^2}$ (233.3 $\frac{ft}{s^2}$)

Simulation 33
Vertical motion vs. time



4.2.6 Cesaroni L1410-Sk

Straight 6" Body

Apogee: 1679m (5508.5 ft)

Rail Exit Velocity: $17.3 \frac{m}{s}$ (56.7fps)

Max Velocity: $200 \frac{m}{s}$ (656.1fps)

Max Acceleration: $70.9 \frac{m}{s^2}$ ($232.6 \frac{ft}{s^2}$)

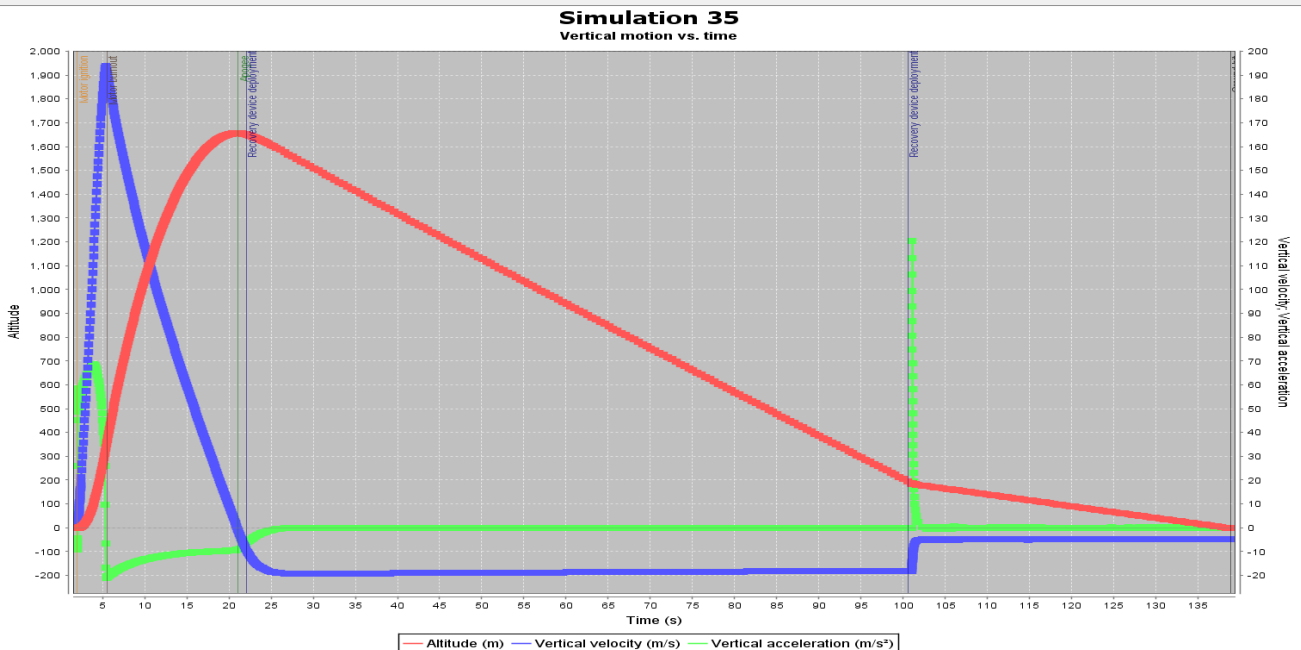
DETS Body

Apogee: 1651m (5416.67 ft)

Rail Exit Velocity: $17.1 \frac{m}{s}$ (56.102fps)

Max Velocity: $191 \frac{m}{s}$ (626.64fps)

Max Acceleration: $68.4 \frac{m}{s^2}$ ($224.409 \frac{ft}{s^2}$)



4.2.7 MatLab Verification

Due to the fact this motor is our ideal engine candidate, hand calculations were done to confirm the data we received in OpenRocket. In Matlab, a simple code using the linear momentum equation:

$$m(v_1) + \int_{t_1}^{t_2} F dt = m(v_2)$$

And the velocity equation:

$$v = \frac{ds}{dt}$$

Together gave us plots of velocity vs time and position vs time our rail exit velocity of:

$$v_{rail\ exit} = 17.7 \frac{m}{s} (58.071fps)$$

Another calculation done with the help of Matlab was a validation of the apogee we received in the OpenRocket simulation. To help simplify some of these equations, we assumed a constant mass for the duration that the engine will burn. Knowing this mass loss would inevitably affect the apogee calculated, a small, but reasonable amount error was expected with these results.

Due to the fact that this motor is our ideal engine candidate, hand calculations were done to confirm the data we received in OpenRocket. In Matlab, a simple code using the linear momentum equation:

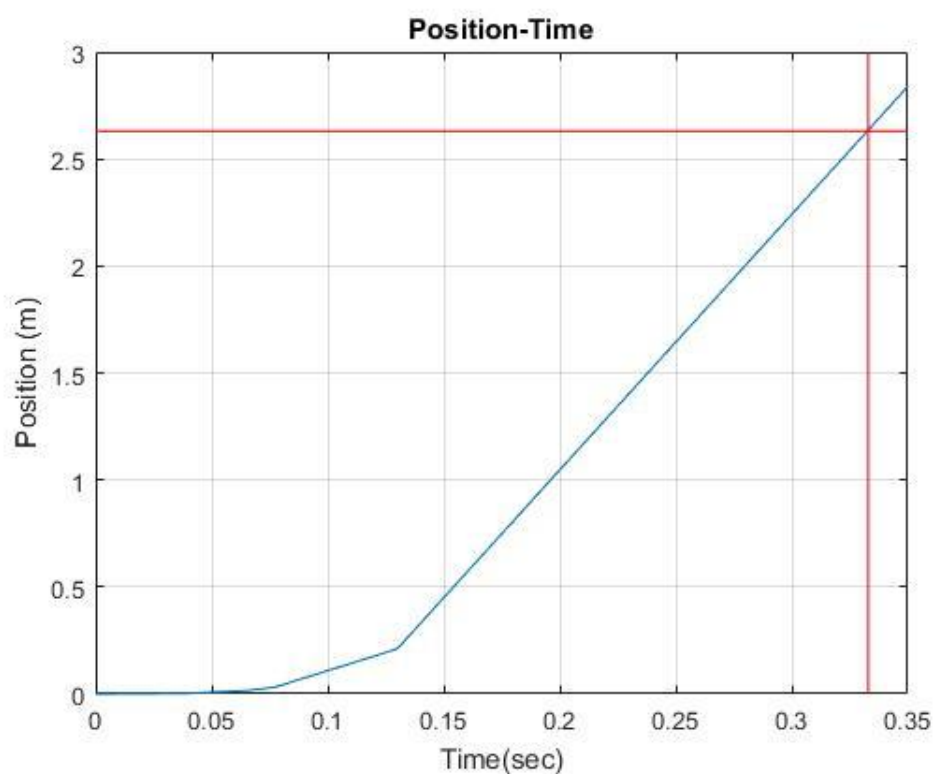
$$m(v_1) + \int_{t_1}^{t_2} F dt = m(v_2)$$

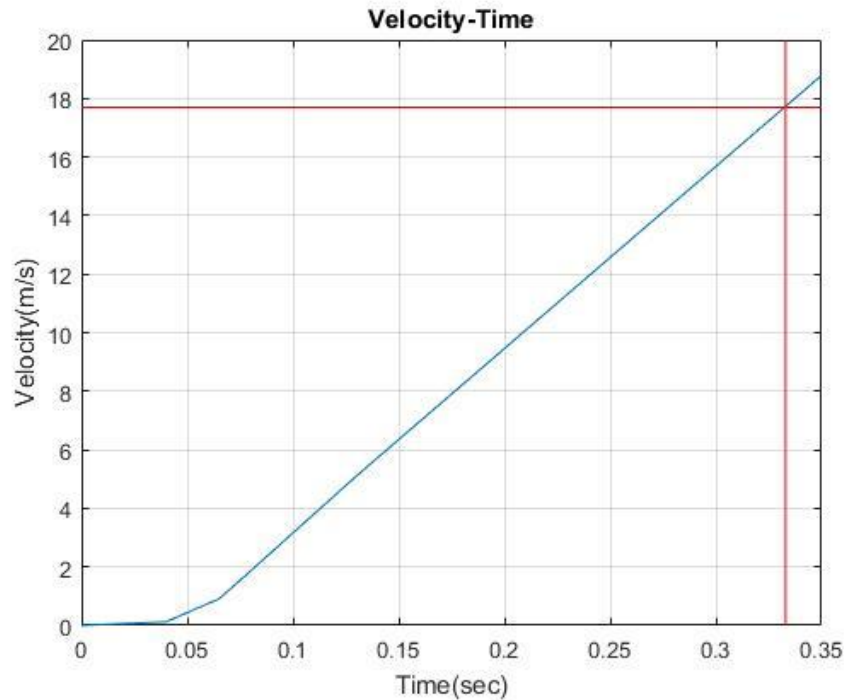
And the velocity equation:

$$v = \frac{ds}{dt}$$

These two together gave us plots of velocity vs time and position vs time our rail exit velocity of:

$$v_{rail\ exit} = 17.7 \frac{m}{s} (58.071 fps)$$





Another calculation done with the help of Matlab was a validation of the apogee we received in the OpenRocket simulation. To help simplify some of these equations, we assumed a constant mass for the duration that the engine will burn. Knowing this mass loss would inevitably affect the apogee calculated, a small, but reasonable amount error was expected with these results. In order to calculate the vehicle's apogee, a burn time was needed to calculate our velocity and height when engine burn out occurred. Our burn time (t_b) equation came out to be the total impulse (I) divided by the average thrust (T):

$$t_b = \frac{I}{T}$$

Before our main velocity and heights could be calculated, a wind resistance factor needed to be accounted for. Using air density (ρ), the coefficient of drag our rocket body (C_d), and the cross-sectional area of our rocket body (A), the equation for wind resistance came out to be:

$$k = \frac{1}{2} \rho C_d A$$

Including both calculated values with the mass of our rocket (m) and the gravitational constant (g), the values for the height (z_b) and the velocity (v_b) at engine burnout were calculated: $z_b =$

$$\left(-\frac{m}{2k} \right) \ln \left(\frac{T - mg - kv^2}{T - mg} \right)$$

After burnout, the value of mass changes to the mass of the rocket without fuel (m_{ab}) and our thrust (T) goes away. This causes the equation for height to be modified to an equation for coasting

$$\text{height}(z_c): z_c = \left(\frac{m_{ab}}{2k} \right) \ln \left(\frac{m_{ab}g + kv^2}{m_{ab}g} \right)$$

Finally, adding our burnout height and our coasting height together we get the estimated apogee:

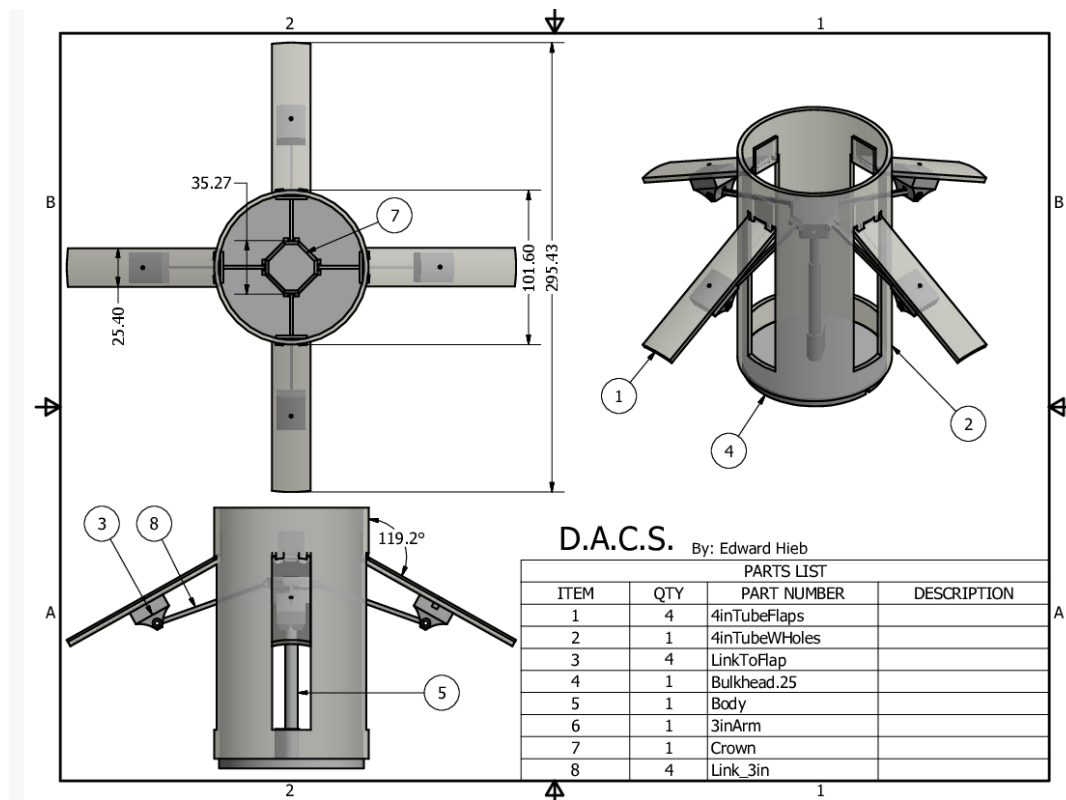
$$Z = z_c + z_b$$

V Dynamic Apogee Control System (D.A.C.S.)

The team has decided on adding an additional payload to the launch vehicle. The chosen payload is a dynamic apogee control system, (DACS) and it will serve the function of regulating maximum altitude to get as close to a mile as possible. This system will consist of a micro-controller, sensor package, and a mechanism that will translate motion from either a linear actuator, or servo to open and close a set of four flaps upon command. DACS is going to require the understanding of advanced subjects such as; fluid dynamics, control of dynamic systems etc. to be successfully implemented.

5.1 Designs

Many different mechanisms were considered for DACS such as an offset slider-crank, utilizing either a linear actuator, or a power screw as the linear driving component. Various gear and cam systems were also proposed and considered thoroughly.



(Conceptual drawing of DACS)

5.1.1 Offset slider-crank

The offset slider-crank mechanism is a dynamic system that uses a slider, connecting rod, and crank to translated linear motion into rotational motion. There is a relationship between the location of the slider (y) and the angular position of the crank, or the flaps in this case (θ). This method can be modeled to determine the exposed surface area which will ultimately

determine the force of drag acting on the system using a system of equations. This mechanism will utilize either a linear actuator or power screw assembly that is rated for the force that will be applied via four drag flaps. The linear actuator will have a feedback sensor that will make control of the system easier due to knowing the location of the (y) on the stroke. If this route is taken, we plan on sourcing the linear actuator through progressive automation and working to obtain a reimbursement sponsorship by posting a link to their website and sending in videos of the linear actuator in action. The power screw assembly will be driven by a motor causing the (y) of the stroke to change thus extending our control arms and flap panels.

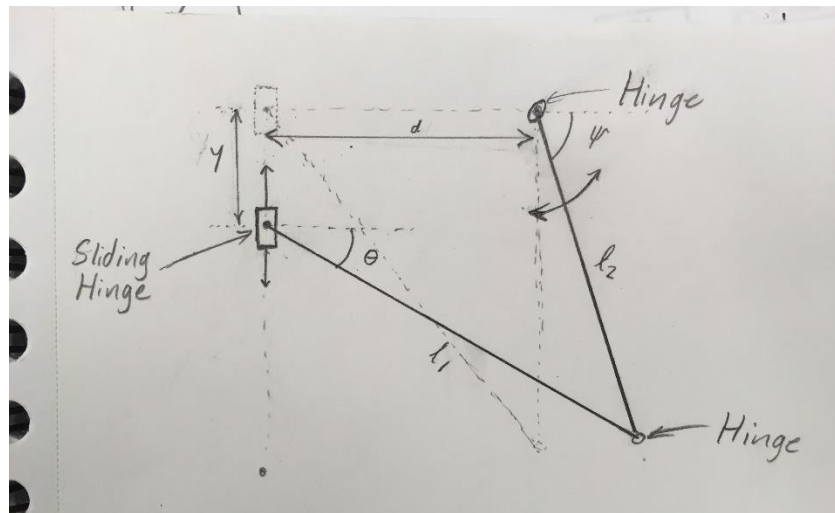


(Diagram of Offset slider-crank used with equations below)

The following system of equations has been derived from the law of cosines to determine the relationship between the slider position y and the angles ψ and Θ .

$$l_1 \cos(\Theta) = l_2 \cos(\psi) + d$$

$$l_1 \sin(\Theta) + y = l_2 \sin(\psi)$$

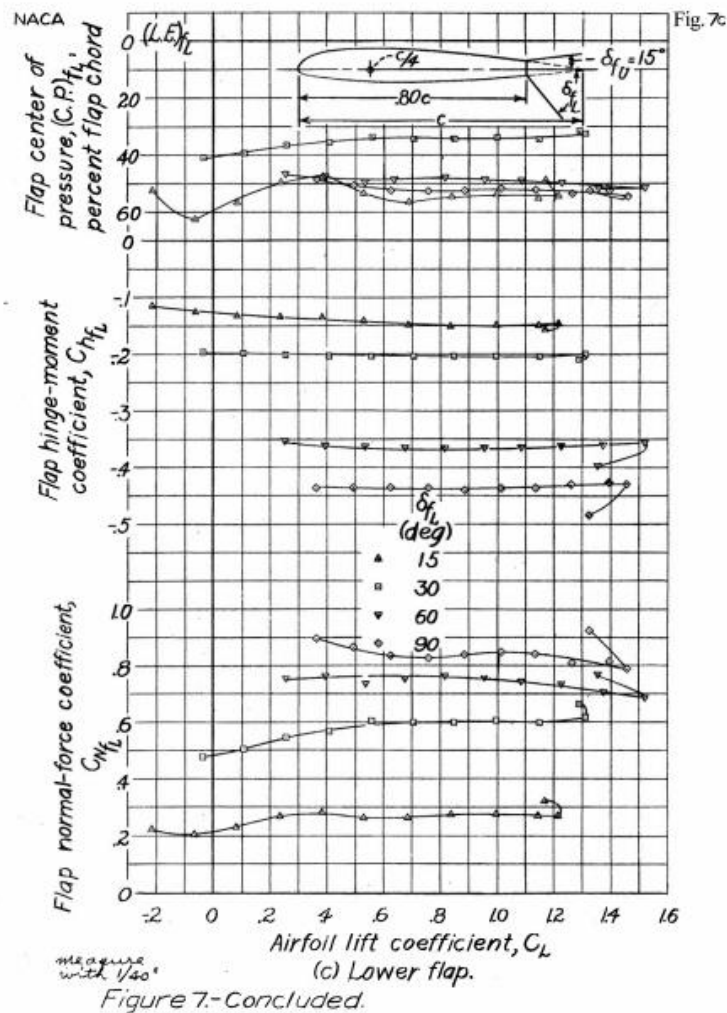
5.2 Parts selection

Multiple ideas were generated when considering flap styles, drive components and mechanisms. Research presented below has gone in to determining a favorable option.

5.2.1 Rectangle flaps:

Rectangular flaps are considered as the simplest option for DACS to their straightforward geometry. This parameter can be seen affecting multiple equations such as the drag force in the form of a changing surface area. The rectangular flaps would be made out of a stiff and strong material due to the requirement of being resistant to bending and supporting high loads created from drag. They would have hinges located at the forward end, a hinge bracket halfway down the internal surface, and a spine that runs down the length of the internal surface. Thoughts of milling holes in the surface of the flaps were thrown around and from further research in a

declassified NACA document, as the angle of attack on a drag flap increases, so does the coefficient of normal force acting on the flap.

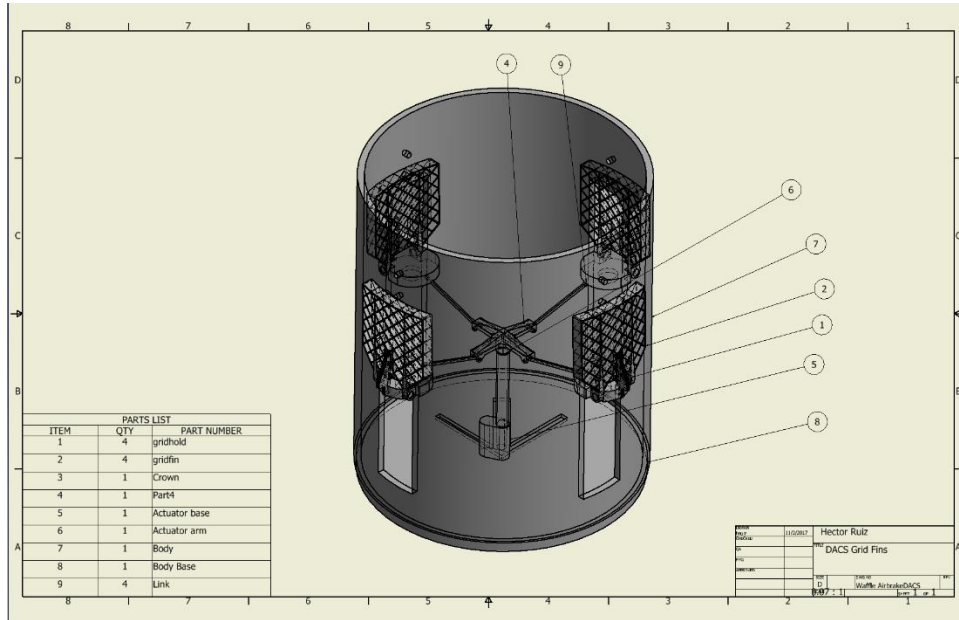


(NACA Declassified document)

5.2.2: Grid Fins

Grid fins have been used since the late 1900's and have been popularized by SpaceX. The Lattice fins create a normal shock wave. For the most part grid fins perform better and are more stable even at differing angles of attack. Additionally, the boxy arrangement of the grid within the fin decreases weight, material needs, and thus, reduces manufacturing costs. Ideally, a grid fin would produce more drag than a planar fin while being lighter and cheaper. However, research from Research Journal of Recent Sciences claims grid fins' drag is "often not higher than a conventional planar fin due to the thin dimensions of the lattice walls which generates less perturbation in the air flowing through the grid." At subsonic speeds, which is the case for the goals of this project, grid fins perform similarly to planar fins. A comparison of grid fin and planar fin drag coefficients and aerodynamics will be tested in The National Wind Institution.

Furthermore, grid fins are much shorter than conventional fins and thus will generate a much smaller hinge moment and require considerably smaller actuators or servos to deploy.



(grid fin concept)

PROGRESSIVE AUTOMATIONS
FORWARD THINKING

**PA-14P
LINEAR ACTUATOR
WITH POTENTIOMETER**

HOW TO ORDER
1.800.676.6123
sales@progressiveautomations.com
www.progressiveautomations.com

SPECIFICATIONS

- Input Voltage: 12 VDC
- Current: 5A at full load
- Load Capacity: 35 lbs, 50 lbs, 150 lbs
- Static Load: 2 x Load
- Speed: 0.59"/sec - 2.00"/sec
- Stroke length: 2" to 40"
- Mounting holes: 0.25" diameter
- Potentiometer: 10K ohm
- Screw: ACME Screw
- Duty Cycle 25%

- Operational Temperature: -25°C–65°C (77°F–150°F)
- Limit Switch: built-in non adjustable
- IP Grade: IP54
- Certification: CE and RoHS
- Housing: Aluminum Alloy
- Gears: Powder Metallurgy
- Wire Length: 40"
- Gear Ratio: 20:1

For Custom Options See Page 5

DIMENSIONS IN INCHES

Page 1 of 5

(Linear actuator drawing)

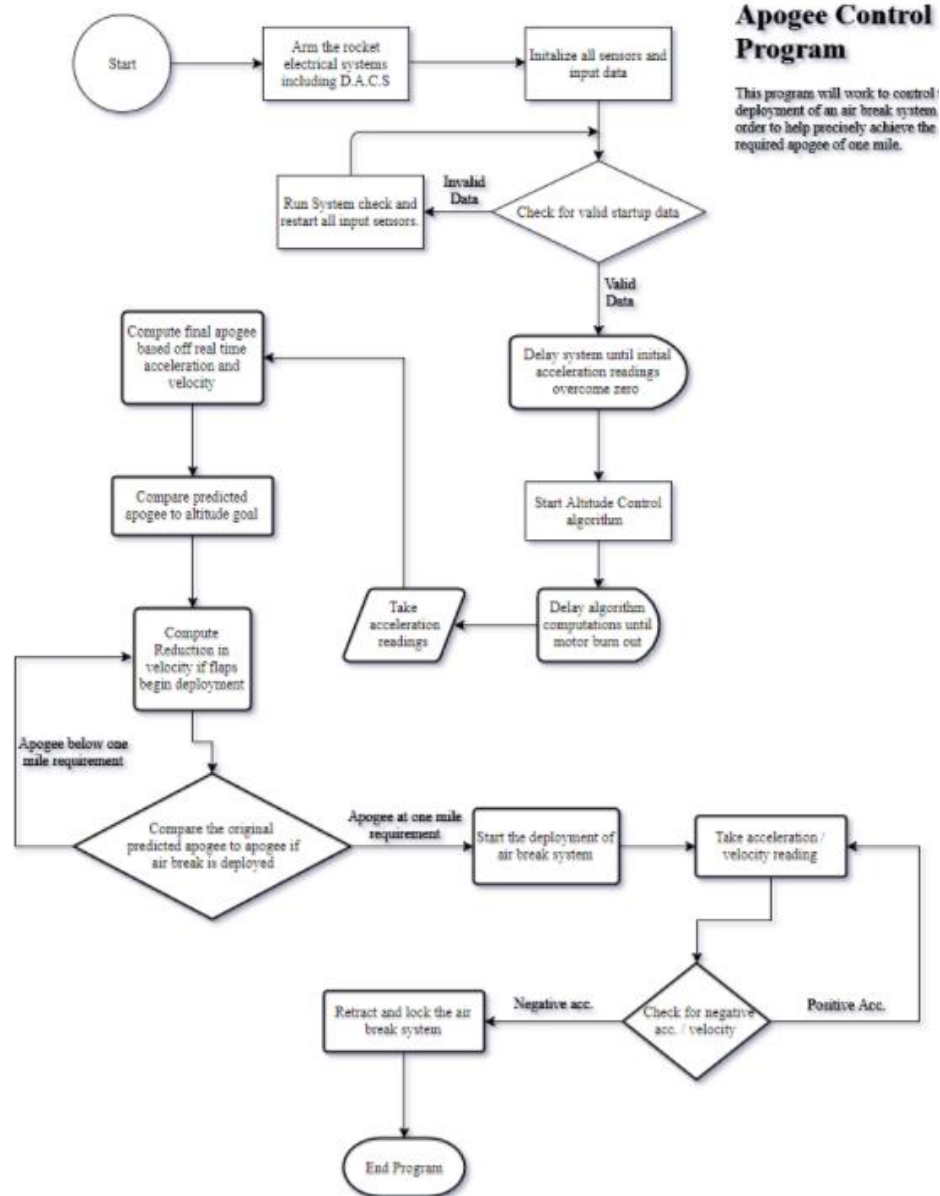
Parts chosen for DACS mechanism are not final yet, however prospected selection of rectangle flaps is priced out above.

Component	Quantity	Price	Material	Total cost
Linear Actuator	1	\$120	Assem	\$207
Arduino	1	0	Electronics	
Battery	1	0	Electronics	
Links	4	0	ABS Plastic	
Crown	1	0	ABS Plastic	
Flaps	1 sheet	\$27	1/8in G10	
Control board	1	\$20	Electronics	
Sensors	1	\$20	Electronics	
Bulkhead	1	5\$	Plywood	
Various electrical	1	\$20	Electrical	

(Due to pre-existing ownership of Arduino and raspberry pi and free access to 3D printing, cost for those parts have been set to zero)


5.3 Logic

The algorithm that will be controlling DACS will run calculations with input parameters of altitude, velocity, acceleration, and feedback of the drive component ie. (linear actuator or power screw mechanism). The input data will be gathered by sensors in real time. The microcontroller will be pre-programmed with a target altitude and using the following logic, will be able to predict the actual altitude and then control the linear actuator to open the control flaps and apply an increased aerodynamic drag force to rapidly decelerate the rocket to correct its predicted altitude. This system will use various coefficients of drag that will be directly correlated with the angle of attack of the flaps. The coefficient of drag (C_d) will be determined from wind tunnel testing and stored in a matrix.





5.4 Testing

The DACS system will need to undergo strenuous testing to determine the coefficient of drag at every instance of the flaps opening. This will then give us a means of calculating the force of drag acting upon the system. The drag will then be controlled by exposing surface area of the attached flaps to slow down the launch vehicle. Because the angle is a changing parameter as the flaps open and close, advanced computation must take place to make accurate predictions. Once we have the coefficient of drag for every angle we can run calculations that can predict the apogee of the rocket given initial altitude and velocity.



The Drag Equation






$$D = C_d \frac{\rho V^2 A}{2}$$

Drag = coefficient x density x velocity squared x reference area
two


Coefficient **C_d** contains all the complex dependencies
and is usually determined experimentally.


Choice of reference area **A** affects the value of **C_d**.

(NASA Drag Equation diagram)



The Drag Coefficient





$$C_d = \frac{D}{\rho V^2 A / 2}$$

Coefficient **C_d** contains all the complex dependencies
and is usually determined experimentally.

Choice of reference area **A** affects the value of **C_d**.

(NASA Drag Coefficient diagram)

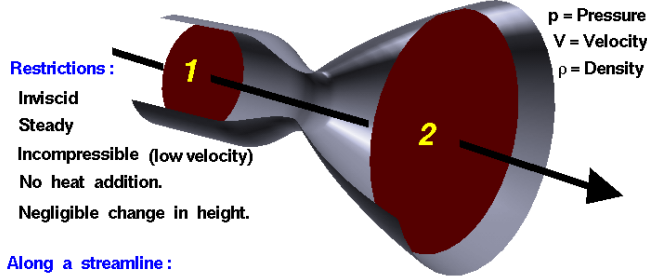
5.4.1 Wind Tunnel:

Testing to determine the coefficient of drag will take place in the Reese Technology Center, under supervision of the National Wind Institute. The Team was given permission to access their wind tunnel for experimentation, and must complete additional safety training as well as organize experiment parameters and procedures before testing begins. The Coefficient of drag can be determined by finding both the force of drag, the dynamic pressure and the exposed area. Dynamic pressure is shown in the C_d equation as "1/2(ρV²)" and force of drag as "D". The dynamic pressure can be found in the test chamber by using a pitot tube as shown in the screenshot below. The relationship of dynamic pressure being equal to (P₁-P₂) is proven in Bernoulli's equation.



Bernoulli's Equation

Glenn
Research
Center



Restrictions:

Inviscid
Steady
Incompressible (low velocity)
No heat addition.
Negligible change in height.

Along a streamline:

static pressure + dynamic pressure = total pressure

$$p_s + \frac{\rho V^2}{2} = p_t$$

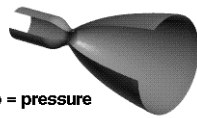
$$\left(p_s + \frac{\rho V^2}{2}\right)_1 = \left(p_s + \frac{\rho V^2}{2}\right)_2$$

(NASA Bernoulli's Equation diagram)



Dynamic Pressure

Glenn
Research
Center



p = pressure
rho = density
u = velocity

From the conservation of fluid momentum:

$$\rho u \frac{du}{dx} = - \frac{dp}{dx}$$

Algebra: $\frac{dp}{dx} + \rho u \frac{du}{dx} = 0$

Simplify: $\frac{dp}{dx} + \frac{d}{dx} \left(\frac{\rho u^2}{2} \right) = 0$

Collect: $\frac{d}{dx} \left(p + \frac{\rho u^2}{2} \right) = 0$

Integrate: $p_s + \frac{\rho u^2}{2} = \text{constant} = p_t$

static pressure

total pressure

$$\text{dynamic pressure} = q = \frac{\rho u^2}{2}$$

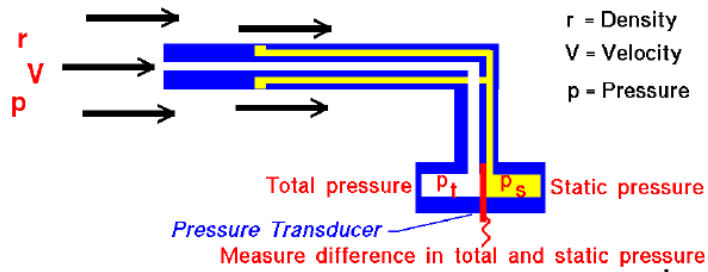
(NASA Dynamic pressure diagram)

Designing the experiment also involves creating a mounting technique to secure DACS in the wind tunnel. We are considering using a sting mount that protrudes from the center rear end of the test model. This is a method of "Internal Balancing" and the wire harness would be ran through the sting mount tube to a module outside of the test chamber. The Sting method is a common mounting technique that is used when testing rockets, with another alternative method being "External Force balancing" which entails mounting sensors on a base plate that is not directly on the test model. Diagrams of these two methods are shown below.



Pitot Tube

Glenn
Research
Center



Bernoulli's Equation:

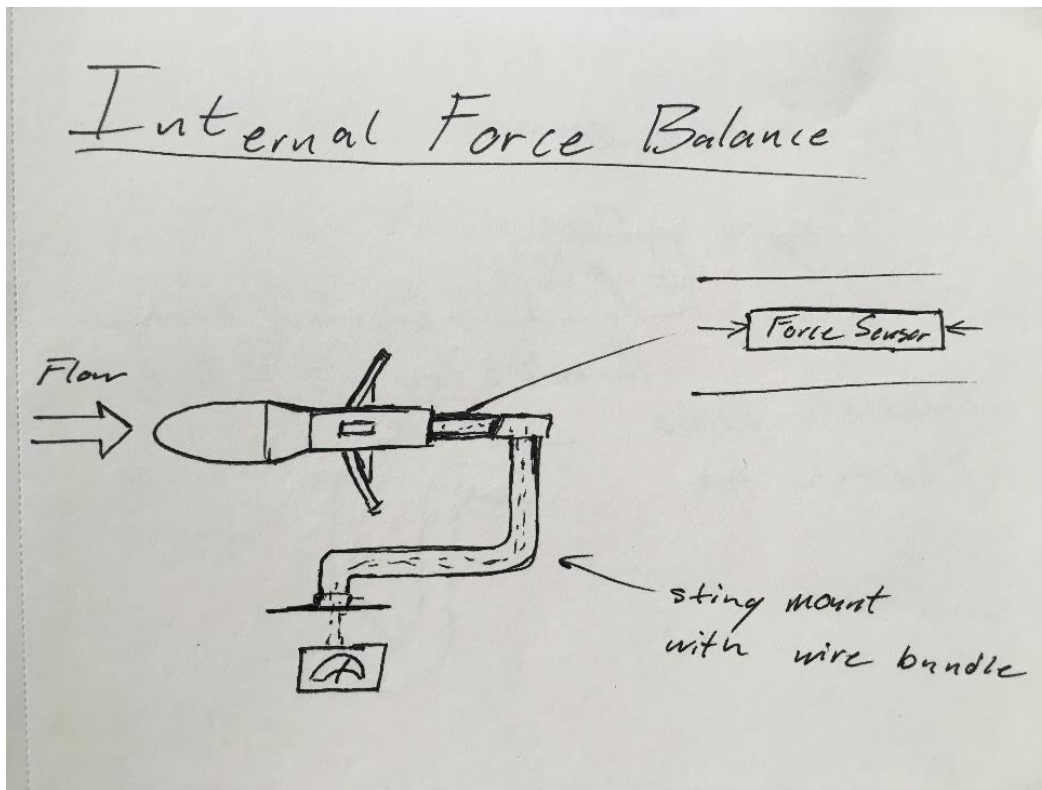
static pressure + dynamic pressure = total pressure

$$(p_s + r \times \frac{V^2}{2}) = p_t$$

Solve for Velocity:

$$V^2 = \frac{2(p_t - p_s)}{r}$$

(NASA Pitot tube diagram)



(sketch of a sting internal balance)

VI) Payload Criteria

6.1 Payload Summary

The Space Raiders payload team will be launching the autonomous rover, R.I.C.K., as the experiment on our vehicle. After landing, the nosecone of the rocket will separate with black powder charges, allowing the rover to exit from its location near the nosecone. The rover will be located on a rotating housing, which utilizes two roller element bearings and an offset center of mass to rotate the rover to an upright position. After attaining an upright position, the rover will be released from its payload housing and will be ejected from the rocket via a compressed spring.

The rover will demonstrate the ability to stow, decreasing its effective volume in order to fit a larger rover into the size constraints of the rocket. The rover will rotate its wheels downward, lifting the chassis of the rover. It will also extend its wheel base by pushing the wheels outward after exiting the rocket.

In order to avoid possible obstacles, the rover will have a simple control system. An ultrasonic sensor at the front of the rover chassis will be calibrated to identify obstacles, and in-wheel motors will allow the rover to be steered using torque differentials. This system will be tested on a variety of obstacles to ensure its reliability in the small chance that the rover does encounter an obstacle.

The rover will travel at least 5 feet from the rocket and deploy a set of 3 solar panels using a tri-fold configuration. In addition, the rover will use its two multi-sensor arrays to test temperature, humidity, altitude, and air pressure. The data obtained from the rover will be transmitted back to mission control.

6.2 Changes Since Proposal

The following are changes made to the payload since submission of the proposal

- Axles removed, motors switched from 2 motors to 4 in-wheel motors
- Extension of the wheel base is driven by motors rather than compressed springs
- 3D printed ball bearings chosen over ceramic or metal due to safety concerns
- Rover was made steerable with in-wheel motors
- Ultrasonic sensor added to identify obstacles in the rover's path
- Solar panels will not be integrated with the electrical system

6.3 Payload Experiment Goals

The payload team is required to deploy a small rover that will drive 5 feet away from the rocket and then deploy solar panels. The payload team fully expects to reach the goals set by the NASA SLI handbook, as well as additional goals the team has set for ourselves in order to further challenge our engineering capabilities. The goals we have set for our team include the following: a rover that can collapse for storage in the rocket and expand for exploration outside the rocket, the ability to collect atmospheric data once deployed from the rocket, and the ability to navigate independently using an ultrasonic sensor.

6.3.1 Expandable Rover

The object of this experiment is to create a more compact rover that is easily storable in a rocket. The rover will be able to expand once deployed from the rocket in order to better navigate the terrain. Two operations must occur in order for this experiment to be considered a success. The first procedure that must occur is that the wheels must be pushed out, causing an increase in the wheelbase, for both the front and back wheels. This will be accomplished by a set of power screws under the chassis of the rover that will push the wheels apart. There will be a motor attached to the power screws that will expand a spacer bracket that will slowly push the wheels away from each other.

The second maneuver that must take place for the experiment to qualify as successful is that the rover must expand and increase its height. The drive motors and wheels will be attached to a bracket that will be secured at a certain angle while it is stored in the rocket, and will rotate to ninety degrees with respect to the chassis after the rover's departure from the rocket. A small pin will hold the bracket in place, and will be pulled by a tether attached to the rocket. After rotating downward and raising the chassis, a pin will lock the wheel at the desired ninety-degree angle.

6.3.2 Atmospheric Data Collection

The goal of the payload team was to treat the rover as if it was traveling to another planet, and this led to the desire to replicate some of the experiments that the Curiosity Rover has been conducting on Mars. Similar to the Curiosity Rover, R.I.C.K. will collect atmospheric data, simulating the collection of data on another planet. Based on the size constraints of the rover, and our budget, the team decided that the most feasible atmospheric data to collect includes the temperature, pressure, altitude, and relative humidity.

After conducting research into the types of sensors that could be used on the rover, the team decided to use a MPL3115A2 sensor board. This sensor board contains pressure, temperature, and altitude sensors on a single board and the payload team decided that this was the cheapest, most compact option. Once the rover departs from the rocket body and completes its 5 ft journey, the sensors will be activated and data collection will start for all three sensors. The data collected from these sensors will then be compared to the listed standards at the time of the launch.

The other property the payload team wanted to measure was the relative humidity at the time of the launch. This will be accomplished by an Adafruit Si7021 Breakout Board,

which has a humidity sensor on it. Similarly to the other three sensors, the humidity sensor will start recording data once the rover reaches its final destination and after the deployment of the solar panels. The collected data from the humidity sensor will also be compared to the listed standard values given by a reliable source on the day of the launch.

All of the above mentioned sensor data will be taken over an appropriate amount of time to allow the readings to reach its steady state conditions before it is compared to the actual values. For the payload team to consider these experiments a success, the sensors must turn on and start collecting data at the time the rover reaches its final destination. Another criterion for a successful experiment is that the data collected must be accurate to the specifications listed for each sensor. Collecting data is inadequate if that data is inaccurate, so the most important criterion for classifying this experiment as a success is definitely the collection of accurate data.

6.3.3 Navigation by Ultrasonic Sensor

The final experiment, which the payload team has designed for the rover to complete, is that it must navigate by using an ultrasonic sensor. The object of the ultrasonic sensor is to steer the rover away from any obstacles that could potentially hinder the motion of the rover, preventing the rover from accomplishing its primary objective of autonomously driving 5 feet away from the body of the rocket. The ultrasonic sensor is equipped with ultrasonic transmitters and receivers, which works similarly to echolocation. Since the purpose of the ultrasonic sensor is proximity sensing for object avoidance, the criteria for this being a successful experiment is the detection and avoidance of any obstacle along the rover's exploration outside of the rocket.

6.4 System Level Design

6.4.1 Payload Interface

Because the R.I.C.K. experiment has the unique design challenge of exiting from a cylindrical rocket, the orientation of the rover upon deployment was a critical design consideration. The payload team determined two methods by which the rover could deploy from the rocket: out the side of the airframe, in a hatch-like exit, or out of a separated circular cross-section of the rocket.

6.4.1.1 Hatch Exit:

The immediate design concern was the possibility of landing the rocket with the hatch face down. The team determined that the only way to avoid this mission critical issue was to design an active system to flip the rocket to a position where the hatch is exposed.

6.4.1.2 Cross-Section Exit

With this design, the rover is more likely to have an open exit from the rocket. However, the rocket can land on its side at any angle from 0-360° about its axis. To design against this, the rover either must be able to exit the rocket in any orientation, or must be moved to an upright position by some mechanism within the rocket

6.4.1.2.1 Multi-Orientation Rover

This design for the rover would allow for a larger overall rover size (because there would be no orienting system in the rocket), and a rover that could recover from flipping over in the rough terrain. However, this would add complexity to the rover, which is already very small, and would not guarantee that the solar panels would be pointed toward the sun.

6.4.1.2.2 Rotating Payload Housing

A payload housing within the rocket, where all structures securing the rover are attached to the inner rings of a set of bearings, would allow the rover to rotate to an upright position after landing. Figure 6.1 is the conceptual design of this bearing housing provided in the Space Raider Proposal.

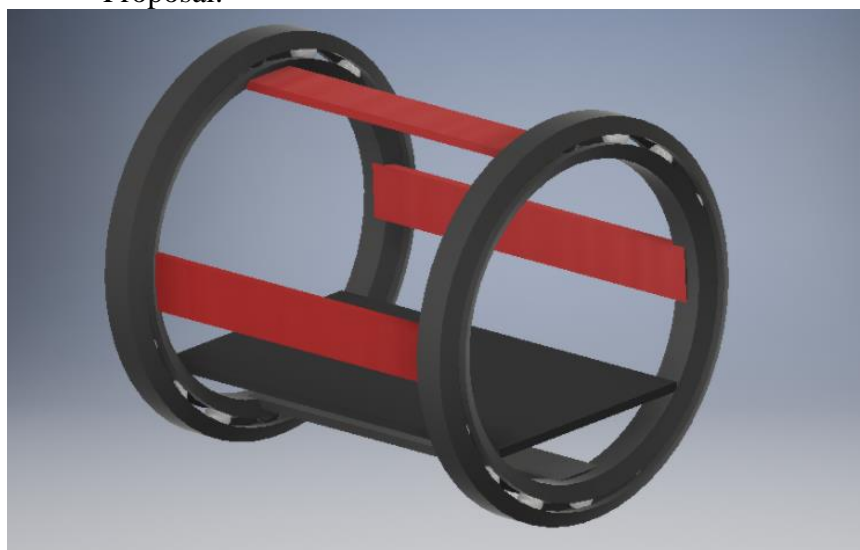


Figure 6.1 - Conceptual design of the payload's bearing housing, which rotates to ensure upright deployment of the rover

This design, which uses an offset center of mass as the driving force, does not require any motors to rotate the rover, and is therefore a simpler design. In addition, the mechanical systems are located on the rocket, rather than on the small rover.

The downside of a rotating payload housing is that the system may be less reliable, as it relies on gravity rather than a motor that the design team can control. This design also decreases the maximum rover size because the rover must fit within a more complex (and therefore larger) housing.

Beyond the overall structure of the payload interface, the physical interfaces between the airframe and the payload are important to keep the payload secure and reduce vibrations during flight. The team evaluated payload interfaces for a rover exiting out of a separated circular cross-section of the rocket, and several alternatives were determined.

6.4.1.3 Axle Pins

The rover has four wheels, and therefore four locations where a pin could be inserted concentrically into the axle to secure the rover in the rocket. This would provide a fairly even distribution of physical constraint across four locations on the rover. These constraints would also be applied to the relatively strong axles. However, a system to remove these pins would require four separate motors, or a very complex system to pull all four pins with one motor. This would also add unnecessary weight to the system.

6.4.1.4 Pins and Tracks

After researching CubeSat deployment methods, the team found that most Cubesats are deployed from rectangular boxes which contain the CubeSat during launch. After reaching the desired orbit, a spring within the box pushes the CubeSat out of the container.

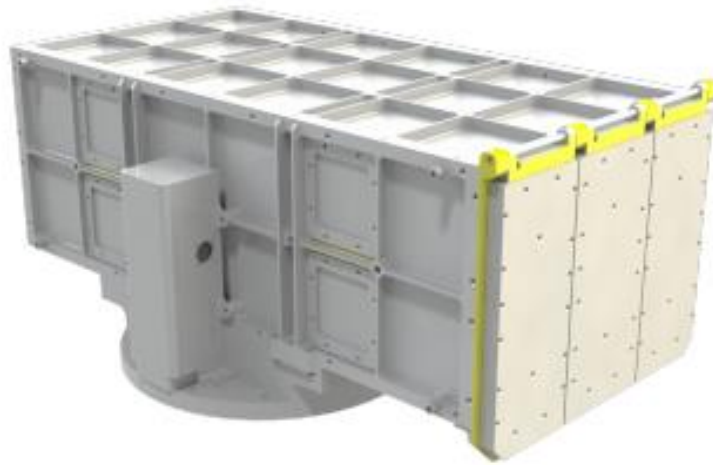


Figure 6.2 - Example of CubeSat housing (Nanoracks External CubeSat Deployer)

http://nanoracks.com/wp-content/uploads/ENRCS D_overviews.pdf

The team determined that matching the payload interfaces in CubeSat launchers would likely lead to a reliable design. According to the CubeSat Design Specification from California Polytechnic State University, CubeSats are required to be ejected using a rail system (https://static1.squarespace.com/static/5418c831e4b0fa4ecac1bacd/t/56e9b62337013b6c063a655a/1458157095454/cds_rev13_final2.pdf). In addition, some CubeSat launchers (such as the Single Picosatellite Launcher by AstroFein), use positioning pins to secure the rover prior to ejection (<https://directory.eoportal.org/web/eoportal/satellite-missions/c-missions/cubesat-concept>).

Drawing from designs used for CubeSats, the payload team developed a payload interface where the ends of the axles are located in horizontal tracks, which constrain the rover in the vertical direction (horizontal before launch). In addition, a vertical pin constrains the front of the rover chassis in both horizontal directions

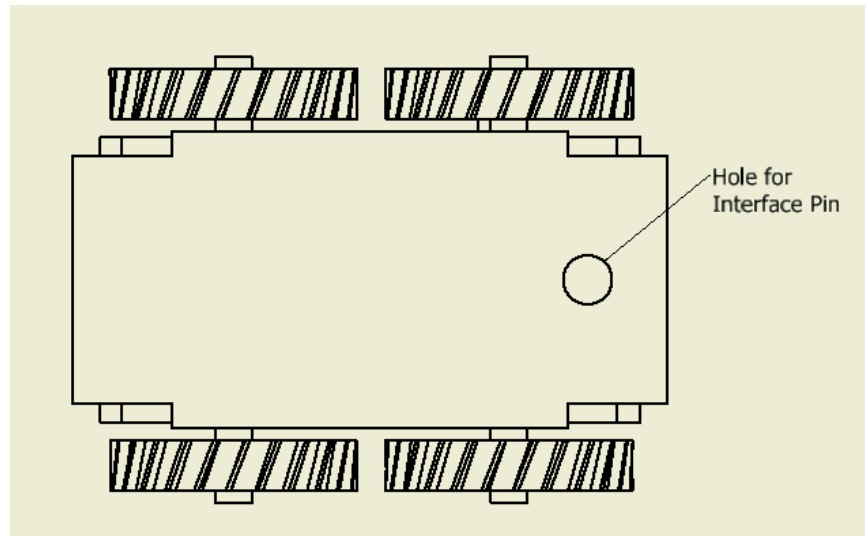


Figure 6.3 - Location of positioning pin at front of rover. Axles can be seen extending from the ends of the wheels, which would be contained in horizontal tracks

This design has the benefits of being documented on CubeSat developers. Although we are not operating a CubeSat, the small size of the rover has some similarities to Cubesats. In addition, this system is simpler, requiring only passive tracks and one motor to remove the pin at the front of the rover. The drawbacks are that the tracks require tight tolerances, and the pin at the front of the rover is not a distributed support.

6.4.1.5 Bayonet Fitting

Research also showed that some small satellite developers use a type of “bayonet fitting” integrated with a push spring to deploy satellites.



Figure 6.4 - Bayonet Fitting by NovaNano (a nano-satellite company) - <http://www.nanosat.jp/images/report/pdf/NSS-05-1002.pdf>

This type of fitting, at the back of the rover, will provide a solid mechanical connection at the bottom of the rover during launch. The release is completed with a simple rotation of the fitting. In addition, it is a design that has been used in the industry. However, the bayonet fitting only interfaces at one location on the payload, and is an active system, requiring a motor to function.

6.4.2 Electrical Systems

The electrical system on the rover is responsible for driving the rover to meet the 5 foot minimum requirement, running the various motors for panel deployment or other functions, and operating the additional experiments on-board the rover.

6.4.2.1 Microcontrollers

Two microcontrollers were originally considered for the logic control of the rover – Raspberry Pi Model 3B and an Arduino. The considerations for choosing between these two options were the size and mass, complexity and capabilities, and power consumption.

6.4.2.1.1 Physical Size

Comparatively, the Raspberry Pi is slightly larger than the Arduino Uno. The Raspberry Pi has approximate outside dimensions of 3.4" x 2.2" and a mass of 2.1 oz. The Arduino, by comparison, has approximate outside dimensions of 2.7" x 2.2" and a mass of .8 oz. Both the smaller size and smaller mass are benefits of using the Arduino.

6.4.2.1.2 Complexity and Capabilities

Overall, the Raspberry Pi is more capable than the Arduino. The Raspberry Pi can run multiple programs simultaneously, and has more processing power than the Arduino.

6.4.2.1.3 Power Consumption

Due to the higher processing power and greater functionality of the Raspberry Pi, it has higher power consumption than the Arduino. The Raspberry Pi does not handle running on batteries as well as an Arduino.

6.4.2.2 Battery

The criteria for selecting the rover battery were mass, voltage, and capacity. The mass of the battery affects the flight of the overall vehicle, but also the torque required from the drive motors on the rover. Given the comparative weight of the battery to the 8.9 foot vehicle, the torque considerations are more critical.

In order to keep the voltage at a reasonable value, the design selection was limited to two cell batteries, for a total voltage of 7.4 V. Finally, the capacity of the battery is a critical design decision because of the high power requirements of the Raspberry Pi.

6.4.2.3 Obstacle Sensors

In order to avoid obstacles, the rover must be able to identify the obstacles that are in its path. These sensors should be on the front of the rover, and calibrated or designed to recognize obstacles at a proper distance to avoid them effectively. Two methods were determined for obstacle sensing: mechanical switches and ultrasonic sensors.

6.4.2.3.1 Mechanical Switches

The idea of mechanical switches, which are essentially buttons on the front of the rover that are pressed when running into obstacles, was inspired by a NASA Innovative Advanced Concepts project currently being conducted by the Jet Propulsion Laboratory. This project is concerned with the development of the Automaton Rover for Extreme Environments (AREE), a fully mechanical rover designed to function in the harsh environment of Venus. Because this rover is fully mechanical, a bumper system is used to identify obstacles. Figure 6.5 is from the Phase I Final Report of this NIAC Project, and shows the bumper system designed for AREE.

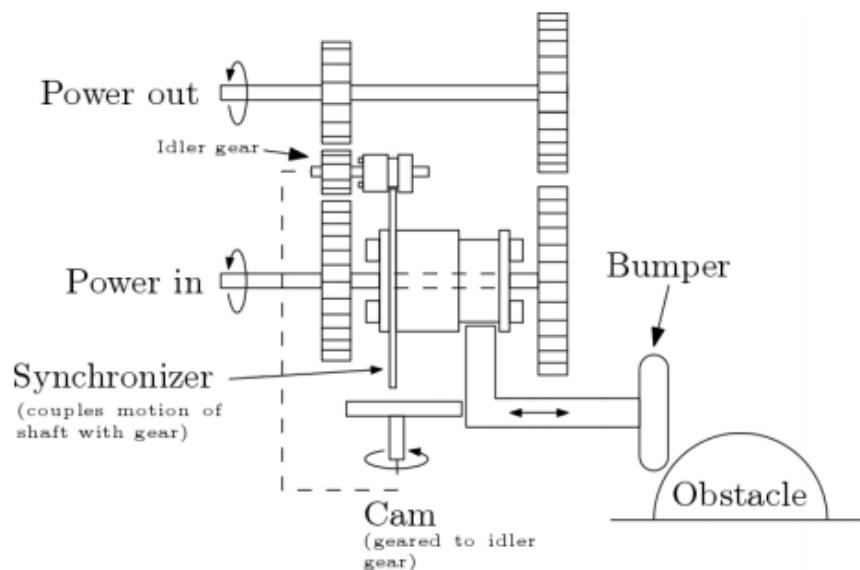


Figure 6.5 - Bumper obstacle avoidance system from NIAC AREE Project https://www.nasa.gov/sites/default/files/atoms/files/niac_2016_phasei_saunders_aree_tagged.pdf

The benefits of the button system are the simplicity, and the fact that the rover can have multiple buttons. By placing a button on the left and right side of the chassis' leading edge, the rover can drive left to avoid an obstacle to the right, and vice versa. However, the difficulty with the button system is

placing the buttons such that they are likely to contact obstacles before any other part of the rover.

6.4.2.3.2 Ultrasonic Sensors

The second possible obstacle avoidance system uses ultrasonic sensors to detect obstacles. Figure 6.6 is an example of an ultrasonic sensor that might be used.



Figure 6.6 - Ultrasonic Sensor for obstacle avoidance

The benefits of an ultrasonic sensor is the ability to calibrate the sensor to detect obstacles at any specified distance that is within range. This feature can be used along with a testing protocol to calibrate the sensors to detect an obstacle with adequate warning, but not detect the hills of the tilled landscape.

6.4.3 Payload Sensors

Every rover is designed to do more than just move away from the launch vehicle and open solar panels, and the R.I.C.K experiment is no different. After research into the instruments included on the Curiosity Rover, the payload team decided to include several sensors to measure air temperature, barometric pressure, altitude, and atmospheric humidity.

6.4.3.1 Pressure/Altitude/Temperature Sensor

Because of the limited space aboard the rover, it is imperative to use sensor boards with multiple functions. The team has had to take the limited power and output pins of the rover's control board into account when selecting sensors. After research, the team found two sensor boards that met all of the required specifications.

6.4.3.1.1 MPL3115A2 Sensor Board

The MPL3115A2 Sensor Board has pressure, altitude, and temperature sensors all contained in a single board. Due to its ultra-low power usage and high precision measurements ($\pm 2\text{ }^{\circ}\text{C}/\pm 1.5\text{ Pa}/\pm .3\text{ m}$), the MPL3115A2 fits the payload team's requirements. The MPL3115A2 is commonly used as an altimeter for model rockets so it can withstand the stress of flight and landing undamaged. The payload team chose this board as the best fit for the R.I.C.K

6.4.3.1.2 BME280 Atmospheric Sensor Breakout

The BME280 is very similar to the aforementioned MPL3115A2 board. It contains altitude, temperature, and barometric pressure sensors. While the BME280 is 133mm² smaller than the MPL3115A2, it is much less accurate. It is 3 times less accurate while dealing with altitude ($\pm 1\text{ m}$) and 8 times less accurate in measuring pressure ($\pm 12\text{ Pa}$) compared to the MPL3115A2. Because of the relative lack of accuracy and the higher cost, the payload team chose not to use the BME280.

	MPL3115A2	BME280
Cost	\$9.95	\$19.95
Dimensions	18mm x 19mm x 2mm / .7" x .8" x .1"	11mm x 19mm x 2mm
weight	1.2 g	1.1 g
Communications	I2C 7-bit address 0x60	I2C & SPI
Operation Voltage	3-5V	3.3V
Temp. Accuracy	$\pm 2\text{ }^{\circ}\text{C}$	$\pm 3\text{ }^{\circ}\text{C}$
Temp. Range	-10 to +85 $^{\circ}\text{C}$	-40 to +85 $^{\circ}\text{C}$
Pressure Accuracy	$\pm 1.5\text{ Pa}$	$\pm 12\text{ Pa}$
Pressure Range	50-110 kPa (up to 10Km altitude)	30-110 kPa (up to 10Km altitude)
Altitude Accuracy	.3 m	1 m

6.4.3.2 Humidity and Temperature

The Rover Environmental Monitoring Station (REMS) on the Curiosity Rover contains a humidity sensor, so the team wanted the ability to gauge the relative humidity in the atmosphere to be included on R.I.C.K. We were unable to find a sensor board that contained a humidity sensor and another sensor that was not already part of any other board on the rover. Because of this, the humidity board will also contain a redundant temperature sensor. After research, two boards became the most logical choices.

6.4.3.2.1 Adafruit Si7021 Breakout Board

The Si7021 has very accurate reading for both temperature and humidity, with .4 and 3% accuracies respectively. The Si7021 has very similar dimensions to the MPL3115A2 Sensor Board making them prime candidates for a space-saving stacked configuration. This board meets the 5v capacity of the control board. The space saving capabilities of the SI7021 make it the prime choice for the payload team.

6.4.3.2.2 DHT22 temperature-humidity sensor

The DHT22 is almost equal to the Si7021 in specs save for in size. It boasts comparable accuracy in temperature ($\pm 0.5^{\circ}\text{C}$) and humidity (2-5%) readings. However, the DHT22 is almost 3 times larger than the Si7021, and its massive size makes it impossible to implement onto the rover without compromising other systems on the rover.

	Si7021	DHT22
Cost	\$6.95	\$9.95
Dimensions	17.8mm x 15.3mm x 3.0mm / .7" x 27mm x 59mm x 13.5mm (1.05" x 2.32" x .6" x .1"	13.5mm x 59mm x 13.5mm (1.05" x 2.32" x 0.53")
weight	1.0 g	2.4 g
Communications	I2C 7-bit address	4 pins I2C
Operation Voltage	3 to 5V	3 to 5V power and I/O
Temp. Accuracy	$\pm 0.4^{\circ}\text{C}$	$\pm 0.5^{\circ}\text{C}$
Temp. Range	-10 to $+85^{\circ}\text{C}$	-40 to 80°C
Humidity Accuracy	$\pm 3\%$	$\pm 2-5\%$
Humidity Range	0-100%	0-100%

6.4.3.3 Other Sensors

The Curiosity rover and other rovers like it contains dozens of sensors and instruments. During research, the team worked to find which sensors would best fit the R.I.C.K. Some sensors that we wanted to include were impossible to add due to various limitations.

6.4.3.3.1 UV Radiation Sensor

Knowledge of UV Radiation levels is key for planning any future missions to an unknown environment. The team wanted to include a UV sensor aboard the R.I.C.K. but were unable to include one without compromising other necessary systems. To take any relevant measurements, the UV sensor must be subjected to direct sunlight. The solar panels are positioned in such a way that make it impossible get light on to the UV sensor consistently.

6.4.3.3.2 Wind Speed Sensor

Some sensors had to be excluded simply for being too large. The smallest wind speed sensor within budget was bigger than the whole R.I.C.K. There was talk of attempting to add a wind speed sensor to the solar panel mast, but we dismissed this idea after we calculated the torque that would be placed on the mast would cause a high chance of the panels or deployment system to be damaged.

6.4.3.3.3 Spectrometers/Radiation Detectors

Radiation Detectors and Spectrometers are a necessity on any interplanetary rover. They are large and complex systems that are next to impossible to compress. We are working with a micro rover so any attempts to add something like this to the rover would waste the team's time and resources for a non-essential purpose.

6.4.4 Solar Panel Deployment

One of the main objectives of the rover is to deploy solar panels after exiting the rocket. Because of this, the mechanism that will deploy the solar panels upon the rover's departure of the rocket was a major consideration of the payload team. The team decided that three solar panels was an appropriate amount to fulfill the requirement of increasing the surface area of solar panels in use by the rover. The decision to start with the solar panels initially stacked was also made, and from these decided upon initial conditions, two methods of expanding the solar panels were determined and are as follows: using a spring loaded rail system to extend the solar panels out of their initially stacked formation, or by using a hinge to unfold the panels.

6.4.4.1 Rail System

The rail system had immediate design concerns having to do with vibration. Since the rocket will have significant vibrations throughout its body the entire flight, the question of how to keep the spring locked in place until the necessary time to release it arose. Similarly, the problem of how to keep the solar panels from sliding down the rails and deploying prematurely emerged. The solution to both of these problems involved adding a set of blocking pins to constrain the motion of both the spring and the solar panel, which would require more motors. The team felt that this added an unnecessary amount of weight and complexity to the deployment system and decided that a better solution to this issue was to make the entire solar panels deployment system self-locking and thus the payload team considered a hinge system.

6.4.4.2 Hinge System

The hinge system was considered for its simplicity and its ease of making the system self-locking. It was found that we could reduce the weight of the deployment system by using a hinge, as well as reduce the amount of space this system would require. Since making the system self-locking was the primary focus, the initial design involved a system of gears to reduce the high speed of the selected motor and increase the torque in order to safely unfold the panels. However, upon farther research, we found that we could simply use a servo that could produce a sufficient amount of torque so that we could get rid of the gear

system and save weight and space. The inspiration behind the hinge system to unfold the solar panel came from NASA's Pathfinder rover (https://docs.google.com/presentation/d/1LYrrmL_mjf8kJD5BYmI8sshaXzsLSO_ghKvL1e8jrFU/edit#slide=id.p) and this can be seen in our designs. We chose to model our system after the way the Pathfinder rover deployed its solar panels, which is why our current design implements the hinge system to unfold the stacked solar panels.

6.4.4.3 Gear System

The concept of a self-locking mechanical system is what led the payload team to design a system that would use gears. Because of the self-locking capability of gears, the team decided that this was an acceptable option to further pursue. The payload team considered three different types of gears to control the rotation of the unfolding solar panel, rack and pinion, bevel gear, and a worm and wheel gear system.

The rack and pinion was considered first due to its stability and cheap cost. The rack and pinion system would be lightweight and would give us more control of the system than other options. However, for the objective that we were trying to accomplish, the rack and pinion system would not be as compact as the other researched gear systems. Upon further research, it was also found that the rack was used mainly for converting rotational motion into linear motion, which would mean our system would become more complex by adding more gears, which would add weight and take up more space. Because of these reasons, it was determined that the rack and pinion was not the best option to accomplish our necessary task.

Bevel gears are used mainly to transmit power between two rotating shafts that are orthogonal to each other, which is the goal we are trying to accomplish, and thus research was done to see if they would be the best option for us. Bevel gears were also considered because of their compactness and efficiency. Through our research, we discovered that bevel gears would be good for our application because they have a high torque capacity and traction between gear teeth prevents the gear from slipping. However, our research uncovered that bevel gears were more expensive, and they also have a limited gear range which would force us to create a larger gear box, taking up unwanted space on our rover. The team discovered that the same task could be accomplished by using a worm and wheel gear system for a reduced cost and thus decided that the best gear system to use is a worm and wheel gear system.

The worm and wheel was chosen for its capability to reduce the speed and increase the torque between two rotating shafts. Since the worm can create high gear ratios, it would be a more efficient use of space on the rover. Another advantage of the worm is that it is self-locking because of the high friction between the worm and wheel gears. Some disadvantages of using a worm is that they have a low efficiency and a high operating temperature because of the high friction between the gears. We came to the conclusion that advantages of using a worm would compensate for the disadvantages and a decision was made to move forward with a conceptual design of this system as shown in figure 6.7.

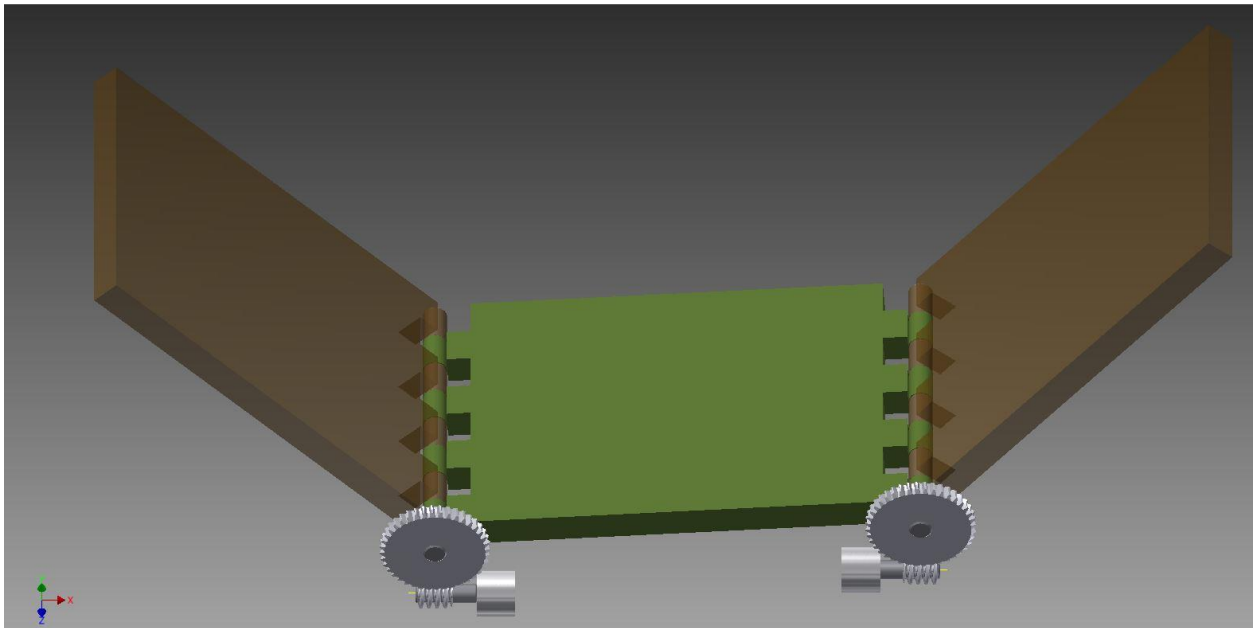


Figure 6.7: Hinge system using worm and wheel gears

Upon farther development of our research however, the team found a servo that offered continuous rotation which could accomplish the same task as the motor and gear system, which led to the current design of our solar deployment system.

6.4.4.4 Rotation Using a Continuous Servo

The current design that the payload team made uses two servos to control two different shafts that will rotate the solar panels similarly to a door hinge as shown in figure 6.8. The decision to use only servos, as opposed to a bigger motor with a gear system, was made because of the reduction in weight to the system and the compactness it offered. Research showed that a servo is ideal for accomplishing our task because servos operate at a low speed with a high torque, which eliminates the need for a gearbox like our previous design. This also reduces the weight of the deployment mechanism and reduces the overall cost of the deployment system which was a significant deciding factor when deciding between the motor and gear system and a continuous rotation servo. The servo is also easily controllable and is the most compact design we have made which was another significant deciding factor for the payload team.

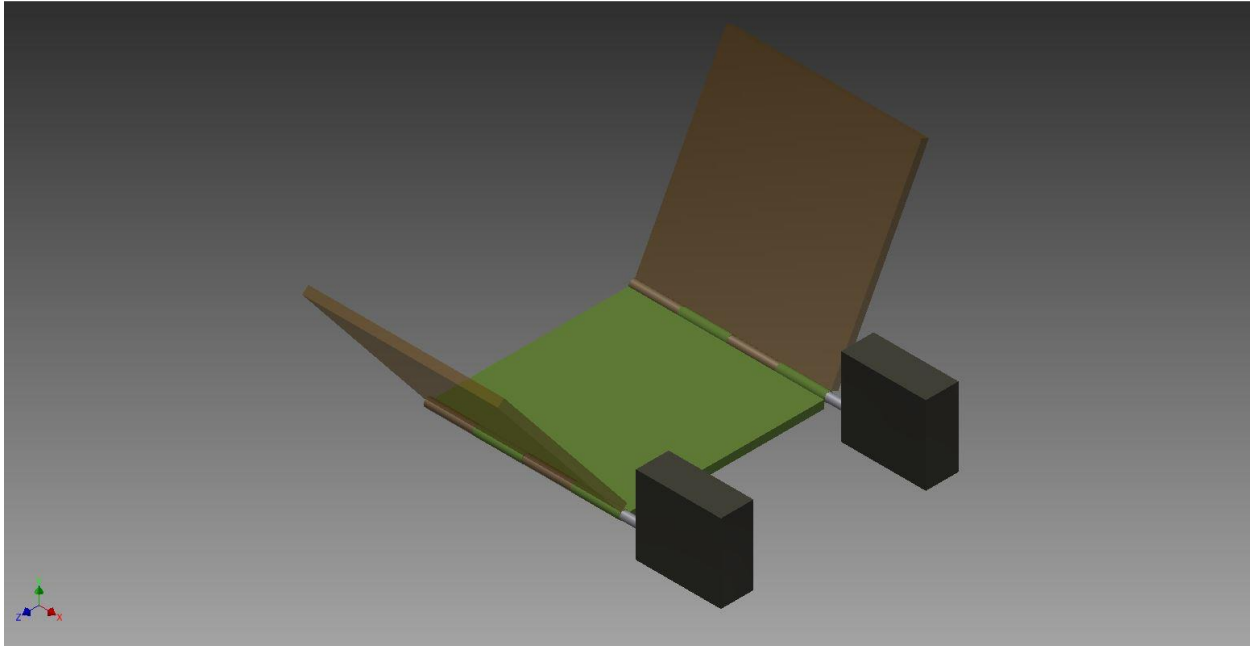


Figure 6.8

6.4.5 Stowaway, Drivetrain and Steering System Configuration

Creating a system to not only drive the wheels but also turn the rover is a unique challenge due to the nature of the small dimensions required in stowaway. Two operations to negate the negative affect of small dimensions were looked into for the stowaway, drivetrain and steering systems.

6.4.5.1 Steering Systems:

6.4.5.1.1 Traditional Ackermann Steering System

This system incorporates a steering shaft that is driven by a motor and turns the sway bar, which moves the control arm a precise way, and in turn changes the angle of wheels with the ground. When turning left, the front of the left front wheel makes a considerably larger movement to the left than the right wheel as shown in figure 1. One of the advantages for this system is the ability to turn without coming to a dead stop, turning, and then accelerating through the turn. However, an Ackermann steering system is quite complex given the rover's small geometry and would require many complex 3d printed parts and the rover would be limited in how much weight it can handle.

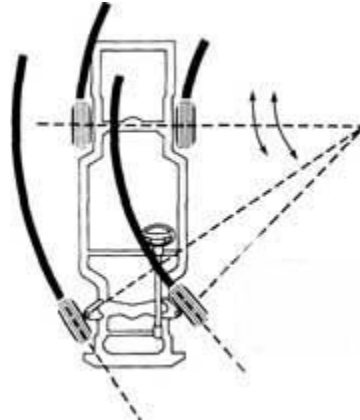


Figure 6.9

<http://www.wheels-inmotion.co.uk/forum/uploads/post-2-1148242025.jpg>

6.4.5.1.2 In-Wheel Motor Steering

In-Wheel Motor Steering would take a page from robotics. The rover would be required to come to a stop, where it would then power opposite wheels in different directions. For example, driving the right front reverse and left rear forward, while keeping cutting power to the two other wheels, would cause the rover to turn right. The biggest disadvantage to this system is the need for one motor on each wheel, although these motors can be significantly smaller than a single motor turning an axle moving a pair of wheels. One major advantage is how mechanically simple the in-wheel motor steering system is.

6.4.5.2 Payload Stowing:

6.4.5.2.1 Axle Extension System

A short wheelbase is one of the major disadvantages of having limited room in the payload housing for the rover to fit. This can be circumvented with a system that will extend the wheelbase after the rover leaves the rocket. The major disadvantage of extending the wheelbase would be the extra weight required by the motors and housing. Nevertheless, the largest benefit would be increasing the stability of the rover over rough terrain.

6.4.5.2.2 Wheel Lift System

Ground clearance is a challenge when working with such tight dimensions. The wheel lift system will tuck the wheel axle up to the chassis during stowaway, and then rotate the wheel axle out and down using a spring. The biggest disadvantage to this system would be raising the rover's center of gravity, increasing the likelihood the rover tips over when traveling over a hill at an angle. The biggest advantage would be increasing the ground clearance of the rover and allowing the wheels to sink in the dirt a little more while still having the center of the rover above the ground.

6.4.5.3 Drivetrain:

6.4.5.3.1 Belt Driven Drivetrain

The belt drivetrain is by far the simplest and lightest. This drivetrain would only require one motor per pair of wheels. A motor mounted toward the center of the chassis would drive a belt through a pinion gear, and the belt would then rotate a much larger spur gear attached to the axle. One of the biggest disadvantages of this system is the lack of variability in the torque to each wheel, potentially causing problems when driving over dirt hills.

6.4.5.3.2 In-Wheel Motor Drivetrain

The in-wheel motor drivetrain requires an individual motor, axle, spur and pinion gears for each wheel. The use of sensored brushless motors will allow the Raspberry Pi to know how much each wheel is turning and be able to adjust the power to each wheel to keep the rover moving completely straight. The biggest drawback to in-wheel motors are the added electronic complexity of four motors instead of one. The largest advantage is being able to drive the rover and steer the rover without any mechanical parts outside the motors and wheels.

6.5 Leading Payload Design

The payload team conducted a significant amount of research that went into the design of each subsystem of the payload before coming to any conclusion regarding the best design to pursue. The subsystems are as follows: The payload interface, rover drivetrain and steering system, rover storage system, sensors for additional experiments, and the solar panel deployment system. A detailed description of the leading design for each subsystem is explained below.

6.5.1 Payload Interface

6.5.1.1 Housing

The payload housing will be a rotating, double bearing structure, with struts in between the bearing, and a bottom platform for the rover. The front of the housing will have a front plate to protect the rover from the nosecone charge, as well as a ramp for the rover to exit the housing. The back of the housing will have a back plate to support the rover during the relatively high forces during launch.

The rotating bearing housing was chosen over the hatch exit because it solved the issue of landing the rocket in any orientation, and still deploying the rover. It also allows for a mechanically simpler rover, because the rover only needs to be able to operate in one orientation after the housing rights itself. Although using the offset center of mass as a driving force may be unreliable, rigorous testing will be done to ensure that the rover will right itself from any orientation. The housing, which the rover is secured in during the flight of the rocket, can be clearly seen in figure 6.10.

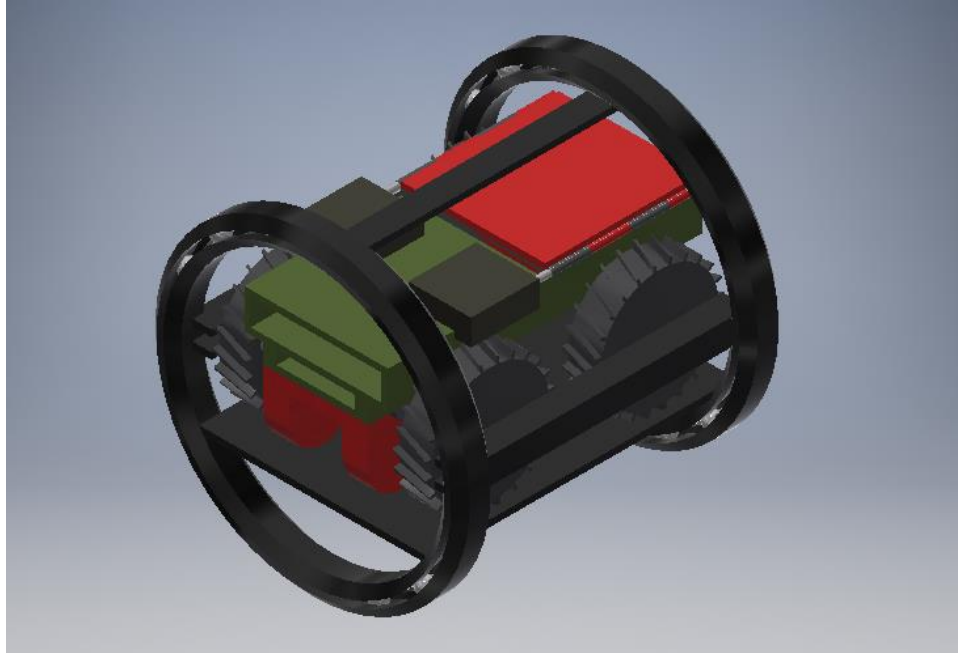


Figure 6.10: Housing with the Rover Secured

6.5.1.2 Interface

The goal of the payload positioning and constraint methods was to secure the rover in all three degrees of freedom in at least two locations. This decision drove the selection of payload interfaces.

First, the team chose to use a bayonet fitting at the back of the rover, because of the benefits of securing the rover at its lower-most part during launch. This interface constrains 3 degrees of freedom at a structurally secure section at the back of the chassis. Figures 6.11 and 6.12 show the initial and final states of the bayonet fitting. The bayonet fitting is also integrated with the system that will release the inner bearing ring from the outer bearing ring of the payload housing. Before the bayonet fully releases the rover, the inner ring will separate from the outer ring and rotate freely to put the rover in an upright orientation.

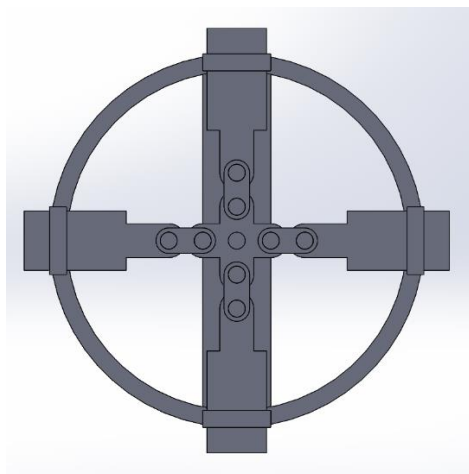


Figure 6.11: Initial state of the bayonet fitting and bearing ring release

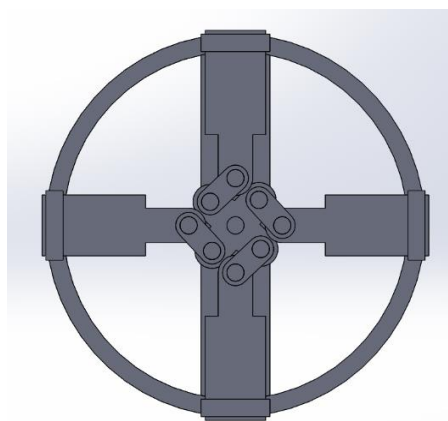


Figure 6.12: Final state of the bayonet fitting and bearing ring release

Second, the team selected the tracks and pins method discussed previously. This method uses two tracks that the ends of the axles are constrained within, as well as a vertical (at landing) pin through the front of the rover chassis. This interface design constrains 1 degree of freedom due to the rails, in the vertical direction, and 2 degrees of freedom due to the pin, in the horizontal directions. Figure 6.13 shows a better view of this track and pin system of locking the rover in the housing.

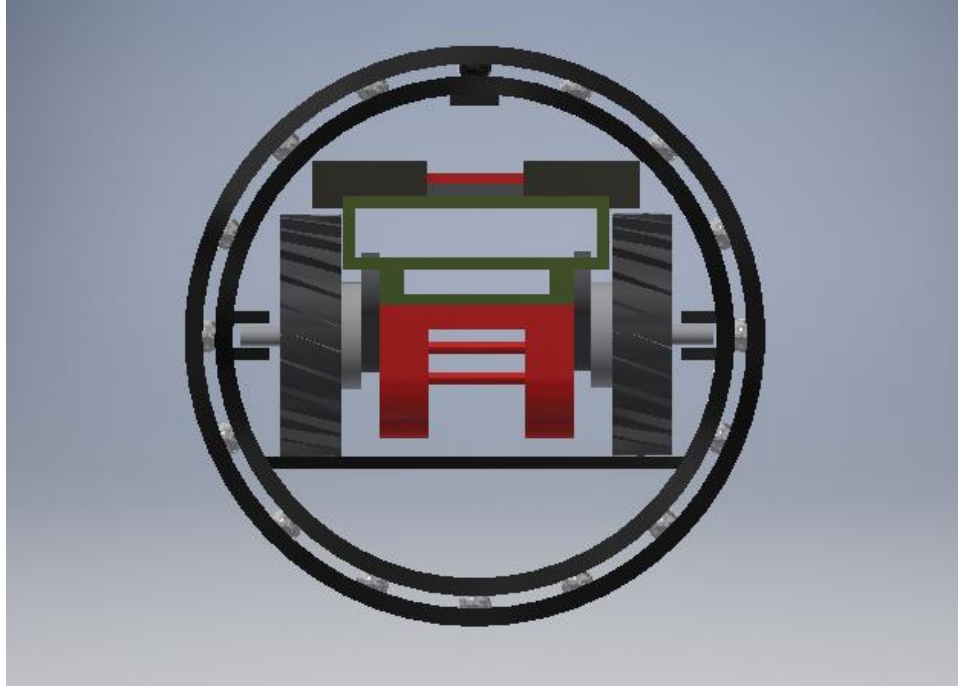


Figure 6.13: Front view of the track and pin system

Additionally, the wheels of the rover will be constrained against the front and back plates of the housing. This additional constraint will provide more support for the rover during launch.

The team decided against securing the rover with concentric pins in the axles. The required complexity and weight of a design using one motor to accomplish this was a major factor in this decision. Alternatively, using a single motor for each of the four pins was too heavy and expensive to be feasible.

6.5.2 Rover Drivetrain Method

The need to constantly adjust the power in each wheel while traveling over loose dirt to maintain a straight velocity is a challenge.

6.5.2.1 Leading Design for Drivetrain System

The goal of the drivetrain system is to have as much control of the rover's velocity and ability to climb over the small dirt hills. This led to our decisions for the drivetrain.

The use of sensed in-wheel brushless motors will allow each wheel's rotational velocity to be the same over loose dirt. The Raspberry Pi will know the rotational velocity of each motor from the electronic speed controller's signals.

The Raspberry Pi will then vary the power sent to each wheel to maintain a constant rotational velocity across all four wheels. The motor will use a small pinion gear in sync with a larger spur gear on each wheel to increase the torque produced. The motors being used are designed for model airplanes, so they occupy a smaller volume. The motor and wheel will be attached to the independent sleeves used to extend the axle.

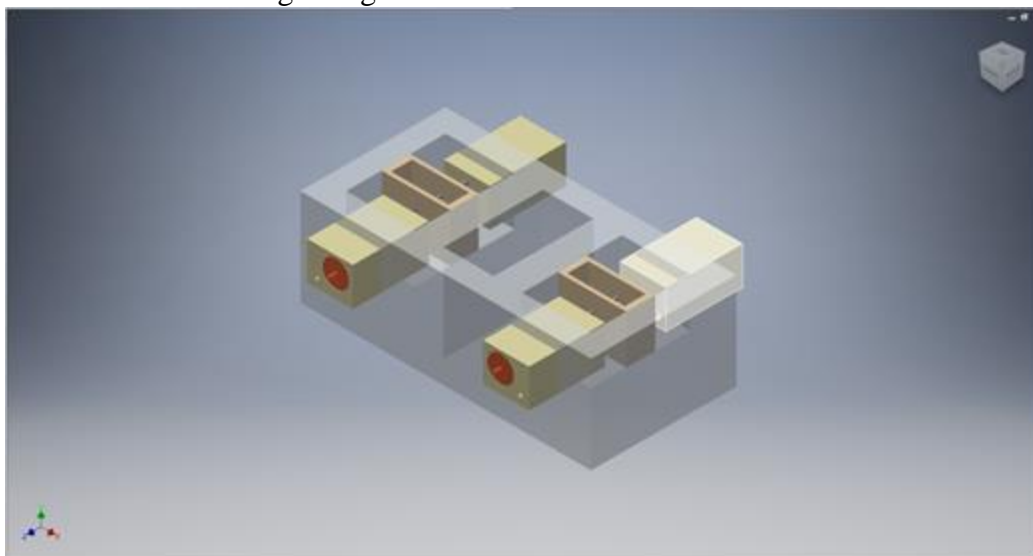
6.5.3 Rover Steering Methods

The space inside the rocket limits the options for a complex steering system. The goal for the steering system is to allow the rover to have as small of a turning radius as possible. This led the team in the decision to use the in-wheel motors independence to alter the movement of the rover without a traditional mechanical steering system. When the rover is travelling, and needs to turn, it will come to a complete stop. Then if it needs to turn right it will rotate the front right wheel in reverse while simultaneously rotating the left rear wheel forward. This will allow for a very small turning radius, similar to how a zero-turn lawn mower works.

6.5.4 Rover Stowing Methods

Because the size of the rover is constrained by the inner diameter of the rocket, storing the rover in the rocket with all of its equipment was a major concern of the payload team.

6.5.4.1 Leading Design for Axle Extension



The goal for the axle extension is to extend the wheelbase of the rover so it has more stability under motion, while not compromising in structural integrity. This goal led the team to our decision for how to extend the axle, which can be seen in figure 6.14.

The housing will secure a power screw lift that will push the wheels out extending the wheelbase. The motor will be mounted to this housing and the motor will then rotate the two ACME power screws through the threaded holes in the housing, pushing the sleeve through the key hole in the chassis. The sleeve will house the motor as well as the axle for each wheel and will have threaded holes to secure each motor to the sleeve itself. These screws within the sleeve will cause the motor housing to be rotationally static while running. Each sleeve will have a hole for the axle of each wheel to be secured to. Pins will secure each sleeve, on the inside of the chassis, to keep them from sliding out of the key hole while the rover is moving. The motion of the axle extension system can be

seen in figures 6.15 and 6.16, which show the system in the initial and final states.

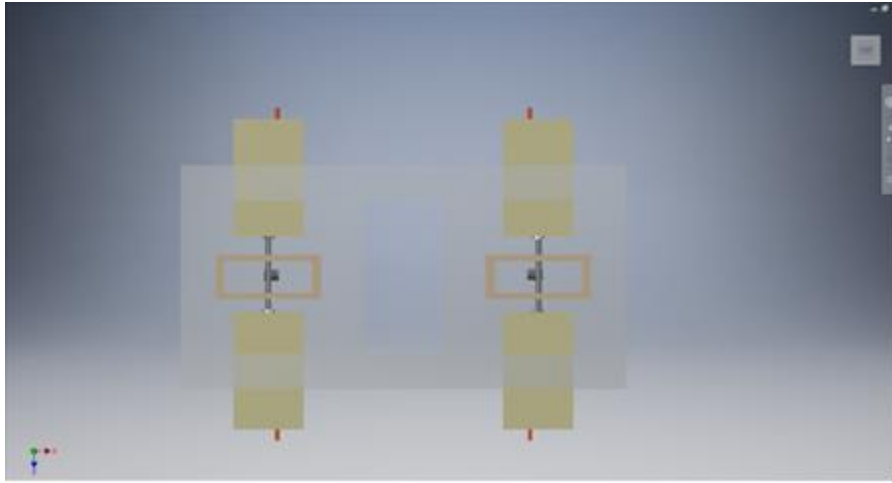


Figure 6.15: Initial state of the axil expansion system

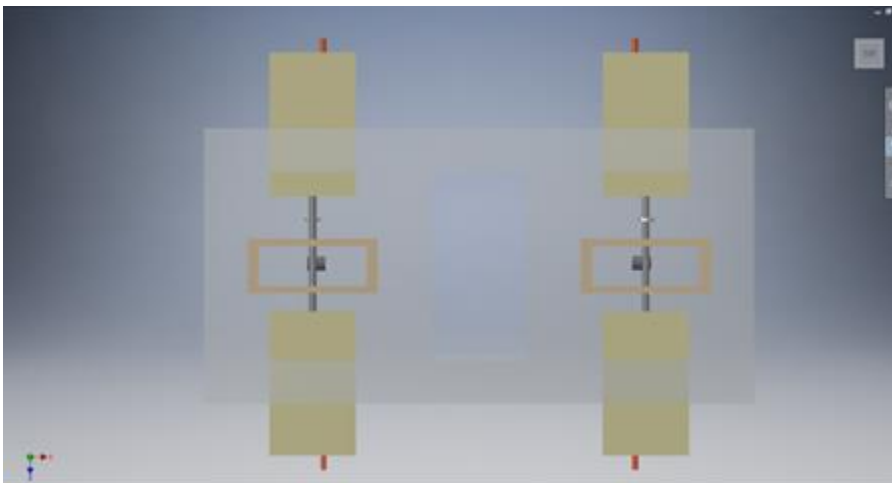


Figure 6.16: Final state of the axil expansion system

6.5.5 Sensors

The goal of the additional sensors is to gather as much data while using as little space and power as possible. The payload team decided that two sensor boards would provide the results for the investment. The first sensor board that we are using is the MPL3115A2 Sensor Board. The MPL3115A2 Sensor Board measures pressure, altitude, and temperature with an acceptable range and accuracy. The MPL3115A2 Sensor Board is a better choice than the BME280 Atmospheric Sensor Breakout because the BME280 is

twice the cost with no notable advantages over the MPL3115A2. The second board that we decided to use is the Adafruit Si7021 Breakout Board. The Adafruit Si7021 Breakout Board measures the humidity and temperature. The DHT22 temperature-humidity sensor was much too large to fit on the R.I.C.K without disrupting other systems. Due to space concerns, no other sensor boards will be included on the rover.

6.5.6 Solar Panel Deployment System

The solar panel deployment system was a major concern because the deployment of solar panels is a primary objective of the rover. The leading design for the storage of the solar panels while in the rocket is to have three stacked on top of each other, with the bottom one being attached to the chassis of the rover. The two other solar panels will be attached to high density polyethylene plates which will unfold in opposite directions at a specified time.

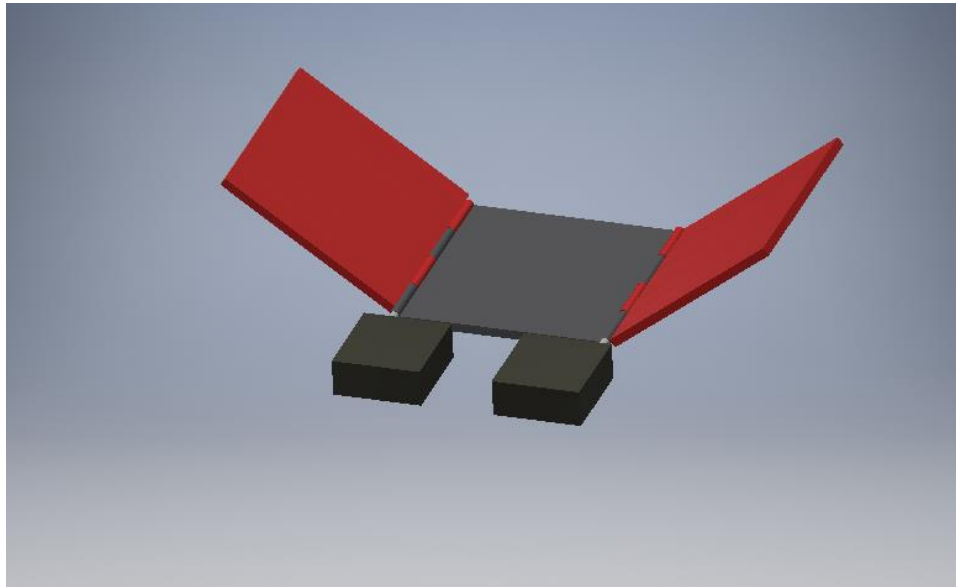


Figure 6.17: Solar Panel Deployment System

The panels that are unfolding are going to be hinged to the chassis of the rover and will be held together by a small shaft that will run through the hinges. There will be a loose fit tolerance between the shaft and the hinge on the chassis, allowing the shaft to freely rotate without creating a torque on the chassis so that the panel will stay stationary. There will be a tight fit tolerance between the shaft and the hinge on the stacked solar panels. This will allow a torque to be created, causing the panel to unfold with the rotation of the shaft. The current leading design is to use a continuous rotating servo to rotate the shaft that is causing the unfolding action. This design was chosen over the alternatives mentioned in the earlier sections because of its simplicity and compactness, as well as its cost efficiency and weight reduction. Figure 6.17 shows the solar panel deployment system in the process of unfolding the two panels. Figure 6.18 shows the solar panels attached to the chassis of the rover in its initially stacked formation. Once the rover departs

from the rocket and reaches its final destination, the final orientation of the solar panels can be seen in figure 6.19.

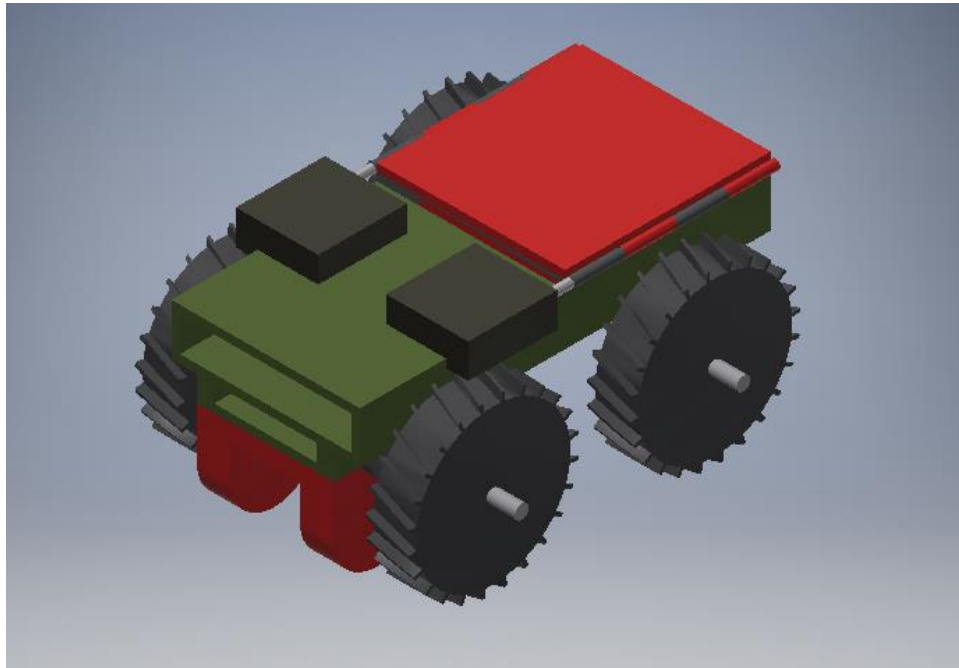


Figure 6.18: Solar Panels Initial State

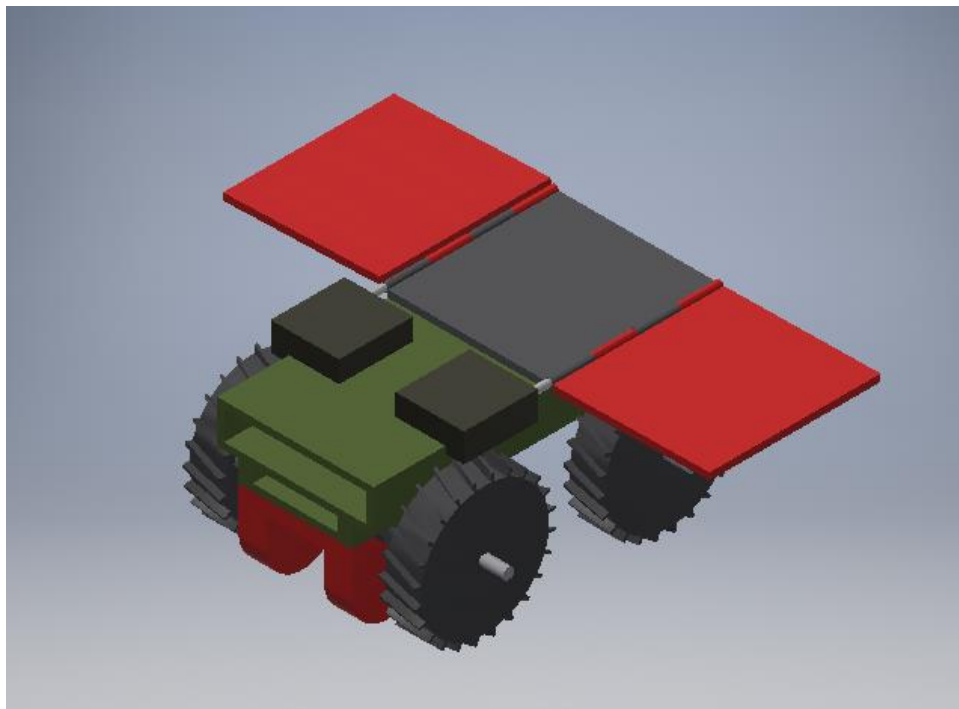


Figure 6.19: Solar Panel Final State

The payload team determined that the hinged system of unfolding solar panels was the best option because of its compactness and simplicity. Another reason this design was selected was its ability to be self-locking, which was a key design criterion because of the constant changing orientation of the rover during flight and landing. Another critical parameter of this design that led to its selection as the leading design is the fact that servos operate at low speeds with high torques, which is ideal for the task we are trying to use the servo to accomplish.

6.5.7 Electrical Design

6.5.7.1 Raspberry Pi and Operating System

The rover will be controlled with a Raspberry Pi model 3-B (1.2 GHz, 64-bit quad core ARMv8 CPU 1GB RAM), the operating system for the Pi module will be Rasbian which is an optimized version of linux. All rover functions will be handled through python scripts maintained within the linux system.

The Pi module will be activated upon receiving a signal (2.4 GHz) from ground operators. The decision to use a Raspberry Pi over an Arduino was primarily due to the increased functionality of the Raspberry Pi, given the required additional experimentation on the rover.

6.5.7.2 Motors

An ESC will connect from the Raspberry Pi to the driving motor for each of the four wheels. These motors will be brushless DC motors with a kV of 2400. Additionally, a wheel base expansion rig will be powered by two additional motors with their own gearbox set up. The Raspberry Pi will be receiving input from an ultrasonic sensor (40 kHz bursts at a range of between 2 cm and 450 cm) in front of the rover to identify obstacles in the rover's path.

6.5.7.3 Wiring Diagram

Figure 6.20 shows an approximate wiring diagram, including all motors, servos, and sensors that will be connected to the Raspberry Pi and battery.

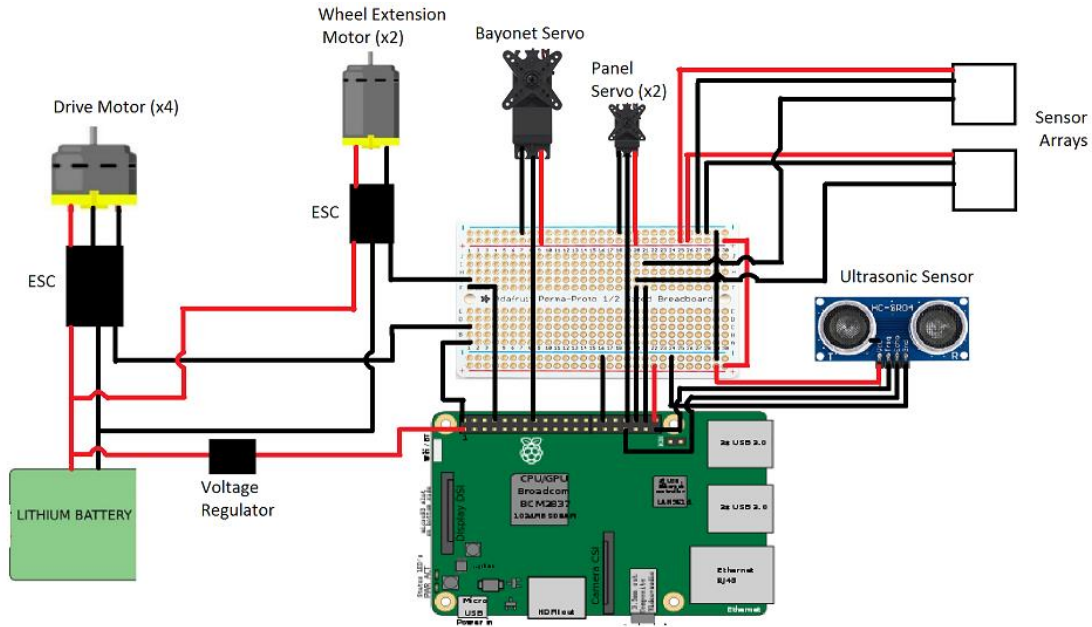


Figure 6.: Wiring diagram for the rover electrical system

Page Break

6.5.8 Mass Estimate for Leading Design

Mass estimates were calculated for both the housing and payload interface and the rover itself. Below are the line item spreadsheets for the mass estimates.

Table 6.1: Mass Estimate for Payload Housing and Interface

The total estimated mass of the housing and interface is 18.049 oz, while the total estimated mass of the rover is 33.877 oz, so the total mass of the payload is expected to be 51.926 oz, or 3.25 lb.

6.6 Verification Plan

6.6.1 Bearing Housing

The test and analysis for the bearing housing system will be conducted with full size models and computer simulations. The bearing system full-size models will be stress tested with mock rovers with similar weights. All possible landing orientations will be tested with mock rovers to ensure functionality. These tests must be conducted prior to any test launches aboard the vehicle.

6.6.2 Payload Interface

The payload interface system includes the inner ring pin lock, the bayonet fitting, and the pins and tracks. The pins and tracks will be tested with full sized models of both the rover and payload housing. Stress simulations will be run on the vault pin lock and the bayonet fitting prior to creating full scale models. All the tests for scale models will be run in cognition with the testing of the payload housing.

6.6.3 Drivetrain and steering

Drivetrain and steering systems are defined as systems responsible for the movement and the automated steering of the rover. All motors will be tested prior to installation to ensure all they are able to meet the required minimum forces. The steering system will undergo testing in controlled environments to ensure all sensors are accurate and the system will respond to obstacles as planned. The team will conduct a full-scale test in corn or cotton fields like the expected performance environment.

6.6.4 Solar Panel Deployment

Solar panel deployment consists of the panel housing, the deployment gear assembly, and the deployment motor. The entire system will undergo computer simulated stress testing prior before any scale models are constructed. The motor output will be tested and measured to ensure it meets projected forces. The panel housing will be tested with mock solar panels in all configurations.

6.6.5 Electrical Systems

The electrical systems include all electrical components outside of pre-fabricated sensors and motors. The heart of the Electrical system and the rover itself, the Raspberry Pi will be inspected for any faults before installation and after any test of the rover.

6.7 Team Derived Requirements

NASA's rover requirements are for the rover to travel 5 feet through a plowed field of dirt and then deploy a solar panel that does not have to charge or power the rover. Rover R.I.C.K. will go beyond these requirements with the following:

6.7.1 In-Wheel Motors

Using in wheel-motors allows complete control and knowledge of each individual wheel at all times.

6.7.2 Autonomous Steering System

6.2.7.1 Incorporates an ultrasonic sensor to detect objects the rover needs to avoid.

6.7.2.2 Uses the in-wheel motors like a zero-turn lawn mower to allow extreme navigation requirements without mechanical parts.

6.7.3 Axle-Extension System

Extending the wheelbase will allow for a lower center of gravity while allowing the rover to still fit in the stowaway.

6.7.4 Wheel-lift system

The wheel-lift system raises the ground clearance to circumvent the extreme requirements to fit in the stowaway.

6.7.5 Sensors

Environment sensors provide accurate measurements of atmospheric pressure, humidity, altitude, and temperature.

6.8 Verification plan for additional team requirements

The payload team wanted to go beyond the requirements set by NASA, and decided on added experiments to conduct. Additional testing to ensure that these experiments are feasible will be required, and thus various testing techniques were discussed.

6.8.1 Rover Stowing

Rover stowing systems are defined as systems responsible for compressing the rover while in flight and prior to exit from the payload housing. These systems include axle expansion systems and other compression systems. Computer simulated stress tests will be run on the compressed states of all rover stowing systems. The motor output will be tested for each motor and measured to ensure it meets projected forces. The team plans on conducting multiple full-scale tests of the system, making sure that the rover compresses and expands to the desired dimensions.

6.8.2 Sensors

The onboard sensors will undergo calibrating measurements and a -series of tests to ensure that the data we collect from them is accurate. The environmental sensors will be tested in different controlled environments to again guarantee that our collected data will be accurate. All sensors will be run through computer simulated launches and landings to ensure they will hold up under any stresses during flight.

6.9 Rover Line Item Budget

VII) Project Plan

a. Requirements Verification

7.1 Vehicle Requirements

Vehicle Requirements	Design Features to fulfill the requirements
<i>The vehicle will deliver the payload to an apogee altitude of 5,280 feet above ground level (AGL)</i>	Make sure the simulation is around 1609 meters and stays below 1700 meters (5577.428 feet).
<i>The vehicle will carry one commercially available, barometric altimeter for recording the official altitude used in determining the altitude award winner. Teams will receive the maximum number of altitude points (5,280) if the official scoring altimeter reads a value of exactly 5280 feet AGL. The team will lose one point for every foot above or below the required altitude.</i>	We will have two Stratologger CF altimeters for main and backup altimeters. The backup altimeter will be the designated altimeter for NASA.
<i>Each altimeter will be armed by a dedicated arming switch that is accessible from the exterior of the rocket airframe when the rocket is in the launch configuration on the launch pad.</i>	We will have the switches built into the body frame which can be accessed from the outside body. Each altimeter will have its own designated switch.
<i>Each altimeter will have a dedicated power supply</i>	We will have two 9-volt batteries which are connected to each altimeter
<i>Each arming switch will be capable of being locked in the ON position for launch (i.e. cannot be disarmed due to flight forces)</i>	We will have the switch built in into the body near the e-bay.
<i>The launch vehicle will be designed to be recoverable and reusable. Reusable is defined as being able to launch again on the same day without repairs or modifications.</i>	We will design the rocket to be recoverable and reusable by putting focus on the recovery system to land the rocket in a recoverable state and not to damage the rover.
<i>The launch vehicle will have a maximum of four (4) independent sections. An independent section is defined as a section that is either tethered to the main vehicle or is recovered separately from the main vehicle using its own parachute.</i>	The design of our rocket is in four sections being the nose cone,
<i>The launch vehicle will be limited to a single stage.</i>	The rocket is a single staged rocket

<i>The launch vehicle will be capable of being prepared for flight at the launch site within 3 hours of the time the Federal Aviation Administration flight waiver opens</i>	We will have the rocket prepared and ready for flight no later than the day before launch so that no problems arise before the 3 hours the FAA flight waiver opens.
<i>The launch vehicle will be capable of remaining in launch-ready configuration at the pad for a minimum of 1 hour without losing the functionality of any critical on-board components.</i>	We will design the electronics of the rocket and rover to be ready for at least an hours' time of launch.
<i>The launch vehicle will be capable of being launched by a standard 12-volt direct current firing system. The firing system will be provided by the NASA-designated Range Services Provider.</i>	The launch vehicle will have rail buttons to slide onto the launch rail to launch the vehicle.
<i>The launch vehicle will require no external circuitry or special ground support equipment to initiate launch (other than what is provided by Range Services).</i>	The launch vehicle will only have the electronics for altimeter and rover which are already included inside the vehicle.
<i>The launch vehicle will use a commercially available solid motor propulsion system using ammonium perchlorate composite propellant (APCP) which is approved and certified by the National Association of Rocketry (NAR), Tripoli Rocketry Association (TRA), and/or the Canadian Association of Rocketry (CAR).</i>	The motor will be a commercially availb Cesaroni L1410-SK
<i>Pressure vessels on the vehicle will be approved by the RSO and will meet the criteria of 2.14.1, 2.14.2, and 2.14.3 in the handbook</i>	We will perform pressure tests on the rocket to make sure it is passing.
<i>The total impulse provided by a College and/or University launch vehicle will not exceed 5,120 Newton-seconds (L-class).</i>	We made sure to choose motors which have the total impulse below the 5120 Newton-seconds limit.
<i>The launch vehicle will have a minimum static stability margin of 2.0 at the point of rail exit. Rail exit is defined at the point where the forward rail button loses contact with the rail.</i>	The launch vehicle will have a simulation stability margin of at least 2.1.
<i>The launch vehicle will accelerate to a minimum velocity of 52 fps at rail exit.</i>	We will calculate the rail exit velocity to confirm the minimum velocity of 52 fps will be achieved
<i>All teams will successfully launch and recover a subscale model of their rocket prior to CDR. Subscals are not required to be high power rockets. 2.18.1-2.18.2</i>	We will launch a subscale model of our rocket.

<p><i>All teams will successfully launch and recover their full-scale rocket prior to FRR in its final flight configuration. The rocket flown at FRR must be the same rocket to be flown on launch day. The purpose of the full-scale demonstration flight is to demonstrate the launch vehicle's stability, structural integrity, recovery systems, and the team's ability to prepare the launch vehicle for flight. A successful flight is defined as a launch in which all hardware is functioning properly (i.e. drogue chute at apogee, main chute at a lower altitude, functioning tracking devices, etc.). 2.19.1 – 2.19.7</i></p>	<p>The launch vehicle we fly during the FRR will be the same launch vehicle used on launch day. We will however use a weight in place of our rover during FRR.</p>
<p><i>Any structural protuberance on the rocket will be located aft of the burnout center of gravity.</i></p>	<p>It will be located at the burnout center of gravity.</p>
<p><i>Vehicle Prohibitions</i></p>	<p>Our motor will <u>not</u> be a hybrid, a cluster, utilize forward canard and firing motors, utilize friction fitting, and will not exceed Mach 1 at any point during the flight. In addition, the vehicle ballast will not exceed 10% of total weight of our rocket.</p>

7.2 Pre-Launch Checklist:

- Motor is secure in rocket
 - a. Motor has bulkhead preventing it from shooting through rocket
 - b. Motor has thrust plate to disperse force of motor from acting on just the centering rings
- Motor is properly assembled
 - a. Inspect configuration
- Drogue and main chutes are packed properly and protected against pyro charges
 - a. Drogue chute is packed and attached to shock cords
 - b. Shock cords are secured to bulkheads by a strong and sturdy knot on the U-bolt Drogue chute does not get tangled
 - c. Main chute is packed and attached to shock cord
 - d. Main chute does not get tangled
 - e. Both chutes are protected from when the pyro goes off
- DACS is properly secured and working functionally
 - a. Rectangular flaps move
 - b. Can run through the calculations and adjust while in flight
 - c. Secured and mounted correctly
 - d. Wired correctly
- E-bay is secured on sled
 - a. E-bay is protected from pyro charges
 - a. E-bay is between bulkheads to prevent altimeters and batteries from getting damaged
- Each altimeter is properly armed by an on/off switch
 - a. Inspect wiring to make sure there is no exposed wire or break
 - b. Inspect to make sure the altimeter goes through the beeping sequence when the switch is flipped on
- Check program of both altimeters
 - a. Altimeters are set to deploy drogue chute when the vehicle reaches apogee
 - b. Altimeters are set to deploy main chute when the vehicle reaches 800ft during descent
- Vehicle body is in perfect condition for flight
 - a. No cracks, edges are reinforced with epoxy to prevent wear and tear, body is not bruised in, smooth, cracks filled in
- Rail buttons are secured to bulk heads by screw
 - a. Rail buttons are lined up with each other vertically
- Payload is secured and functional
 - a. The rover is protected from pyro charge
 - b. The rover has some protection during landing
 - c. The rover has power and motors that function to turn the wheels
 - d. Rover can be triggered to deploy from rocket
- 1. Rover has program running waiting for the trigger signal either from the team sending a signal or an altimeter sending the signal to rover interface that the rocket has landed
 - e. Rover can travel at least 5ft away from rocket autonomously
 - f. Rover can deploy foldable solar panels autonomously
- Nose cone has snug fitting in body
 - a. Nose cone is sturdy
 - b. Nose cone has no lip over body
 - c. Nose cone is smooth with no rough edges

Launch Checklist:

- Wait for approval from RSO and event staff to walk to pad with rocket
- Turn on rover to run program and wait for landing command
- Pack rover back in rocket and secure rover and make sure nose cone is fitted snug
- Set up launch pad
 - a. Tip pad over to lower rail
 - b. Check rail and rail buttons to make sure everything is in perfect condition
 - c. Slide rocket all the way onto the rail
 - d. Tip pad up to raise rail and rocket
 - e. Arm first altimeter
 - f. Listen for the correct series of beeps
 - g. Arm second altimeter
 - h. Listen for the correct series of beeps
 - i. Put fuel in motor and secure it
- Connect ELS to battery
- Clear the launch area
- Wait for approval from the event administration for launch
- Do final check for range being clear and clear sky
 - a. Do not launch with wildlife in sky, airplanes, or into clouds
- Insert key into ELS
- Start countdown from 5
- Launch
- Remove key from ELS
- Disconnect ELS from battery
- Recover rocket and the rover

7.3 Budgeting

Raider Aerospace Society (RAS) within Texas Tech University will acquire all funding. Space Raiders, functioning as a subsidiary of Raider Aerospace Society will be funded by the parent company (RAS). The society's treasurer, Russell Curlee, will continue seeking funding and budgeting for RAS. Space Raiders funding will be spearheaded by Hector Ruiz with the assistance of Reid Yentzen. A line item budget with parts and prices are detailed below. All prices are subject to an 8.25% sales tax unless otherwise noted. Furthermore, income will be separated into three categories: Funding, Material acquisition, and Facilities/services.

Expenses		Income	
Recovery Parts	\$1,200.00	RAS	\$2,000.00
Vehicle Parts	\$2,200.00	Top Tier	\$1,700.00
DACS Parts	\$530.00	Sponsor 1	\$1,000.00
Payload Parts	\$310.00	ME Dept.	\$1,000.00
Travel	\$2,000.00	Eng. College	\$1,500.00
Shipping	\$300.00	Sponsor 2	\$500.00
Sponsor investment	\$1,160.00	Sponsor 3	\$250.00
Miscellaneous	\$500.00	Sponsor 4	\$750.00
Safety	\$250.00	Sponsor 5	\$750.00
Scale Model	\$550	Sponsor 6	\$500.00
	\$9,000.00		\$9,950.00
All values rounded to highest dollar			
10% + accounted for spare parts			
Taxes and Shipping accounted for			

Figure	List
6.3	Recovery Parts
6.4	Vehicle Parts
6.5	DACS Parts
6.6	Payload Parts
6.7	Safety
6.8	Sponsor Investment

Funding:

Top Tier- Texas Tech University uses Top Tier catering services. Each member will participate in a 10-hour shift which will incur \$100 per shift to the organization. The Whitacre College on Engineering has agreed to aid in the fundraising process. The Development Director will personally oversee the progress as well as aiding with a contribution.

The Texas Tech Mechanical Engineering department has had a history of matching funds, dollar-dollar, an organization can fundraise on its own. The organization must demonstrate the funds are to be used for goals aligning with the department's mission, ethics, and standards.

Rush Enterprises has demonstrated interest in sponsoring the project in an effort to support the caliber of engineering students graduating from the university.

Raider Aerospace Society has allocated \$2000 towards Space Raider's mission in NASA's university student launch initiative.

Local businesses popular with the university will be offered a presence in the organization’s literature as well as potential company logos on the rocket’s body which will appear in local news channels. Further negotiations with local businesses will seek a mutually beneficial relationship. All businesses who contribute to the organization’s mission will also receive tax exemption credits. See figure 6.2.

Sample Fundraising Portfolio:

TEXAS TECH UNIVERSITY

RAIDER AEROSPACE SOCIETY

TEXAS TECH UNIVERSITY

NASA Student Launch Initiative

- 8-month challenge to design, build, and launch a high-powered rocket 5,000 feet, recover and deploy a solar-powered rover
- 200+ Universities proposed designs
- 45 were accepted into the challenge
- Texas Tech University one of the two universities representing Texas
- Student Launch contributes to the future development of NASA projects and aligns with current research, such as addressing potential technical issues for the agency's Journey to Mars

Schedule:

- Preliminary Design Report—Nov. 4*
- Critical Design Review and Model Prototype—Jan. 11*
- Launch Day—April 22*

TEXAS TECH UNIVERSITY

TEXAS TECH UNIVERSITY

SPONSORSHIP

	<i>Bronze</i>	<i>Silver</i>	<i>Gold</i>	<i>Platinum</i>
Contribution	\$250	\$500	\$750	\$1000
Email Blast	•	•	•	•
Logo	Small	Medium	Large	Extra Large
Plaque		Small	Large	Large
Rocket Logo			Small	Large
Monthly Event				5

*All Sponsors receive Tax break certificate
*Logos will have presence on presentations, email announcements, T-shirts, and advertisements

TEXAS TECH UNIVERSITY

10,000

Material Acquisition:

The following institutions would serve as sources for materials taken as donations. Some might require purchasing and will later on be refunded once materials are demonstrated to be used for collegiate project purposes.

- Texas Tech Industrial, Manufacturing, & Systems Engineering Department
- Home Depot

Vehicle Parts					
Part Name	Amount	Cost (ind.)	Weight Total (g)	Material	Part Total
Nose Cone	1	\$0.00	1443	ABS Plastic	\$0.00
					\$0.00
Airframe					\$0.00
Coupler (6in)	1	\$20.00	334.98	Blue tube	\$20.00
Coupler (5.5in)	1	\$20.00	301	Blue tube	\$20.00
6in Frame	1	\$67.00	806	Blue tube	\$67.00
Bulkhead (3/4in)	1	\$10.00	840	Plywood	\$10.00
Bulkhead (1/4in)	1	\$5.00	70	Plywood	\$5.00
5.5in Frame	1	\$56.00	1164	Blue tube	\$56.00
Fins	2	\$54.00	1146	G10	\$108.00
Transition	1	\$0.00	50	ABS Plastic	
RocketPoxy (2 quarts)	1	\$60.00	453	Epoxy	\$20.00
					\$0.00
Motor Assembly					\$0.00
Thrust Plate	1	\$60.00	254	Aluminum	\$60.00
Hardware set	1	\$310.00	2268	Aluminum	\$310.00
Centering Rings	1	\$10.00	128	Plywood (1/4in)	\$10.00
Fuel Grain	2	\$600.00	5115	Amonium Perchloarate	\$1,200.00
				Total	\$1,886.00

DACS Parts List

Component	Quantity	Price	Material	Total cost
Linear Actuator	1	\$120	Assem	\$292
Arduino	1	\$40	Electronics	40
Battery	1	\$10	Electronics	10
Links	4	\$10	ABS Plastic	40
Crown	1	\$20	ABS Plastic	20
Flaps	1	\$27	1/8in G10	27
Control board	1	\$20	Electronics	20
Sensors	1	\$20	Electronics	20
Bulkhead	1	\$5	Plywood	5
Various electrical	1	\$20	Electrical	20
				\$494

Payload Parts List

1	Item	Descriptions	Price	Qty	Total Price	Part No	Link
2	General						
3	.125" Plastic Stock	12" x 12"		\$4.23	1	\$4.23	8619K441 https://www.mcmaster.com/#standard-plastic-sheets/=1a2foqx
4	.25" Plastic Stock	6" x 12"		\$4.62	1	\$4.62	8619K751 https://www.mcmaster.com/#standard-plastic-sheets/=1a2foqx
5	.5" Plastic Stock	12" x 12"		\$7.46	1	\$7.46	8619K461 https://www.mcmaster.com/#standard-plastic-sheets/=1a2foqx
6	1" Plastic Stock	6" x 6"		\$13.23	1	\$13.23	8619K614 https://www.mcmaster.com/#standard-plastic-sheets/=1a2foqx
7	3D Printing Materials	-		\$0.00	1	\$0.00	https://www.depts.ttu.edu/its/services/3dprint/faqs.php
8	3D Printing Machine Time	-		\$0.00	1	\$0.00	https://www.depts.ttu.edu/its/services/3dprint/faqs.php
9							
10	Bearing Housing						
11	Motor for Bayonet	Servo		\$13.99	1	\$13.99	900-00008 https://www.alliedelec.com/parallax-inc-900-00008/70372373/7r
12	Spring for Bayonet	.2 OD, .36" CL, .49 LB		\$0.61	1	\$0.61	965K46 https://www.mcmaster.com/#compression-springs/=1a2fu8h
13							
14	Rover						
15	Raspberry Pi	3 Model B	\$34.90	1	\$34.90		https://www.amazon.com/Raspberry-Model-1-2GHz-64-bit-quad
16	Pressure/Altitude/Temp.	MPL3115A2 - I2C	\$9.95	1	\$9.95	MPL3115A2	https://www.adafruit.com/product/1893
17	Temp & Humidity Sensor	Adafruit SI7021	\$6.95	1	\$6.95	SI7021	https://www.adafruit.com/product/3251
18	ZIPPY Compact Battery		\$10.56	2	\$21.12	9067000018-0	https://hobbyking.com/en_us/zippy-compact-1500mah-2s-40c-lip
19	Step Down Regulator		\$3.95	1	\$3.95	2098	https://www.pololu.com/product/2098
20	Wires	80 pc set	\$5.99	1	\$5.99	4330587431	https://www.amazon.com/GenBasic-Solderless-Ribbon-Breadboa
21	Breadboard	Solderable Breadboard	\$4.95	1	\$4.95	PRT-12070	https://www.sparkfun.com/products/12070
22	Ultrasonic sensor		\$3.95	2	\$7.90	474-SEN-13959	https://www.mouser.com/ProductDetail/SparkFun-Electronics/SE
23	Solar Panel	1.5V, 400mA, 80X60mm	\$3.99	3	\$11.97	16240	https://www.xump.com/science/Solar-Cell-1-5V-400mA-80x60mm
24	Panel Deployment Servo	1.3"x1.2"x0.5" servo	\$7.50	2	\$15.00	2442	https://www.adafruit.com/product/2442
25	Torsion Springs	1 in-lb torque, 6 pk.	\$6.41	1	\$6.41	9271K31	https://www.mcmaster.com/#torsion-springs/=1a2fy96
26	Wheel Bracket Pins	1/16" x 3" Shaft	\$2.70	1	\$2.70	1327K83	https://www.mcmaster.com/#rotary-shafts/=1a2fzaw
27	Wheel Extension Motor	Brushed motor 256:1 ratio	\$4.96	2	\$9.92	225000049-0	https://hobbyking.com/en_us/brushed-motor-15mm-6v-2000kv
28	Wheel Extension Screw	ASTM A193 Steel ACME Lead Sc	\$8.98	2	\$17.96	93420A881	https://www.mcmaster.com/#93420A881
29	Drive Motor	4 pk	\$13.99	4	\$55.96	RV2306	https://www.hobby-wing.com/aakfly-rv2306-2400kv-brushless-m
30	ESC	BLHeli Series, 30Amp	\$13.00	2	\$26.00	XT60	https://store.flitetest.com/blheli-series-30a-esc-xt60/
31							
32				Total		\$285.77	

Safety Parts List

Equipment	Qty	Price	Total	Vendor Link
Eye Goggles	14	\$1.20	\$16.80	rds&id=294714
Safety Glasses	12	\$1.85	\$22.20	rds&id=40789
Disposable Gloves	200	\$0.06	\$12.00	https://www.t
Disposable Coveralls	25	\$1.24	\$31.00	d=CjwKCAjwh
Breathing Mask	20	\$0.60	\$12.00	ype=pla&id=S-
Wool/Nylon Fire Blanket	1	\$55.50	\$55.50	/UMO3AAAAG
Poly Plastic Tarp	4	\$2.80	\$11.20	iwAx2nhLovM
First Aid Kit	1	\$25.00	\$25.00	293&gclid=Cjw
ABC Class Fire Extinguisher	1	\$60.00	\$60.00	=S-9873&gclid
			\$245.70	

Sponsor Investmet	
Plaque small	\$90.00
Plaque Large	\$120.00
logo rocket	\$20.00
email	\$30.00
shirts	\$500.00
polos	\$400.00
TOTAL	\$1,160.00

7.4 Timeline

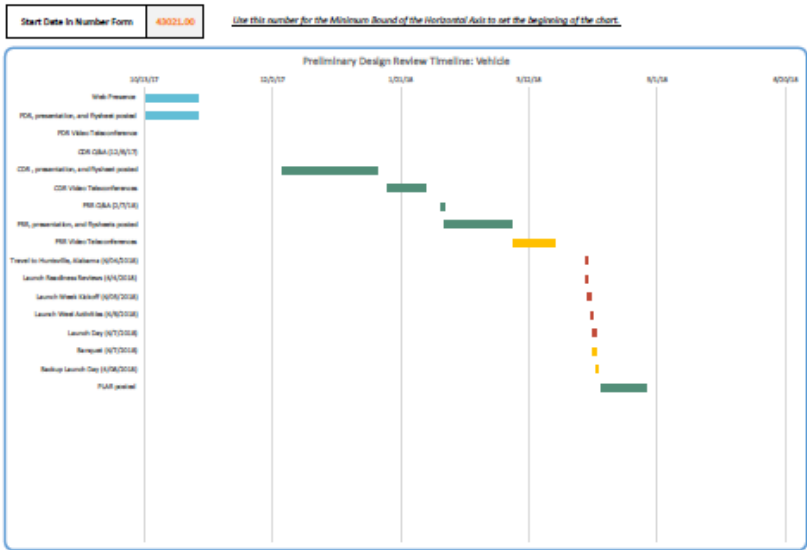
FREE GANTT CHART TEMPLATE FOR EXCEL



TeamGantt is much more than a spreadsheet. Try our web based project management app with simple drag and drop scheduling, easy sharing, and much more! Create your free account today

START BUILDING FOR FREE

Task Name	Start Date	End Date	Duration
Web Presence	10/13/2017	11/3/2017	23
PR, presentation, and flybair posted	10/13/2017	11/3/2017	23
PR Video Teleconference	11/5/2017	11/5/2017	0
CDR O&A (12/6/17)	12/6/2017	12/6/2017	0
CDR, presentation, and flybair posted	12/6/2017	1/12/2018	37
CDR Video Teleconferences	1/16/2018	1/31/2018	15
PR O&A (2/7/18)	2/5/2018	3/7/2018	1
PR, presentation, and flybair posted	2/7/2018	3/5/2018	26
PR Video Teleconferences	3/5/2018	3/23/2018	18
Travel to Huntsville, Alabama (4/4/2018)	4/3/2018	4/4/2018	1
Launch Readiness Review (4/4/2018)	4/3/2018	4/4/2018	1
Launch Week Kickoff (4/5/2018)	4/4/2018	4/5/2018	1
Launch Week Activities (4/5/2018)	4/5/2018	4/5/2018	1
Launch Day (4/7/2018)	4/5/2018	4/7/2018	1
Barquet (4/7/2018)	4/6/2018	4/7/2018	1
Backup Launch Day (4/9/2018)	4/7/2018	4/9/2018	1
PL&R posted	4/9/2018	4/27/2018	18



Key:	Calculated Cell	Manual Entry Cell
	These cells will be automatically calculated based on the inputs on other cells.	These cells require manual input so the calculated cells have data to work with.

VIII) Safety

8.1 Safety Procedures

Vehicle Safety:

G10 Fiberglass will be utilized for the fins and the Dynamic Apogee Control System (DACS) flaps. When cutting, or shaving down this material certain safety precautions will be taken since it is deadly when shavings are inhaled. Everyone in the proximity MUST wear the proper PPE: disposable coveralls, respirators, gloves, and safety goggles. The area will be removed of any shavings before removing PPE and continuing any other work.

When handling any adhesives such as Epoxy, proper PPE will be provided on site and worn by those within a 6-foot radius. Epoxy will be used only for bonding parts together for the USLI rocket and will be given the appropriate time to dry. Epoxy will be stored on the bottom shelf of the flammable cabinet to compensate for any falling damage. Proper PPE consists of but not limited to: disposable coveralls and gloves.

Regarding rocket motors, they will be stored in the appropriate container and locked away in the flammable cabinet. These motors will only be used for our USLI rocket scaled down model and full-scale model. Lastly, these motors will be disposed of in the proper fashion.

E-match's will be used for ignition to ensure appropriate distance of personnel from the launch pad. They will be secured and locked away in the appropriate container in the flammable cabinet. E-match's will be tested and properly fixed into the rocket motor.

Wind tunnel safety: Only authorized personnel permitted to use and be in the area of the wind tunnel. This is done to avoid overcrowding. All personnel will wear the PPE provided by the National Wind Institute (NWI) department. All personnel will abide by the lab safety rules of the NWI department and only use this equipment for USLI research. According to the NWI policies, anyone who uses these facilities must attempt and pass the following tests:

- Shop/Studio Safety
- Safety Awareness
- Hazardous connections
- Laser safety

Payload Safety:

Battery use and storage – Among the batteries we're considering, all of them are Lipo-batteries. Lipo-batteries must always be stored at a storage charge and never completely discharged during use. For this reason, we will check our batteries at the beginning of every design period to ensure the battery condition is maintained. A battery voltage checker will always be on site, which confirms the voltage across each cell and if they are balanced.

ESC use – The Electronic Speed Control is dependent upon what current the motors require to function at a given voltage. Otherwise, the ESC would shut off at a given value pre-

programmed or overheat causing an electrical fire. Clearly, to avoid overheating is desired, so many cross referencing and testing our connections will be executed to guarantee proper implementations. The ESC will be stored away from any exposure to water to avoid short circuiting.

Electric Motor – Our motor is the control when considering purchasing electronics. When selecting a motor, we concern ourselves with the kv value and required current to perform at certain voltages. This current is then cross referenced with other electronics to avoid any overheating resulting in electrical fires. Electric Motors will always be stored in its provided casing in order to avoid dust collection and exposure to water.

Recovery Safety:

Black powder: Will be utilized for the separation stages and the following safety measure will be followed by Space Raiders personnel. The flammable cabinet will be used for all black powder products of which will be ensured are sealed tightly. The cabinet will be securely locked inspected daily to upkeep cleanliness. When handling the black powder, the proper PPE will be provided and worn by all those within a 6-foot radius: disposable coveralls, gloves, safety glasses, fire hydrant, fire-blanket, and a first aid kit. Quantities will be tested before implementing into the rocket itself. Tests will be executed safely by following these procedures: e-match ignition, all personnel at least 30 yards away, notified fire marshal and appropriate remote testing location.

Packing procedures: Only the safety officer and the Recovery Team Lead are permitted to pack the black powder discharging stages of the rocket. Appropriate PPE will be provided and worn. All other personnel will remain at least 30 yards away.

Personal Protective Equipment:

- Eye Goggles
- Safety Glasses
- Wool/Nylon Fire Blanket
- Disposable Coveralls
- ABC Class Fire Extinguisher
- Disposable Gloves
- Leather Gloves
- First Aid Kit
- Plastic Tarp
- Breathing Mask

**The following safety procedures are posted on site frequently as a constant reminder.*

RAIDER AEROSPACE SOCIETY
REESE TECHNOLOGY CENTER
SAFETY PROTOCOL

Document Disclosure: This document has been drafted per request of Texas Tech professor, Dr. Gale, in order to appropriately ensure efficiency and safety during the use of this facility.

Tool Disclosure: For specific procedures and regulations, refer to the RoboRaider's Safety Exam:

https://docs.google.com/forms/d/e/1FAIpQLSep1fB0_4bH5-M5h1R-F5xtqwybu_13TJ_1IAHWV1XpgKnpQ/viewform

****Equipment is used at your own risk and neither the Raider Aerospace Society nor Reese Technology Center accepts any responsibility***

Members of R.A.S. will adhere to the following:

Behavior and Conduct:

- Horseplay or aggressive actions towards any and all persons at the facility will not be tolerated
- The consumption, possession, and the presence of alcohol will not be tolerated on the facility property
- Members will be limited to a maximum of two guests to avoid overcrowding
- All food and drinks must be kept out of construction zones
- Access to equipment other than that owned by R.A.S. must be approved by a credible representative of ownership
- Members should NEVER run inside of the workspace building
- NEVER use equipment you are not familiar with and haven't been introduced to by an authorized officer
- Never work in poor lit areas
- Keep yourself well balanced and never overreach.
- Never work with material that is broken or unclean.
- Always consult a RAS officer before using any special equipment or setups.
- Never stand near danger zones or close to anyone operating equipment.

General Equipment Behavior:

- Always keep hands, arms, or legs out of the cutting path of equipment.
- Position your body out of harms way while operating any equipment.
- NEVER use faulty equipment that is subject to replacement.
- NEVER test the sharpness or temperature of a tool with an appendage of a body.
- Equipment will be used solely for its functions and are not to be considered toys.
- The appropriate use of tools for a given action must be considered in order to. avoid error in equipment performance and protection.
- Only authorized members may use both the given equipment of the facility and equipment purchased by the organization.
- Equipment is not to be removed from the premises unless for club events or repairs.
- Properly use secure support surfaces while operating any equipment in order to ensure safety to both equipment and adjacent people.

- Always store or secure tools away from potential harm to yourself, other person(s), or the equipment itself.
- Cutting edges must be sharp and within operating conditions.
- Equipment should always be adjusted and calibrated before attempting a given task.
- Always consult a RAS officer before making adjustments or performing maintenance to equipment.
- Never force or apply uneven pressure while performing any tasks with equipment.

Cleanup and Awareness:

- Keep workspaces clear and organized.
- Keep isles clear of loose materials.
- Never use your hand or body parts to remove scraps or shavings away from equipment operating area.
- Remove any special attachments from equipment as well as reset both safety guards and standard settings to equipment.
- Don't leave spills or hazardous materials unattended.
- All equipment and tools will be returned to their designated storage area(s)/container(s).
- Maintain cleanliness of equipment to insure equipment functions properly.

Clothing Standards and PPE (Personal Protective Equipment):

- Always use personal protective equipment while operating any equipment.
- Complete coverage of feet must be worn.
- Hair should be secured with proper hair accessories.
- Jewelry must be removed before using any equipment.
- No baggy clothing will be worn while using equipment.
- Pants must be worn while using equipment..
- Shirts should be tucked in and long sleeves neatly rolled up.
- Do not wear gloves while operating equipment unless handling rough materials.
- Wear ear protection while around working around loud equipment.
- Use proper ventilation and wear masks to avoid breathing in harmful material debris.

Shop Maintenance:

- If you are not certain on cleaning procedures or cannot identify spilled substances, notify a RAS officer immediately.
- Always know location of fire extinguishers and how to use them.
- Always keep cabinet doors and drawers closed.
- If you disconnect power to a machine at the circuit breaker, use a lock out system or put up a sign: "Don't Connect."

Chemical Use and Storage:

- Chemicals include but are not limited to:

- Potassium nitrate, ammonium, perchlorate, ammonium nitrate and potassium chloride, liquid oxygen, oxidizers, lithium, fluorine, methane, water, etc.
- All chemicals must be properly secured and stored when not in use.
- Any chemicals with noxious and flammable fumes must remain in airtight containers until directly in use.
- All flammable materials must be properly stored within given fire cabinets.
- While handling any dangerous fumes proper use of the fume hood, masks, goggles, lab coat, and gloves must be enforced.
- Chemical expiration's must be documented and properly disposed of.
- Disposal of chemicals must be done properly and safely.
- Chemicals must be properly and eligibly labeled.

Materials:

- Materials include but are not limited to:
 - PVC pipe, wood, aluminum, steel, carbon fiber, polyethylene, G10 blue tube, polyurethane, polystyrene, various plastics and foams, ABS plastic, black powder, Epoxy, etc.

Hand Tools:

- Tools include but are not limited to:
 - Non-powered equipment such as: screwdrivers, pliers, hammers, etc.
- Hand tools are to be used in a safe manner at all times and should never be used outside of their designed purpose.
- Proper maintenance and replacement of hand tools should be exercised by all RAS members.

Power Tools:

- Tools include but are not limited to:
 - Table saw, Band saw, power drill, drill press, routing tools, sander, jig saw, circular saw, lathe, etc.
- Electric Power tools must be grounded or double insulated to prevent electric shock. If equipment does not meet that standard, it will not be used.
- Re-assure power tool as been turned off before connecting to a power source to avoid any unscripted equipment actions.
- Always make sure equipment has been turned off and unplugged before any adjustments or maintenance is performed.
- Always wait for machine to reach operating position/speed before use.
- Unplug or turnoff any equipment not being used

Specialized Machine and Equipment:

- Policies and procedures for any heavy equipment not listed above will be added under this given section as the need arises.

**Failure to adhere to the policies listed above will result in being given a warning appropriate to the offense. Repeated offenses will prompt a suspension and possible removal from construction activities*

8.2 Safety Budget

Equipment	Qty	Price	Total
Eye Goggles	14	\$1.20	\$16.80
Safety Glasses	12	\$1.85	\$22.20
Disposable Gloves	200	\$0.06	\$12.00
Disposable Coveralls	25	\$1.24	\$31.00
Breathing Mask	20	\$0.60	\$12.00
Wool/Nylon Fire Blanket	1	\$55.50	\$55.50
Poly Plastic Tarp	4	\$2.80	\$11.20
First Aid Kit	1	\$25.00	\$25.00
ABC Class Fire Extinguisher	1	\$60.00	\$60.00
			\$245.70

XI) Bibliography

DACS Sources:

Purser, Paul E., and Thomas R. Turner. *Wartime Report*. NACA, 1943, pp. 13–68, *Wartime Report*. Aerodynamic characteristics and flap loads (angle of attack changes force on flaps)

Progressive Automations. “Feedback Linear Actuator.” *Linear Actuator with Potentiometer / Progressive Automations*, Progressive Automation Inc., 2017, [www.progressiveautomations.com/linear-actuator-with-potentiometer#ig_lightbox2\[gal\]/0/](http://www.progressiveautomations.com/linear-actuator-with-potentiometer#ig_lightbox2[gal]/0/).

“The Drag Equation.” Edited by Tom Benson, Glenn Research Center, NASA, National Aeronautics and Space Administration, 12 June 2014, spaceflightsystems.grc.nasa.gov/education/rocket/drageq.html.

“The Drag Coefficient.” Edited by Tom Benson, Glenn Research Center, NASA, National Aeronautics and Space Administration, 12 June 2014, spaceflightsystems.grc.nasa.gov/education/rocket/dragco.html.

“Bernoulli's Equation.” Edited by Nancy Hall, Glenn Research Center, NASA, National Aeronautics and Space Administration, 5 May 2015, www.grc.nasa.gov/www/k-12/airplane/bern.html.

“Dynamic Pressure.” Edited by Nancy Hall, Glenn Research Center, NASA, National Aeronautics and Space Administration, 5 May 2015, www.grc.nasa.gov/www/k-12/airplane/dynpress.html.

“Pitot Tube.” Edited by Tom Benson, Glenn Research Center, NASA, National Aeronautics and Space Administration, 12 June 2014, www.grc.nasa.gov/WWW/k-12/VirtualAero/BottleRocket/airplane/pitot.html.

“External Force Balance.” Edited by Nancy Hall, Glenn Research Center, NASA, National Aeronautics and Space Administration, 5 May 2015, www.grc.nasa.gov/www/k-12/airplane/tunbalext.html.

“Internal Force Balance.” Edited by Nancy Hall, Glenn Research Center, NASA, National Aeronautics and Space Administration, 5 May 2015, www.grc.nasa.gov/www/k-12/airplane/tunbalint.html.

Vehicle Sources:

“Shape Effects on Drag.” Edited by Nancy Hall, *Glenn Research Center, NASA*, National Aeronautics and Space Administration, 5 May 2015, www.grc.nasa.gov/www/k-12/airplane/shaped.html. (DETS design inspiration (Low Cd of teardrop shape))

“Our Materials.” Markforged.com, Markforged, Inc., 2017, markforged.com/materials/.

“Apogee Components.” Apogee Components, 2017, [webcache.googleusercontent.com/search?q=cache:G7mLKMpxPXEJ:https://www.apogeerockets.com/ &cd=1&hl=en&ct=clnk&gl=us](https://www.apogeerockets.com/).

“Rocket Equations.” Rocketmime.com, Rocket Mime, 14 Jan. 2012, www.rocketmime.com/rockets/rckt_eqn.html.

“Resources.” Aerotech-Rocketry, RCS Rocket Motor Components, Inc., 2009, www.aerotech-rocketry.com/resources.aspx?id=7.

“6061-T6 Aluminum.” MakeItFrom.com, Make It From, 2017, www.makeitfrom.com/material-properties/6061-T6-Aluminum.

“What Is Blue Tube 2.0.” Alwaysreadyrocketry.com, AfterDark Creative, 2017, www.alwaysreadyrocketry.com/blue-tube-2-0/.

“Material Safety Data Sheet - Acculam™ Epoxyglas (NEMA Grades G10, G11, FR4, FR5).” Ifa.hawaii.edu, Accurate Plastics, Inc., 30 Nov. 2001, www.ifa.hawaii.edu/instr-shop/SDS/G10.pdf.

“Average Weather in Huntsville Alabama, United States.” Weatherspark.com, Cedar Lake Ventures, Inc, 2017, weatherspark.com/y/14628/Average-Weather-in-Huntsville-Alabama-United-States-Year-Round.

“G9 G10 FR4 Glass Epoxy Sheet.” Eplastics.com, Ridout Plastics Co. Inc. ePlastics, 2017, www.eplastics.com/Plastic/G9-G10-FR4-glass-epoxy-sheet/G10NAT-250X12X24.

“Plywood.” Merriam-Webster.com, Merriam-Webster, Incorporated, 2017, www.merriam-webster.com/dictionary/plywood.

“Carbon Fiber.” Dictionary.com, Dictionary.com, LLC., 2017, www.dictionary.com/browse/carbon-fiber.

Recovery Sources:

“Material Safety Data Sheet - MSDS-BP (Potassium Nitrate) .” Goex Powder, www.Epa.gov, Goex Powder, Inc. , 17 Mar. 2009, www.epa.gov/sites/production/files/2015-05/documents/9530608.pdf.

“Apogee Components.” Apogee Components, 2017, [webcache.googleusercontent.com/search?q=cache:G7mLKMpxPXEJ:https://www.apogeerockets.com/ &cd=1&hl=en&ct=clnk&gl=us](http://webcache.googleusercontent.com/search?q=cache:G7mLKMpxPXEJ:https://www.apogeerockets.com/&cd=1&hl=en&ct=clnk&gl=us).

“Rocket Materials.” Rocketmaterials.org, Rocketmaterials.org, www.rocketmaterials.org/datastore/cord/Shear_Pins/index.php.

Haines, Lestar. “Pyrotechnic boffin poised to light LOHAN's fire.” Theregister.co.uk, Biting the hand that feeds IT, 18 July 2012, www.theregister.co.uk/2012/07/18/lohan_igniter/.

“How To Size Ejection Charge.” Hararocketry.org, Huntsville Area Rocketry Association, 2017, hararocketry.org/hara/resources/how-to-size-ejection-charge/.

Nose Cone Sources:

“Nose cone design.” *Wikipedia*, Wikimedia Foundation, 18 Oct. 2017, en.wikipedia.org/wiki/Nose_cone_design.

Milligan, Ashley Van. *Drag of Nose Cones*. National Association of Rocketry, 2013, *Drag of Nose Cones*, 6. https://www.apogeerockets.com/downloads/Drag_of_Nose_Cones.pdf .

“Nose cone design.” *Wikipedia*, Wikimedia Foundation, 18 Oct. 2017, en.wikipedia.org/wiki/Nose_cone_design.

Payload Sources:

“Rover Environmental Monitoring Station (REMS) - Mars Science Laboratory.” NASA, USA.gov, 2017, mars.nasa.gov/msl/mission/instruments/environsensors/remss/.

Industries, Adafruit. “Adafruit Si7021 Temperature & Humidity Sensor Breakout Board.” Adafruit industries blog RSS, Adafruit, 2017, www.adafruit.com/product/3251.

Industries, Adafruit. “MPL3115A2 - I2C Barometric Pressure/Altitude/Temperature Sensor.” Adafruit industries blog RSS, Adafruit, 2017, www.adafruit.com/product/1893.

“SparkFun Atmospheric Sensor Breakout - BME280.” SparkFun Electronics, SparkFun Electronics, 2017, www.sparkfun.com/products/13676.

Industries, Adafruit. “DHT22 temperature-Humidity sensor extras.” Adafruit industries blog RSS, Adafruit, 2017, www.adafruit.com/product/385.